

**EFAM GTP 02 –
the GKSS test procedure for determining
the fracture behaviour of materials**

Authors:

K.-H. Schwalbe

J. Heerens

U. Zerbst

*(GKSS Research Centre,
Institute for Materials Research,
Geesthacht, Germany)*

H. Pisarski

*(The Welding Institute,
Cambridge, United Kingdom)*

M. Koçak

*(GKSS Research Centre,
Institute for Materials Research,
Geesthacht, Germany)*

Beneficial comments (recommendations, additions, deletions) and any pertinent data which may be of use in improving this document should be addressed to:

Prof. Karl-Heinz Schwalbe
GKSS-Forschungszentrum Geesthacht GmbH
Max-Planck-Str.
21502 Geesthacht, Germany

using the EFAM DOCUMENT IMPROVEMENT PROPOSAL form appearing at the end of this document or by e-mail to:

Schwalbe@gkss.de

While GKSS-Forschungszentrum Geesthacht GmbH (GKSS) believe that the information and guidance given in this document are correct, all parties making use of it must rely on their own skill and judgement. Neither GKSS nor those of its employees responsible for the production of this document can assume any liability for loss or damage caused by any error or omission in the application of the procedure. Any and all such liability is disclaimed.

Neither GKSS nor any of its employees give any warranty or representation whatsoever that the information and guidance given in this document does not infringe the rights of any third party or can be used for any particular purpose at all. Any person intending to use the same should satisfy himself as to its accuracy and the suitability for the purpose for which he intends to use it.

GKSS-Forschungszentrum Geesthacht GmbH, December 2002

Die Berichte der GKSS werden kostenlos abgegeben.

The delivery of the GKSS reports is free of charge.

Anforderungen/Requests:

GKSS-Forschungszentrum Geesthacht GmbH
Bibliothek/Library
Postfach 11 60
D-21494 Geesthacht
Germany
Fax.: (49) 04152/871717

Als Manuskript vervielfältigt.

Für diesen Bericht behalten wir uns alle Rechte vor.

ISSN 0344-9629

GKSS-Forschungszentrum Geesthacht GmbH · Telefon (04152)87-0
Max-Planck-Straße · D-21502 Geesthacht/Postfach 11 60 · D-21494 Geesthacht

GKSS 2002/24

EFAM GTP 02 – the GKSS test procedure for determining the fracture behaviour of materials

Karl-Heinz Schwalbe, Jürgen Heerens, Uwe Zerbst, Henryk Pisarski, Mustafa Koçak

149 pages with 79 figures

Abstract

This document describes a unified fracture mechanics test method in procedural form for quasi-static testing of materials. It is based on the ESIS Procedures P1 and P2 and introduces additional features, such as middle cracked tension specimens, shallow cracks, the δ_5 crack tip opening displacement, the crack tip opening angle, the rate of dissipated energy, testing of weldments, and guidance for statistical treatment of scatter. Special validity criteria are given for tests on specimens with low constraint. This document represents an updated version of EFAM GTP 94.

EFAM GTP02 – die GKSS-Bruchmechaniktestmethode

Zusammenfassung

Der vorliegende Bericht beschreibt eine vereinheitlichte Bruchmechanik-Versuchsprozedur für die quasi-statische Werkstoffprüfung. Sie beruht auf den ESIS-Prozeduren P1 und P2, führt aber darüber hinaus weitere Aspekte ein, wie die Rissspitzenverschiebung δ_5 , den Rissspitzenwinkel, die Energiedissipationsrate, Mittenrisscheiben, kurze Risse, Schweißverbindungen und Berücksichtigung von Streuungen in den Kennwerten. Spezielle Gültigkeitskriterien für Versuche an Proben mit geringer Spannungsmehrachsigkeit werden angegeben. Dieser Bericht stellt eine ergänzte Fassung von EFAM GTP 94 dar.

Manuscript received / Manuskripteingang in TDB: 20. Dezember 2002

CONTENTS

SUMMARY	7
DEFINITIONS	7
NOMENCLATURE	8
1 INTRODUCTION	11
2 SPECIMEN GEOMETRY, DIMENSIONS AND PREPARATION	18
3 TEST REQUIREMENTS	28
4 TEST PROCEDURE	34
5 PLAIN STRAIN FRACTURE TOUGHNESS K_{Ic}	39
6 FRACTURE PARAMETERS δ_{5c} , J_c AND δ_{5u} , J_u	40
7 CRACK EXTENSION RESISTANCE CURVES AND RELATED FRACTURE PARAMETERS $\delta_{5,0.2/BL}$, $J_{0.2/BL}$ AND $\delta_{5,0.2}$, $J_{0.2}$ UNDER HIGH CONSTRAINT CONDITIONS	45
8 CRACK EXTENSION RESISTANCE UNDER LOW CONSTRAINT CONDITIONS	55
9 PRESENTATION OF RESULTS	57
10 REFERENCES	60
APPENDIX 1 Stress Intensity Functions	63
APPENDIX 2 Measurement of Load Point Displacement	64
APPENDIX 3 Measurement of Crack Mouth Opening Displacement on Middle Cracked Tension Specimens	66
APPENDIX 4 Measurement of the Crack Tip Opening Displacement, δ_5	69
APPENDIX 5 Single Specimen Methods to Determine R-Curves	72
APPENDIX 6 δ_{5i} and J_i Determination	88
APPENDIX 7 Determination of Blunting Line from Tensile Properties	92
APPENDIX 8 Offset Power Law Fit to Crack Extension Fracture Resistance Data	96
APPENDIX 9 Testing of Weldments	97
APPENDIX 10 Statistical Analysis of Fracture Resistance Data	113
APPENDIX 11 K-Based Fracture Resistance Curves For Middle Cracked Tension Panels	122
APPENDIX 12 Testing Specimens with Shallow Cracks	124
APPENDIX 13 Relationships Between δ_5 and other Fracture Parameters	125
APPENDIX 14 Determination of δ_5 and J in the Centre Plane of SE(B) and C(T) Specimens	127
APPENDIX 15 Determination of the Crack Tip Opening Angle (CTOA)	132
APPENDIX 16 Determination of the Rate of Dissipated Energy, R	145

SUMMARY

This document describes a procedure for determining the fracture resistance of materials from the linear elastic regime to the fully plastic regime under conditions of various constraint. The fracture resistance is characterised in terms of either the stress intensity factor, K , the crack tip opening displacement, δ_5 , the J-integral or the crack tip opening angle (CTOA), ψ .

Testing requirements and analysis procedures are given which enable K , δ_5 , J , and ψ to be calculated for compact, single edge cracked bend, and middle cracked tension specimens. Fracture parameters are defined for unstable and stable crack extension which estimate the value of K , δ_5 , and J at, or close to, crack initiation.

This procedure closely follows the European Structural Integrity Society Procedure ESIS P2-92 and the draft ISO Standards N-413.6 and ISO/DIS 12135 and includes the following features:

- Crack tip opening displacement measured in terms of the parameter δ_5 ;
- Middle cracked tension specimen;
- Single edge cracked bend specimen under four-point bending;
- Use of specimens under low constraint conditions.

Appendices are also included which provide guidance on the testing of weldments, the evaluation of statistical bounds to the fracture parameters, the testing of specimens with shallow cracks and the determination of δ_5 and J in the centreplane of the specimen, and of the rate of dissipated energy, R .

DEFINITIONS

Stable Crack Extension

Crack extension which, under displacement control, stops when the applied displacement is held constant.

Unstable Crack Extension

An abrupt crack extension which occurs with or without prior stable crack extension and which leads to unstable fracture of the specimen.

Fracture Resistance

The resistance a material exhibits to stable or unstable crack extension, expressed in terms of K , δ_5 , J , CTOA, or R .

Fracture Parameter

Fracture resistance related to unstable crack extension or initiation of stable crack extension.

NOMENCLATURE

Dimensions

a	Crack length.
a_i	Estimated initial crack length.
a_o	Measured initial crack length, Figs. 5 to 8.
B	Specimen thickness.
B_n	Net thickness of sidegrooved specimens.
S	Span of single edge cracked bend specimen, Fig. 12a.
W	Specimen width.
z	Either the distance of the knife edge from the load line, Figs. 5 and 6, or the knife edge height defined in Figs. 9 and 17.

For the middle cracked specimen a, a_i and a_o are the half crack length; and 2W is the specimen width, **Fig. 8.**

Tensile Properties

E	Young's modulus.
ν	Poisson's ratio.
$R_{p0.2}$	Yield strength equivalent to 0.2 percent proof stress.
R_m	Tensile strength.
R_f	Flow stress $(R_{p0.2} + R_m)/2$.

Forces and Displacements

F	Applied force
F_c	Force defined in Section 5.1.2
F_Y	Yield force calculated using $R_{p0.2}$.
F_L	Ultimate force, calculated using R_m .
F_{max}	Maximum sustained force, Fig. 21.
R	Ratio of lower to upper force during fatigue cracking.
q	Load point displacement.
V	Crack mouth opening displacement.

Fracture Parameters and Related Quantities

Δa	Average crack extension including blunting.
Δa_{SZW}	Critical stretch zone width.
Δa_{max}	Maximum amount of crack extension for the evaluation of crack extension resistance in terms of δ_5 , J, or ψ .

J	Fracture resistance in terms of the experimental equivalent of the J -integral, allowing for crack extension.
J_0	J not allowing for crack extension.
J_C	Value of J_0 at unstable crack extension and stable crack extension of less than 0.2 mm.
J_i	Value of J_0 at initiation of stable crack extension.
J_u	Value of J_0 at unstable crack extension after stable crack extension greater than 0.2 mm.
J_{uc}	Value of J_0 at unstable crack extension after an unknown amount of stable crack extension.
$J_{0.2/BL}$	Value of J or J_0 at 0.2 mm crack extension offset to the blunting line.
$J_{0.2}$	Value of J or J_0 at 0.2 mm crack extension including blunting.
dJ/da	Slope of the J - Δa curve.
J_{max}	Value of J or J_0 at the limit for J -controlled fracture behaviour.
J_g	Value of J or J_0 at upper limit of J -controlled crack extension.
ψ	Crack tip opening angle.
$\eta(a/W)$	J -calibration function.
δ_5	Displacement measured at the surface of a specimen either side of the original crack tip over an initial gauge length of 5 mm, see Appendix 4 .
δ_{5c}	Value of δ_5 at unstable crack extension and stable crack extension of less than 0.2 mm.
δ_{5i}	Value of δ_5 at initiation of stable crack extension.
δ_{5u}	Value of δ_5 at unstable crack extension after stable crack extension greater than 0.2 mm.
δ_{5uc}	Value of δ_5 at unstable crack extension after an unknown amount of stable crack extension.
$\delta_{5,0.2/BL}$	Value of δ_5 at 0.2mm of stable crack extension offset to the blunting line.
$\delta_{5,0.2}$	Value of δ_5 at 0.2mm of stable crack extension including blunting.
$d\delta_5/da$	Slope of the δ_5 - Δa curve.
$\delta_{5,g}$	Value of δ_5 at upper limit of δ_5 -controlled crack extension.
$\delta_{5,max}$	Value of δ_5 at the limit for δ_5 -controlled fracture behaviour.
K	Stress intensity factor.
ΔK	Range of stress intensity factor in fatigue.
$f(a/W)$	Stress intensity function, Appendix 1 .
K_{Ic}	Plane strain fracture toughness.
P_f	Failure probability.
R	Rate of dissipated energy.

The SI units to be used in this Procedure are:

F	Force, kN.
V, q	Displacement, mm.
Δa	Crack extension, mm.
K	Stress intensity factor, MPa m ^{1/2} .
J	Experimental equivalent of J-integral, MPa m.
R	Rate of dissipated energy, N/mm.
δ_5	Crack tip opening displacement, mm.

Acronyms

CMOD	Crack mouth opening displacement.
CTOA	Crack tip opening angle.
CTOD	Crack tip opening displacement.
LPD	Load point displacement.
SZW	Stretch zone width.

1 INTRODUCTION

1.1 Scope and Significance

1.1.1 Objective

This document is an updated version of EFAM GTP 94 and describes a procedure for determining the fracture resistance of materials using pre-cracked laboratory specimens. It closely follows the ESIS P1-92 and ESIS P2-92 Procedures and the draft ISO Standard N-413.8 and encompasses the fracture range from linear elastic through to fully plastic material behaviour. The Procedure includes experience gained at GKSS and introduces several additional features not covered by ESIS P1-92 and ESIS P2-92, such as

- Middle cracked tension specimens;
- Four-point bend specimens;
- Crack tip opening displacement, δ_5 ;
- Crack tip opening angle, ψ ;
- Rate of dissipated energy, R ;
- Specimens under low constraint conditions.

Guidance is also given for:

- Testing of weldments;
- Evaluation of statistical bounds to fracture toughness data.

Experience gained during the preparation of the new ISO standard ISO 12135 has also been incorporated.

The Procedure is applicable to a wide range of materials such as ferritic steels, austenitic steels, aluminium and titanium alloys, polymers as well as weldments.

The test method involves loading a pre-cracked specimen at a low rate until either sudden unstable fracture occurs with or without significant stable crack extension or ductile stable crack extension ensues.

The fracture resistance is characterised in terms of stress intensity factor, K , crack tip opening displacement δ_5 , the J-integral and the crack tip opening angle, ψ . δ_5 is measured close to the crack tip and is particularly useful for weldments. It avoids problems which may arise with the evaluation of parameters measured remotely from the crack tip region. Relationships between δ_5 and other fracture parameters are given in **Appendix 13**.

In the case of unstable fracture, these parameters are measured at the point of instability. For ductile crack extension, the variation of the fracture resistance with crack extension Δa is measured. This document contains testing requirements and analysis procedures which enable K and J to be calculated for compact, single edge cracked bend and middle cracked tension

specimens. The determination of δ_5 and ψ is basically independent of the specimen type as these parameters are measured directly at the crack tip.

The crack tip opening angle and rate of dissipated energy are alternative parameters for characterising the fracture resistance for ductile crack extension. However, due to limited experience with these parameters their determination is described in appendices.

Without prior knowledge of the force-displacement behaviour, it is impossible to know whether a specimen will exhibit unstable fracture or ductile crack extension. The force-displacement behaviour dictates the fracture parameters that can be measured. **Fig. 1** shows the main fracture parameters derived in the Procedure in relation to their broad area of application on an idealised force-displacement diagram. The force-displacement behaviour depends on the material and the specimen size and geometry. Temperature can also affect the behaviour. In the case of ferritic steels a distinct ductile-to-brittle transition is observed with decreasing temperature, **Fig. 2**. The fracture parameters are described in the following two sections.

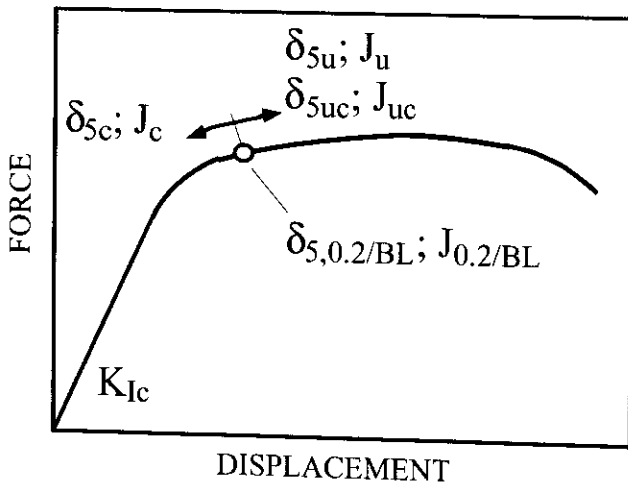


Figure 1:

Fracture parameters relevant to a force-displacement diagram.

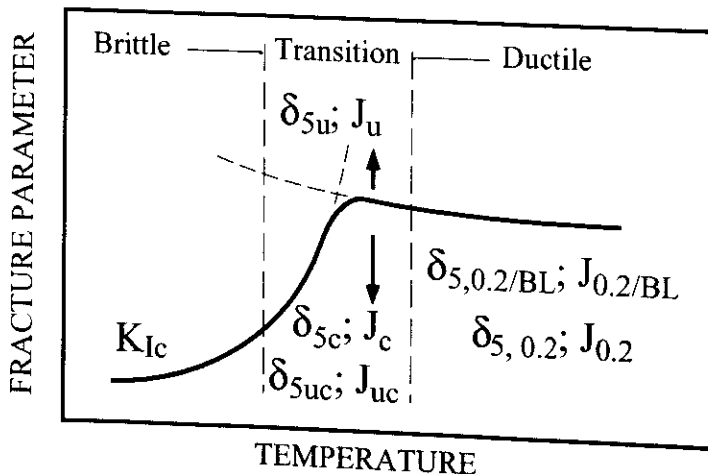


Figure 2:

Fracture parameters relevant to temperature effects of ferritic steels.

1.1.2 Fracture Parameters for Unstable Crack Extension

If the force-displacement record is essentially linear prior to unstable fracture, then the established procedures of linear elastic fracture mechanics are used to determine the plane strain fracture toughness K_{Ic} . This type of test record is exhibited by materials in the brittle regime.

If the force-displacement record is non-linear prior to unstable fracture and crack extension excluding blunting is less than 0.2 mm, then the fracture parameters δ_{5c} and J_c are determined at the point of instability. This type of test record is usually exhibited by materials in the brittle-ductile transition regime.

If the stable crack extension exceeds 0.2 mm prior to unstable crack extension, then the fracture parameters δ_{5u} and J_u are determined. This type of behaviour is usually associated with materials close to the onset of the ductile regime.

When it is not possible to measure the amount of stable crack extension prior to unstable crack extension, then the fracture parameters δ_{5uc} or J_{uc} are determined.

1.1.3 Ductile Crack Extension Parameters

If the force-displacement record is non-linear and only stable crack extension occurs, then the variation in δ_5 , or ψ with crack extension Δa is determined using either the multiple or single specimen method. This type of test record is usually exhibited by materials in the ductile regime. The multiple specimen method requires several nominally identical specimens to be loaded to different displacements. The extent of ductile crack extension is marked and the specimens are then broken open to allow measurement of the crack extension. Single specimen methods based on, for example, the unloading compliance or potential drop techniques can be used to measure crack extension provided they meet accuracy requirements given in the Procedure. The main body of the text contains the requirements of the multiple specimen method which is considered the reference method. Due to the developing nature of the single specimen methods, recommendations for these are described in an Appendix. With either approach the objective is to determine sufficient data points to adequately describe the crack extension resistance behaviour of a material

Three fracture parameters are defined in the Procedure for estimating δ_5 or J close to the onset of initiation of stable crack extension:

- $\delta_{5,0.2/BL}$ or $J_{0.2/BL}$ which measure the material resistance at 0.2 mm of ductile crack extension offset to the blunting line and provide an engineering definition of initiation. A value of 0.2 mm was chosen as it was felt large enough to allow accurate measurements of crack extension in the test specimens, yet small enough to give material resistance values close to crack initiation.

- $\delta_{5,0.2}$ or $J_{0.2}$ which measure the material resistance at 0.2 mm of total crack extension, including crack tip blunting. For many materials, like low to medium strength steels, these parameters provide useful estimates of the initiation toughness which are generally lower bound estimates of $\delta_{5,0.2/BL}$ and $J_{0.2/BL}$.
- δ_{5i} or J_i which correspond to values of the fracture resistance at crack initiation. The derivation of these parameters requires the measurement of the stretch zone width using a scanning electron microscope. It is considered to be the most accurate method for measuring δ_5 or J close to the onset of crack extension. Since there are practical difficulties in using this approach, which makes it unsuitable for routine materials testing, the method is described in **Appendix 6**.

Additionally, parameters δ_{5g} and J_g are defined which give the maximum fracture resistance values that can be measured from a given test specimen. Also $d\delta_5/da$ and dJ/da which are slopes of the δ_5 - Δa and J - Δa curves, respectively, are used to measure the material resistance to crack extension.

In **Appendix 11** a method is described for determining K-based crack extension resistance curves on high strength materials.

Appendices 15 and **16** describe methods for the determination of the crack tip opening angle and the rate of dissipated energy, respectively.

1.1.4 Use of Fracture Parameters

Fracture properties are generally dependent on size and geometry of the specimen. Therefore, the specimen configuration has to be selected according to the use of fracture properties in structural assessment.

In this Procedure, compact and single edge cracked bend specimens are tested with near-square remaining ligaments to provide conditions of high constraint. If certain size requirements are met, then the fracture properties determined by these specimens are considered size independent and define lower bound properties.

In engineering practice, however, there are cases which are not covered by these specimen configurations, for example where:

- The thickness of a structural component is much less than that specified for size independent properties and their use in assessment procedures can be unduly conservative.
- The thickness of available material does not enable the fabrication of specimens meeting the criteria for size independence.
- In many structural configurations the loading conditions are characterised by tension rather than bending.

In these cases constraint in the structural component may be substantially lower than in compact and bend specimens with near-square ligaments, thus leading to higher resistance to crack extension, which in turn provides higher load carrying capability.

Therefore, this Procedure describes also test methods for specimens not satisfying requirements for size independent fracture properties; namely,

- Compact specimens with extended ligaments,
- Middle cracked tension specimens.

The fracture parameters and the crack extension resistance curves can be used to assess the structural integrity of components. They can also be used as an index for material selection and quality assurance purposes or to evaluate the effects of temperature, heat treatment, environment, processing and chemical composition on fracture properties. The choice and applicability of the fracture parameters for structural integrity assessments and materials characterisation is at the discretion of the user.

For structural integrity analyses the procedures described in "**Engineering Flaw Assessment Method (EFAM)**" [10] are recommended. However, the material properties determined with EFAM GTP 02 can also be used in other integrity assessment methods such as the SINTAP procedure [13].

1.2 Selection of Test Method and Analysis Procedure

The geometry, dimensions and preparation of the test specimens and the test requirements are given in **Sections 2** and **3**, respectively. Selection of the test method and analysis procedure depend on the force-displacement behaviour of the test specimen. A specimen of suitable design and size should be tested at the required temperature and loading rate. Load-point displacement should be recorded as a function of applied force. If fracture does not occur the specimen should be unloaded after passing through the maximum force.

Following the test, the force-displacement record should be inspected and the flow diagram in **Fig. 3a** should be consulted for guidance on how to evaluate the fracture behaviour. **Fig. 3a** also gives the relevant section number required in the Procedure to evaluate the appropriate fracture parameter. **Fig. 3b** gives in more detail the evaluation procedure for the ductile fracture parameters. The corresponding test procedures are described in **Section 4**. Typical force-displacement records and categories of fracture behaviour are shown schematically in **Fig. 4**.

The main part of this Procedure describes the testing of homogeneous materials. If weldments are to be tested, additional steps and requirements are needed, as described in **Appendix 9**.

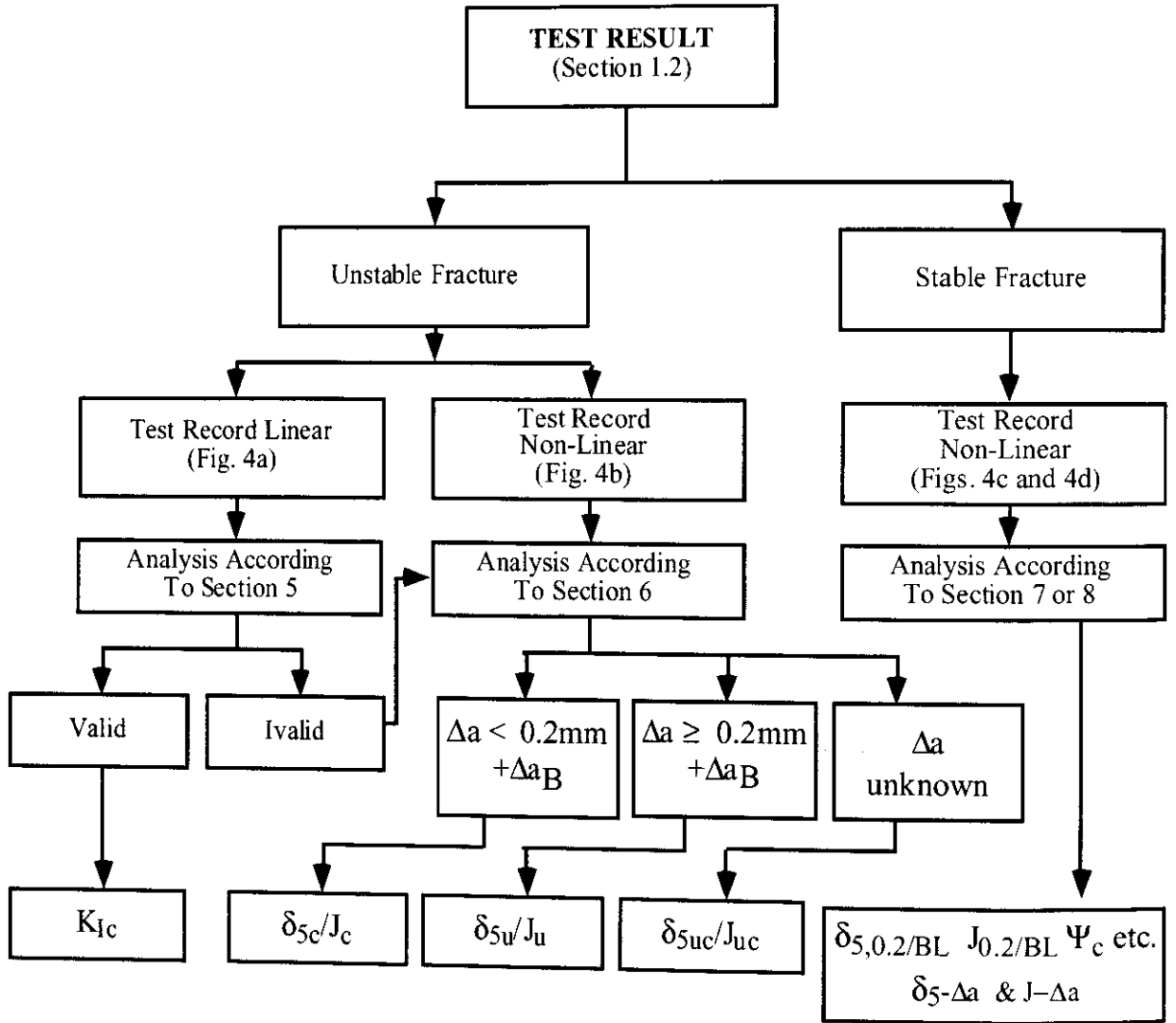


Figure 3a: Evaluation of fracture parameters from force-displacement record.

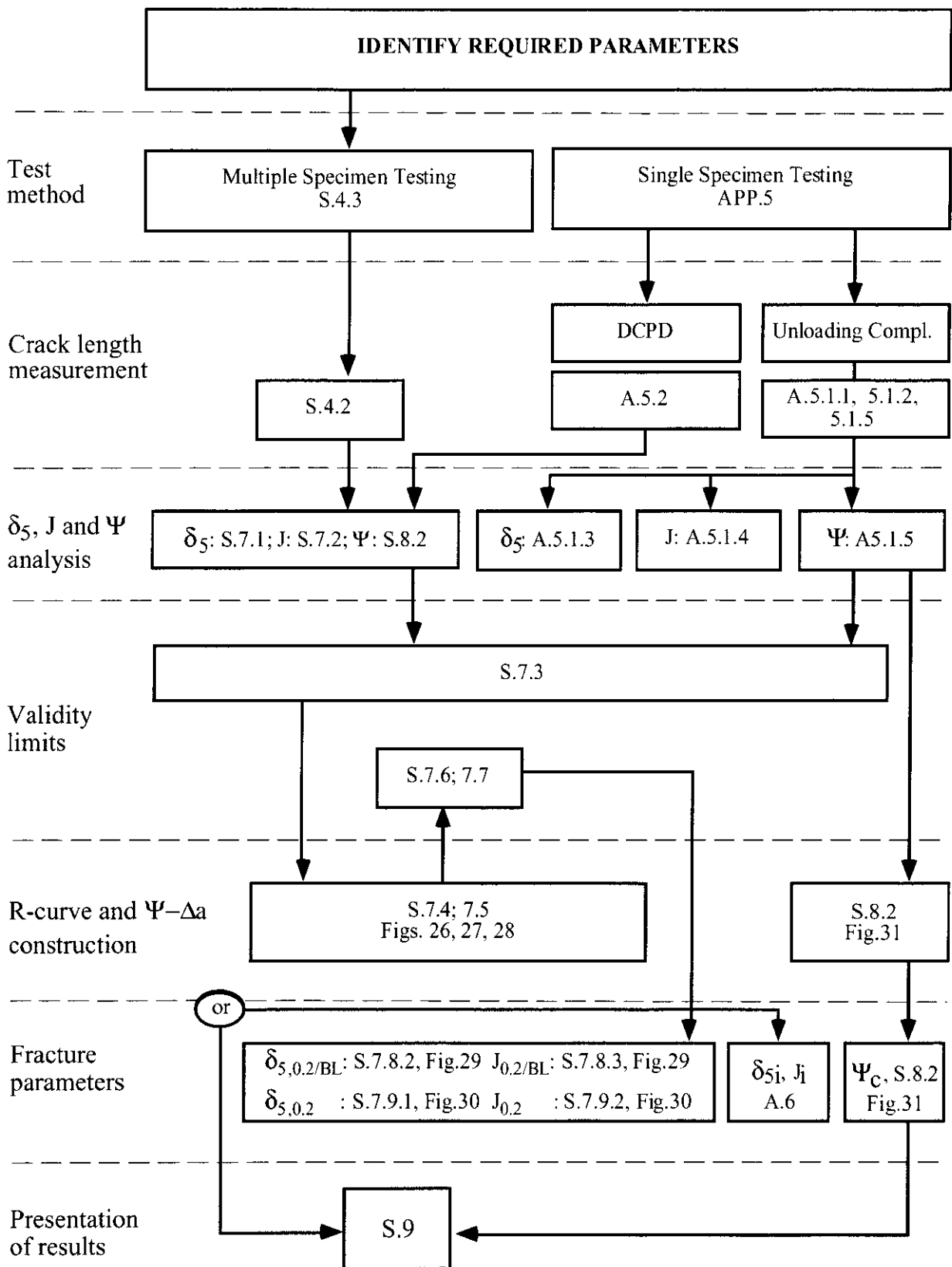


Figure 3b: Flow chart for determining stable crack extension and related fracture parameters.

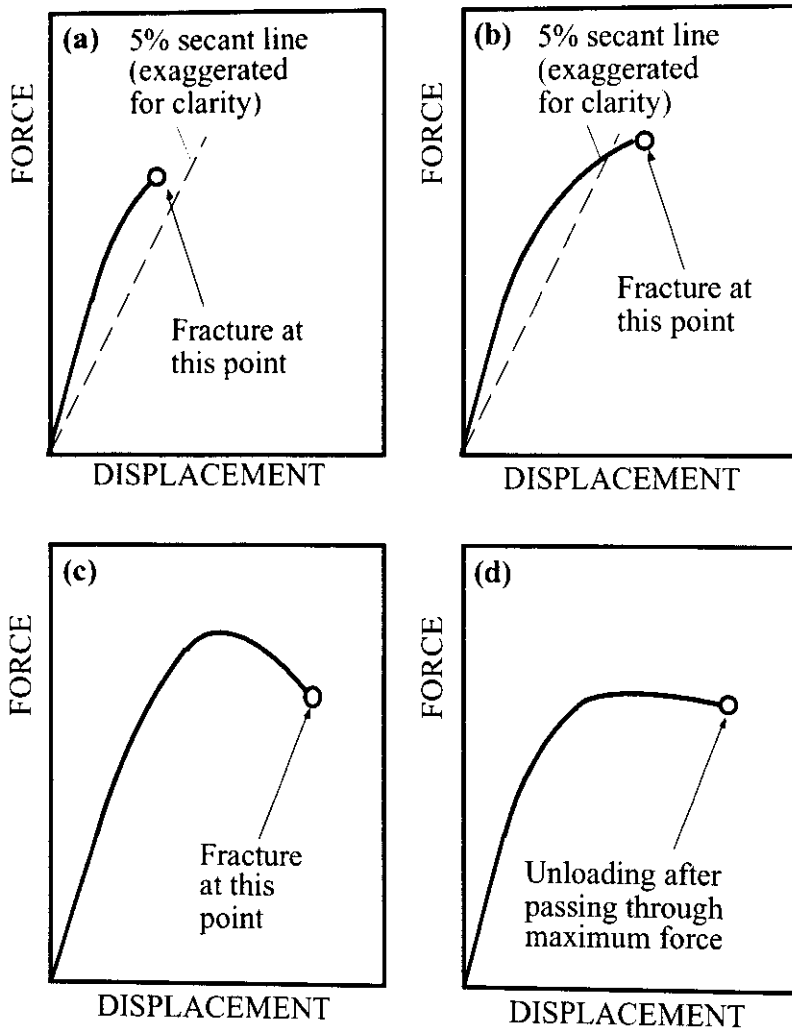


Figure 4:
Schematic force-displacement records and associated fracture behaviour.

1.3 Caveat

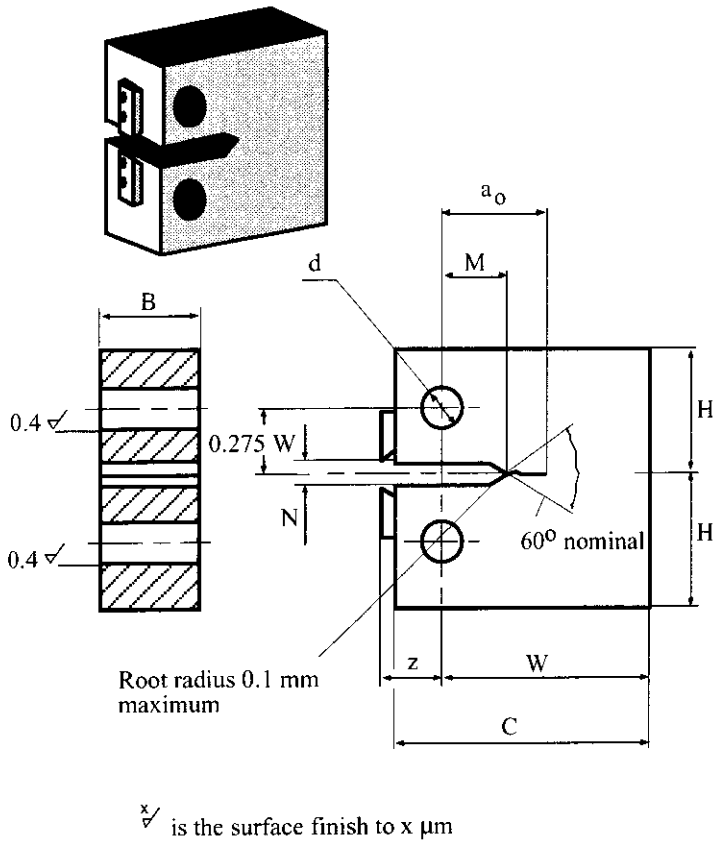
Testing of replicate specimens in the transition region, **Fig. 2**, under the same nominal conditions can often produce non-linear test records for which both unstable and stable fracture occurs, **Fig. 4**. This Procedure enables the appropriate parameters to be determined for the material behaviour. However, care should be exercised in their subsequent use as material characterising parameters.

2 SPECIMEN GEOMETRY, DIMENSIONS AND PREPARATION

2.1 Specimen Geometries

The Procedure allows the use of either compact (C(T)), single edge cracked bend (SE(B)), or middle cracked tension (M(T)) specimens. The suggested designs of compact specimens are shown in **Figs. 5** and **6**. The step notched specimen is recommended for measuring load-

point displacement directly, **Fig. 6**. Other loading hole separations, pin hole diameters and notch configurations can be used but care must be taken to avoid excessive plastic deformation at the pin holes.



Preferred width for high constraint $W = 2B$
 Total width $C = 1.25W \pm 0.01W$
 Half height $H = 0.6W \pm 0.005W \begin{smallmatrix} +0.004W \\ -0 \end{smallmatrix}$
 Hole diameter $d = 0.25W$
 Notch width $N = 0.06W$ max. or 1.5mm max. if $W \leq 25\text{mm}$
 Effective notch length $M = 0.4W$ min
 Effective crack length $a_0 = 0.45W$ to $0.65W$

NOTES:

1. A spark eroded or machined slit can be used instead of the V-notch profile.
2. Squareness and parallelism to be within $0.002W$.
Holes to be square with faces and parallel.

\sqrt{x} is the surface finish to $x \mu\text{m}$

Figure 5: Straight notched compact (C(T)) specimen.

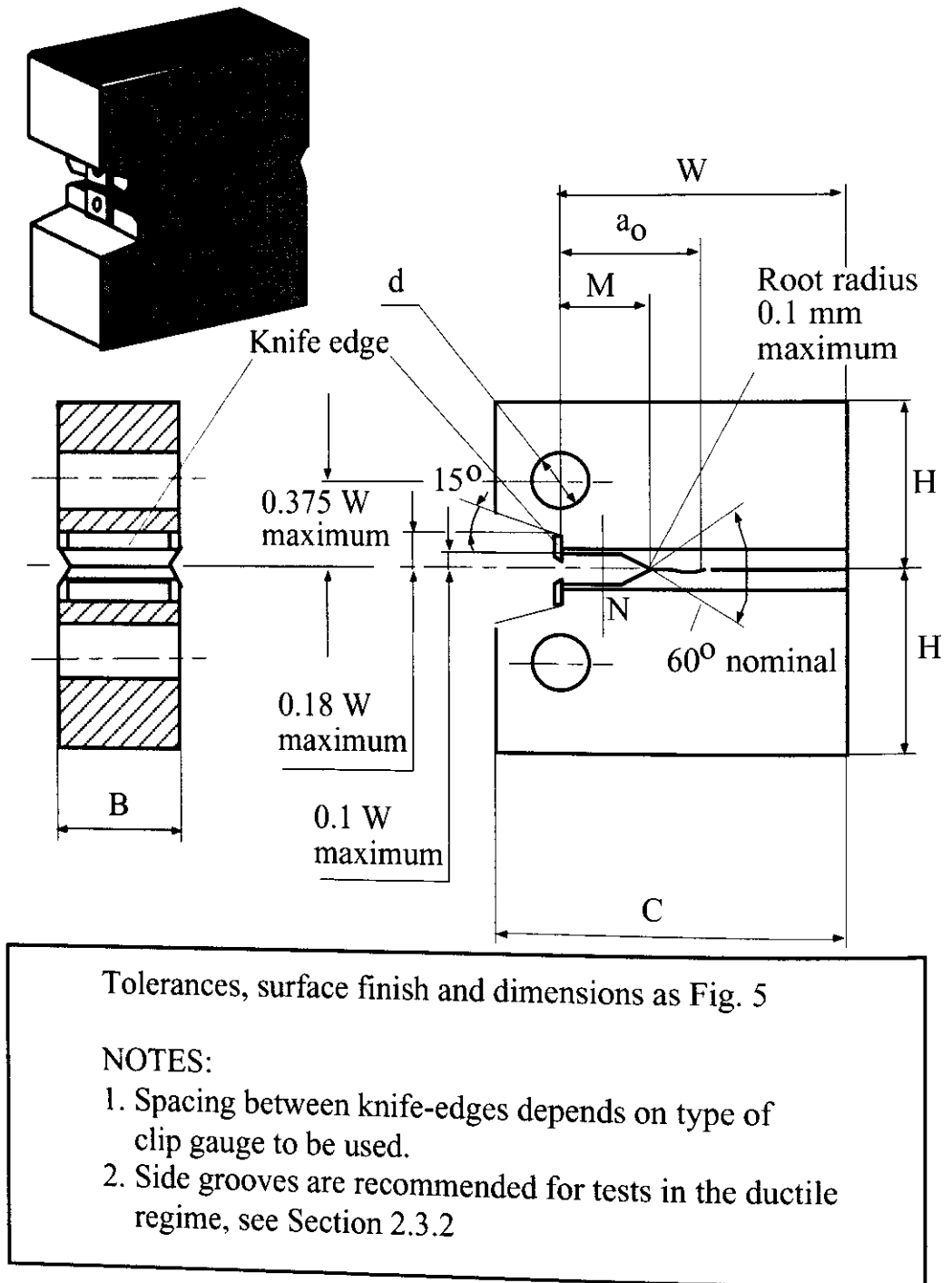
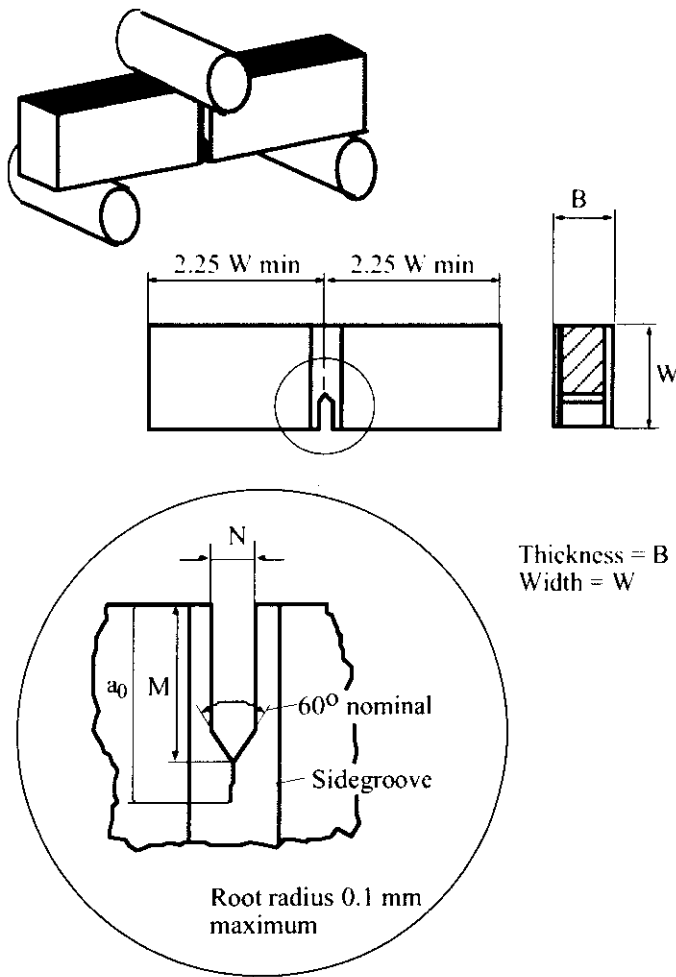


Figure 6: Step notched compact (C(T)) specimen.

The single edge cracked bend specimen is shown in Fig. 7. It can be tested either in three point or four point bending. Fig. 8 shows the middle cracked tension specimen.



Preferred width $W = 2 B$
 Notch width $N = 0.06W$ max. or
 1.5mm max. if $W \leq 25\text{mm}$
 Effective notch length
 $M = 0.4W$ min.
 Effective crack length
 $a_0 = 0.45W$ to $0.65W$.

NOTES:

1. A spark eroded or machined slit can be used instead of the V-notch profile.
2. Squareness and parallelism to be within $0.002W$.
 Notch to be square with specimen faces and notch faces to be parallel.
3. Side grooves are recommended for tests in the ductile regime, see Section 2.3.2

\sqrt{x} is the surface finish to $x \mu\text{m}$

Figure 7: Single edge cracked bend (SE(B)) specimen.

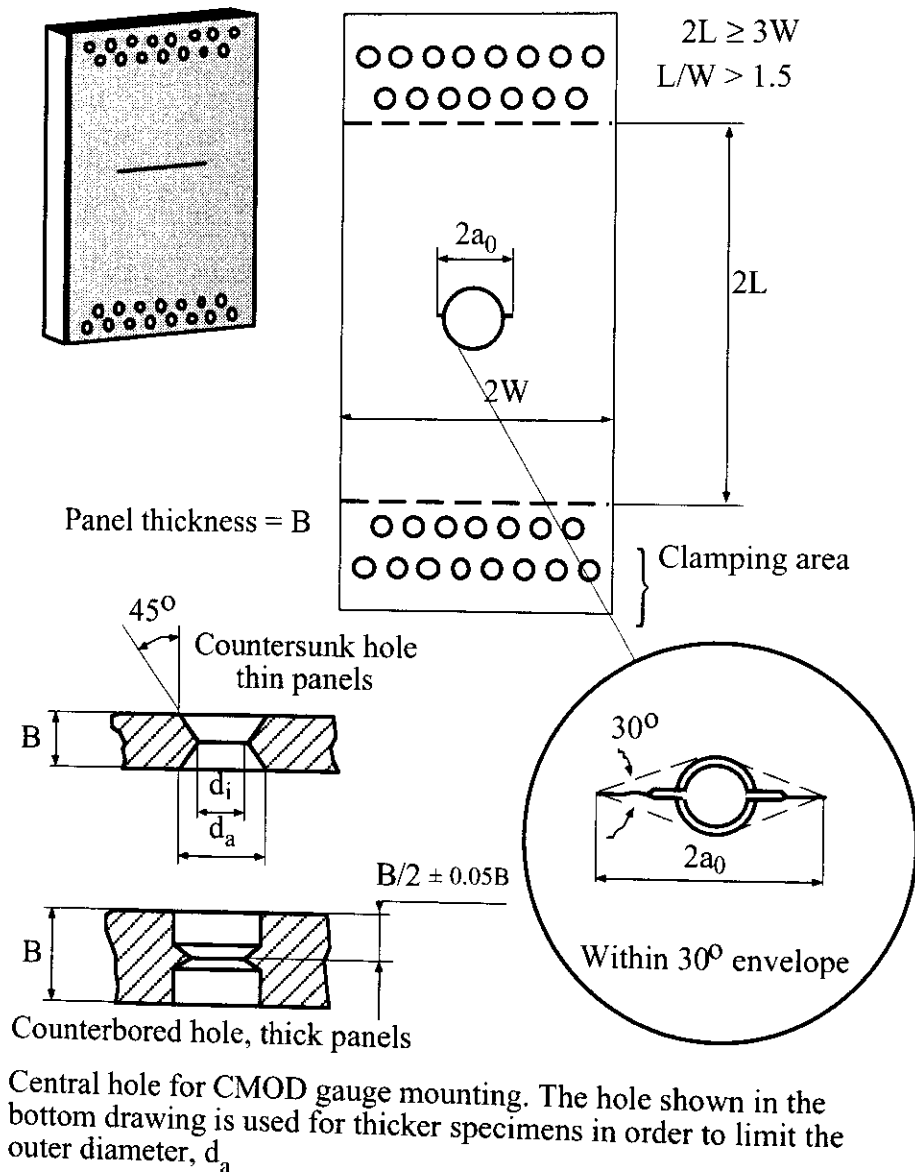
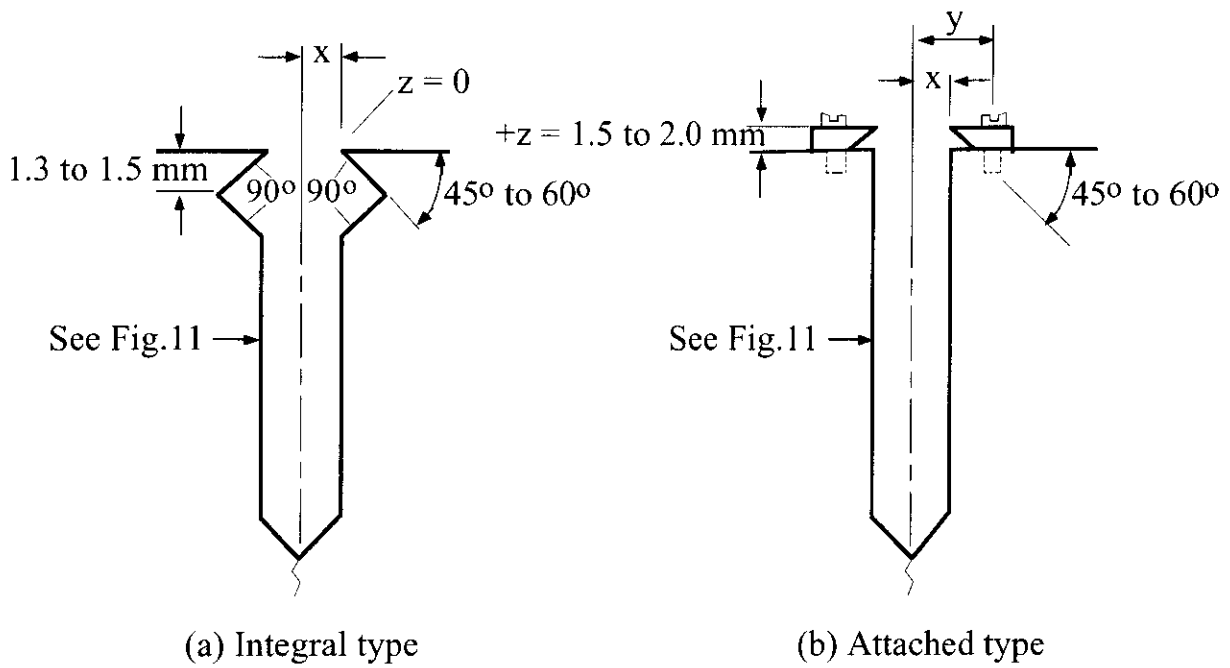


Figure 8: Middle cracked tension specimen.

Knife edges are used to define the gauge length and to attach a clip gauge for measuring the crack mouth opening displacement (CMOD). Specimen knife edges may be integral or attached. Suitable designs for compact and bend specimens are shown in **Figures 9** and **10**. The dimension $2x$ in **Figures 9** and **10** shall be within the working range of the crack mouth opening displacement gauge, and the knife edges shall be square with the specimen surfaces and parallel to each other within 0.5° . For both types, the crack mouth opening displacement gauge is to be free to rotate about the points of contact between the gauge and knife edge. Consequently, when inward pointing knife edges or stiff razor blades are used, it may be necessary to use an enlarged notch mouth, as shown in **Figure 6**. For middle cracked tension specimens the circular knife edge shown in **Figure 8** is recommended. The use of a knife-edge/clip gauge for displacement measurement does not preclude the use of other schemes providing they meet the requirements and accuracy of this method.

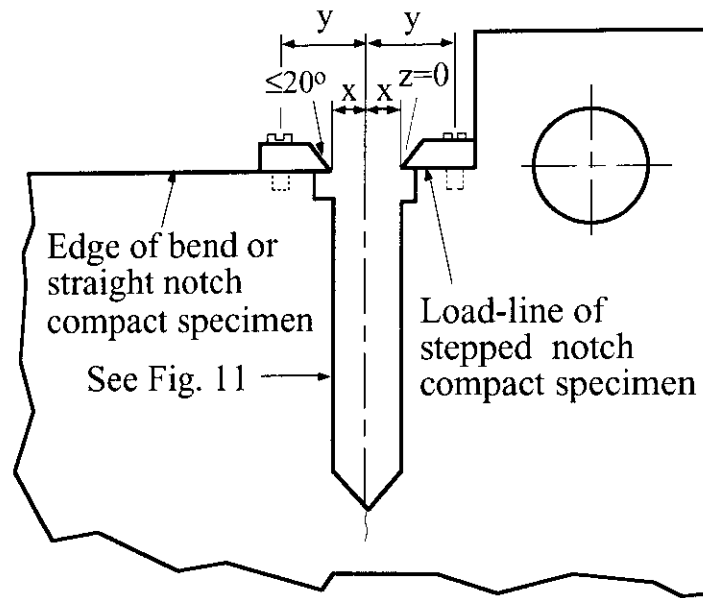


$$2y + \text{screw thread diameter} \leq W/2$$

NOTE:

If the knife edges are glued or similarly attached to the edges of the specimen, $2y$ = distance between extreme points of attachment.

Figure 9: *Outward pointing knife edges and corresponding notch geometries.*



$$2y + \text{screw thread diameter} \leq W/2$$

NOTES:

1. If the knife edges are glued or similarly attached to the edges of the specimen, $2y$ = distance between extreme points of attachment.
2. If razor blades are used instead of inward pointing knife edges, the displacement will normally be measured at a point half the razor blade thickness above the load line.

Figure 10: *Inward pointing knife edges and corresponding notch geometries.*

2.2 Dimensions

2.2.1 Geometrical Considerations

The dimensions of the test specimens shown in **Figs. 5 to 8** are characterised by the specimen width, W .

2.2.1.1 For tests aimed at achieving high constraint conditions (plane strain), compact and single edge cracked bend specimens with thickness B equal to $0.5 W$ are used. The specimen dimensions should satisfy the validity requirements appropriate to the parameter being measured. The thus determined fracture properties are insensitive to the size of the specimen.

Since these requirements depend on the measured properties, they can only be checked after the test has been completed. However, suitable specimen dimensions can be obtained before testing from an estimate of the maximum probable value of the fracture parameter.

Although no requirements for the determination of size insensitive fracture properties are available for M(T) specimens, this specimen type is included since it may be used to model structural situations not covered by **Section 8**. Specific B to W ratios are not suggested.

2.2.1.2 In cases when the size requirements mentioned in **2.2.1.1** cannot be met or are not needed, fracture properties can be determined which depend on thickness B, but are independent of the in-plane dimensions of the specimen.

For compact specimens $W = 8B$ and for middle cracked tension specimens $W = (8 \text{ to } 16) B$ depending on the initial crack length (see **2.3.1.1**). In these situations, the use of antibuckling guides is recommended (see **Section 3.3**). The use of single edge cracked bend specimens is not suitable.

2.2.1.3 All test specimens must be machined to within the tolerances given in **Figs. 5 to 8**.

2.3 Preparation

2.3.1 Fatigue Pre-cracking

2.3.1.1 A fatigue pre-crack must be produced in the test specimen from the end of the machined notch, **Figs. 5 to 8**, to give an initial crack length a_0 in the range $0.45 \leq a_0/W \leq 0.65$ for compact and single edge cracked bend specimens, and $0.25 \leq a_0/W \leq 0.40$ for the middle cracked tension specimen. Test specimens should contain initial crack lengths which are in reasonably close agreement with each other. Guidance for testing single edge cracked bend specimens with shallow cracks when $a_0/W \leq 0.45$ is given in **Appendix 12**.

NOTE: *Compact specimens should not be tested when $a_0/W < 0.45$.*

It is recommended that for those materials in which the ultimate to yield strength ratio, $R_m/R_{p0.2}$ exceeds 2, and stable crack extension is expected to occur, **Section 1.1.3**, the initial crack length in compact and single edge cracked bend specimens should tend towards the upper limit of a_0/W to ensure that plastic deformation is limited to the uncracked ligament.

2.3.1.2 The length of the fatigue pre-crack, or pre-cracks for the middle cracked specimen, must exceed the larger of $0.05 a_0$ or 1.5 mm. The notch geometry must be enclosed within a 30° included angle from the fatigue pre-crack tip, **Fig. 11**. For the middle cracked specimen, the fatigue pre-cracks should also be within $0.05 a_0$ or 1.5 mm, whichever is the greater, of each other.

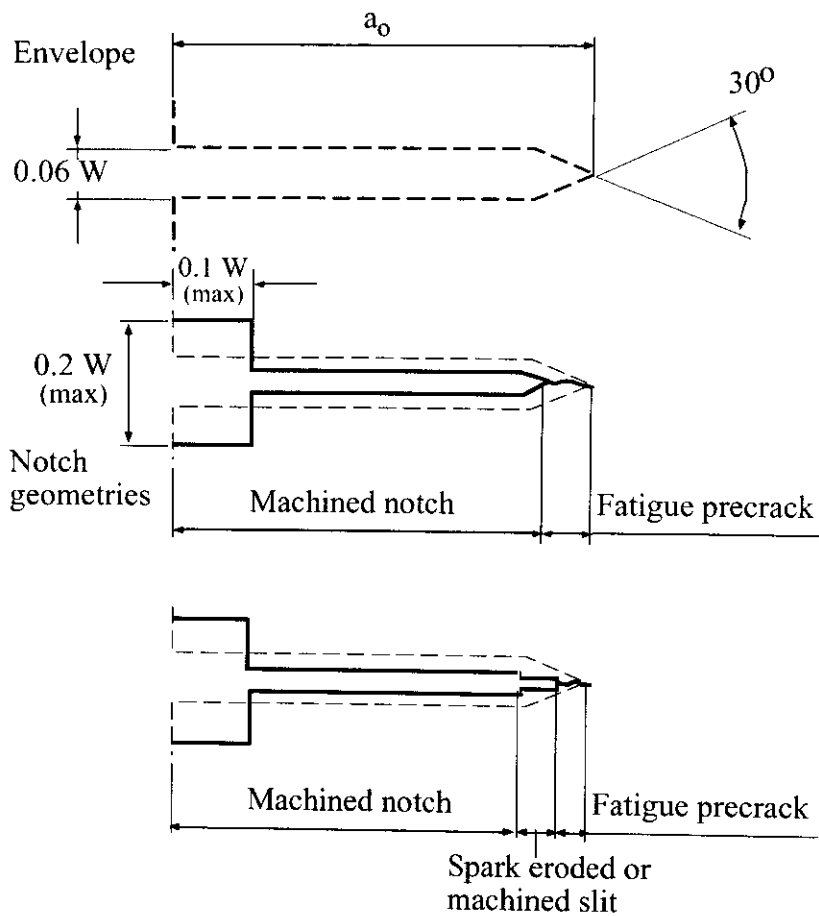


Figure 11:
Acceptable machined notch geometries.

- NOTES:
1. Machined notch width must not exceed 0.06W or 1.5mm if $W \leq 25\text{mm}$.
 2. The intersection of the notch surfaces with the two specimen sides shall be equidistant from the top and bottom of the specimen to within 0.005W

2.3.1.3 The maximum fatigue force, F_{\max} , must not exceed the lower of $0.6 F_Y$ or the force corresponding to a maximum stress intensity factor to Young's modulus ratio (K_{\max}/E) equal to or less than $1.5 \times 10^{-4} \text{ m}^{1/2}$.

The ratio of minimum-to-maximum load in the fatigue cycle shall be in the range 0 to 0.1.

The force F_Y , for a compact specimen, is given for the purposes of fatigue pre-cracking by

$$F_Y = \frac{B(W - a)^2}{(2W + a)} R_{p0.2},$$

for the single edge cracked bend specimen under three-point bending by

$$F_Y = \frac{4B(W - a)^2}{3S} R_{p0.2},$$

for the single edge cracked bend specimen under four-point bending by

$$F_Y = \frac{2.52B(W - a)^2}{\sqrt{3(S_1 - S_2)}}$$

and for the middle cracked tension specimen by

$$F_Y = 2(W - a)BR_{p0.2}.$$

For the significance of S, S₁ and S₂ see **Fig. 12**.

For materials which exhibit a linear force-displacement test record, **Fig. 4a**, use F_c defined in **Section 5.1.2**, instead of F_Y to check the fatigue pre-cracking requirements. F_c is only available after the test.

2.3.1.4 When the fatigue precracking of a specimen is performed at a temperature T₁, and then tested a temperature T₂, K_{max} given in **Clause 2.3.1.3** should be factored by the ratio (R_{p0.2})₁/(R_{p0.2})₂ where (R_{p0.2})₁ and (R_{p0.2})₂ are the yield strengths at the temperatures T₁ and T₂, respectively. In addition, F_Y should be evaluated from the lowest value of R_{p0.2} at the two temperatures.

2.3.1.5 The stress intensity factor K_{max} at force F_{max} is calculated from

$$K_{\max} = \frac{F_{\max}}{\sqrt{BB_n W}} f(a/W)$$

where the stress intensity function f(a/W) is defined in **Appendix 1**.

2.3.2 Sidegrooving

Sidegrooving is recommended for those compact and single edge cracked bend specimens which are expected to exhibit stable crack extension and a non-linear force-displacement record, **Fig. 4c**. When the test specimen thickness is less than the component thickness, it is recommended that the specimens are sidegrooved.

Sidegrooving is not recommended for middle cracked tension specimens.

2.3.2.1 Sidegrooving promotes straight fronted ductile crack extension during a test. Specimens should be sidegrooved after fatigue pre-cracking, although in some instances it may be advisable to have a shallow side groove to promote the fatigue crack extension in the original crack plane.

2.3.2.2 The sidegrooves must be equal in depth on both sides of the specimen and have an included angle of 30° – 90° with a maximum root radius of 0.1 mm. A Charpy V-notch cutter provides a suitable profile. The depth of sidegrooving, $B - B_n$, must exceed 0.10 B and must not exceed 0.25 B where B_n is the net section thickness. For most materials, 20 percent total sidegrooving is recommended.

2.3.3 Measurements

Prior to testing, measure the thickness B, net section thickness B_n , if applicable, and W, as shown in **Figs. 5 to 8**. The accuracy of measurement shall be better than 0.05 mm.

NOTE: *Sidegrooving may significantly affect crack extension resistance.*

3 TEST REQUIREMENTS

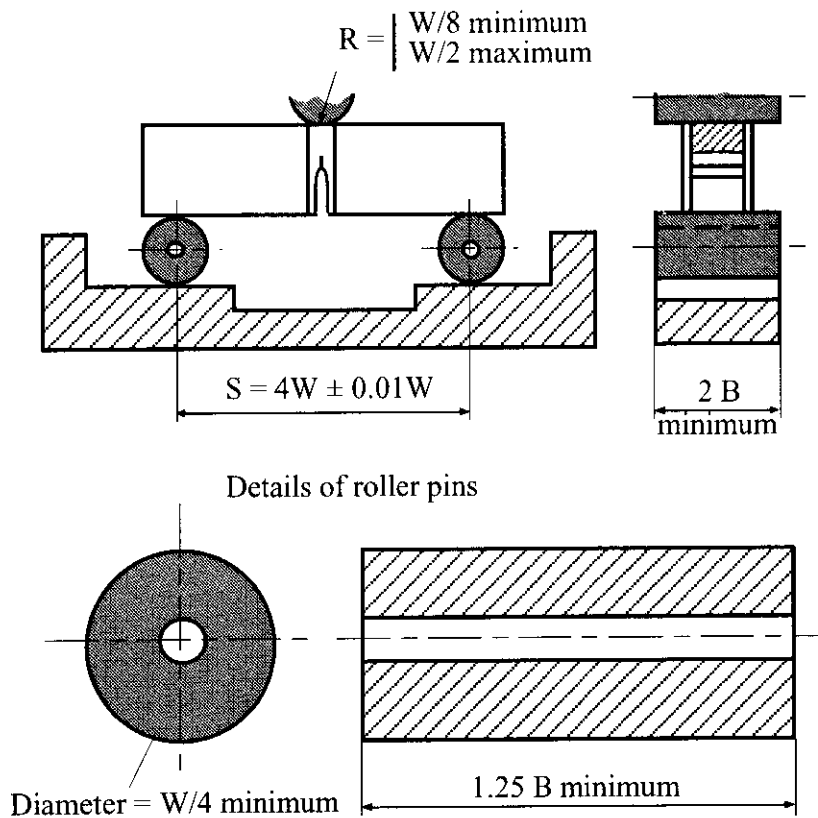
3.1 Test Machine

The test machine must incorporate a rigid loading frame, and a force transducer to provide an autographic recording of the force applied to the specimen. The test machine should be capable of operating at both constant force and displacement rates.

3.2 Test Fixtures

The test fixtures must be designed to be as rigid as practicable. **Fig. 12a** shows a suitable loading frame for three-point bending of a single edge cracked bend specimen. **Fig. 12b** shows the arrangement for four point bending. In both cases, the lower support rollers must be free to move outwards. **Fig. 13** shows a suitable clevis design for the compact specimen. Other testing fixtures can be used providing care is taken to minimise roller indentation and frictional effects between the specimen and fixture.

Figure 12a:
Three point bend fixture
for SE(B) specimen.



NOTES:

1. Roller pins and specimen contact surface of loading ram must be parallel to within 1 degree.
2. Rollers must be free to move outwards.
3. Fabricate fixture from a high strength material sufficient to resist plastic deformations in general use.

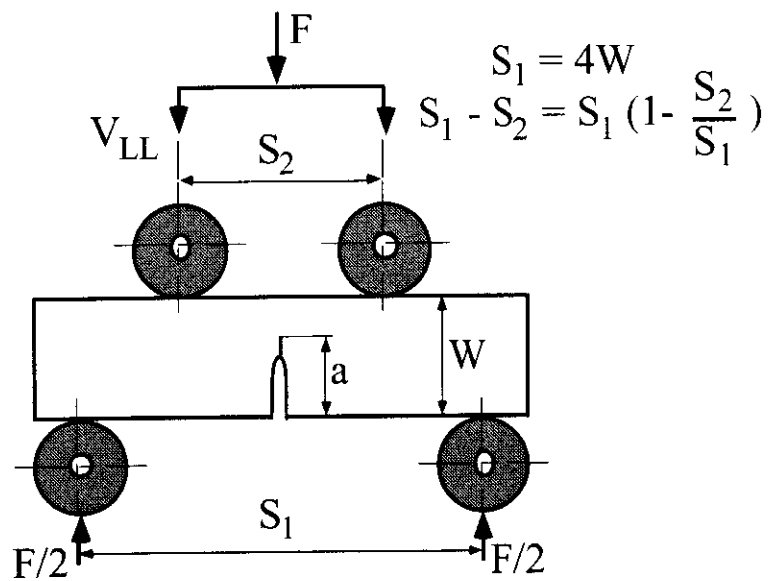
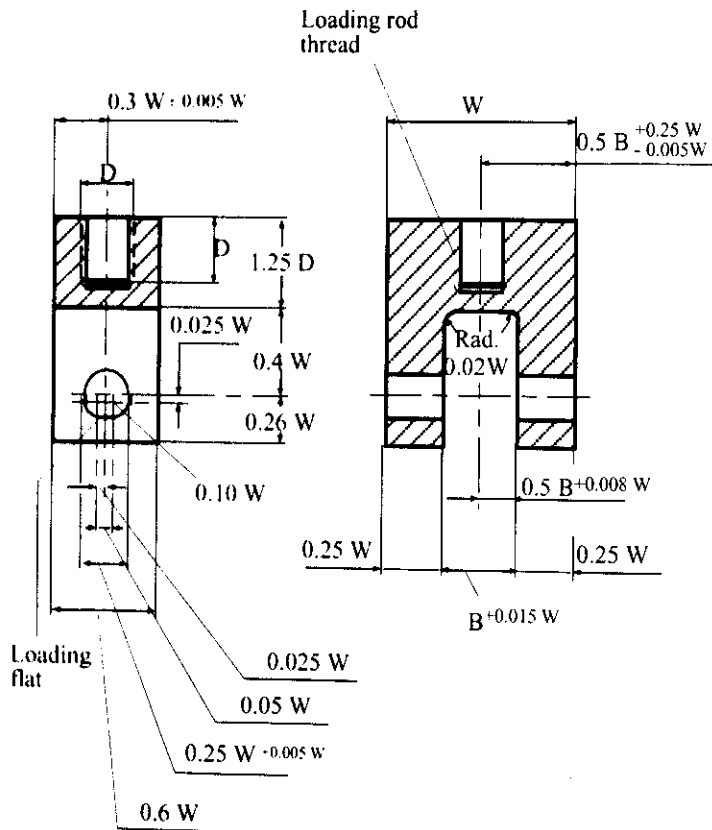


Figure 12b:
SE(B) specimen under
four point bending.



NOTES:

1. Thickness B usually 0.5W, see Section 2.2.1.
2. Loading pin diameter = $0.24W \begin{matrix} +0 \\ -0.005W \end{matrix}$
3. Surface must be flat, in-line and perpendicular as applicable, to within 0.002W.
4. Hardened steel or ceramic inserts in the clevis at the loading flats can be used to reduce indentation.
5. Fabricate pins and clevises from a high strength steel sufficient to resist plastic deformations in general use.
6. The loading pinhole diameter and the width of the loading flat may need increasing for austenitic steels.

Figure 13: Clevis for C(T) specimen testing.

The fixture for the middle cracked tension specimen should be designed to distribute the load uniformly over the cross-section of the specimen. The fixture may be rigidly connected to the machine if uniform loading of the specimen in the machine can be achieved at all loads. Otherwise, pin-loading via detachable grips is recommended, Fig. 14.

3.3 Prevention of Buckling

If specimens with $(W-a_0) \geq 4B$ are to be tested, then it is recommended that anti-buckling plates should be attached to both sides of a specimen covering the expected path of the crack. Frictional forces between the specimen and the plates should be reduced to a minimum with the use of a non-corrosive lubricant such as Teflon® applied to the mating surfaces. An access hole is required in one of the plates for mounting the displacement CMOD and δ_5 gauges onto the specimen or, if the potential method is used, for the attachment of cables. Suitable arrangements are shown in Figs. 15 and 16.

Figure 14:

Examples of fixed and pin-loaded grips for M(T) specimens.

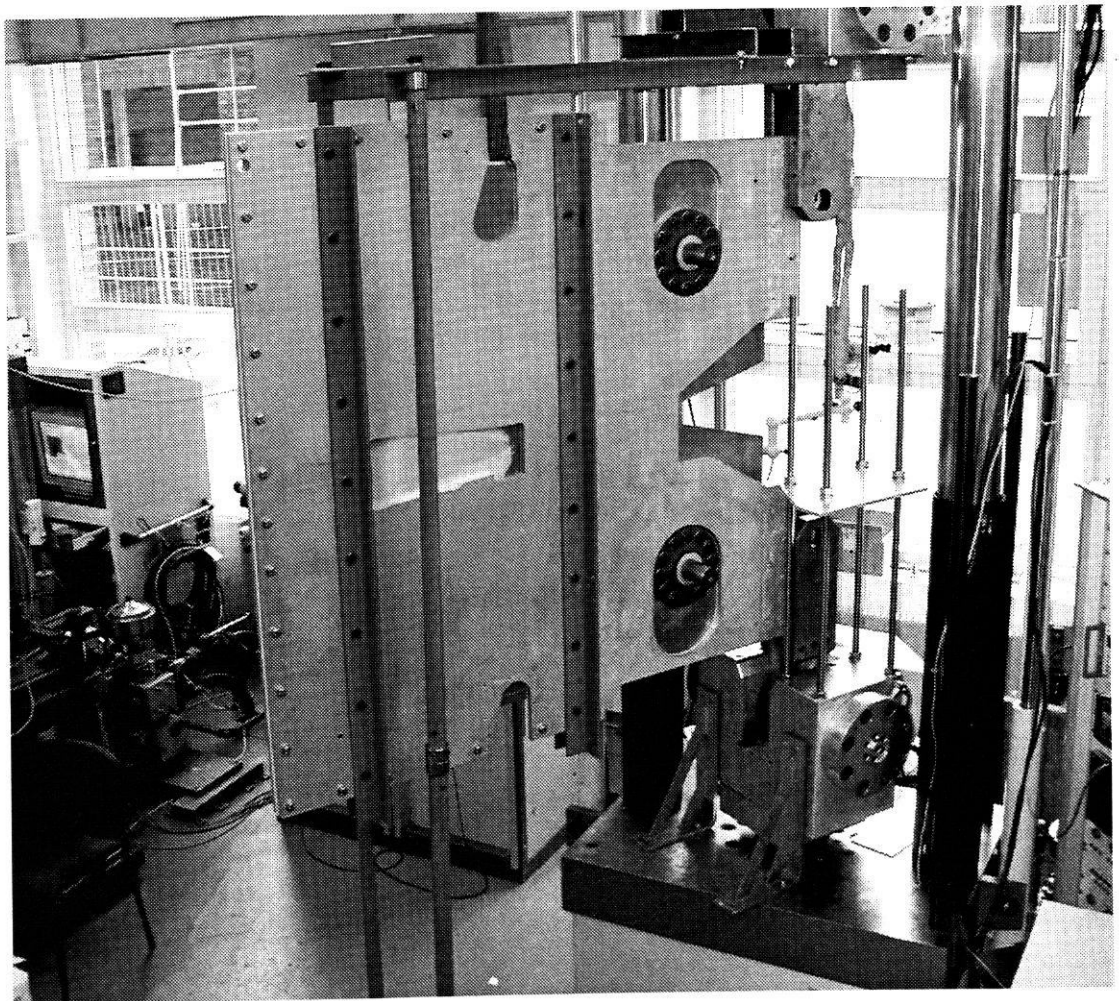
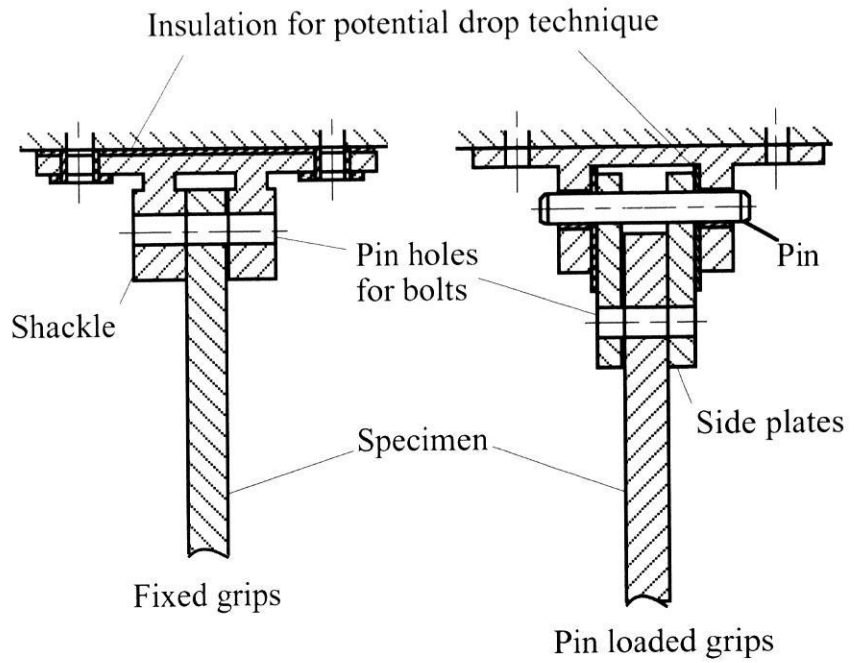


Figure 15: *Suggested design for C(T) anti-buckling guides.*

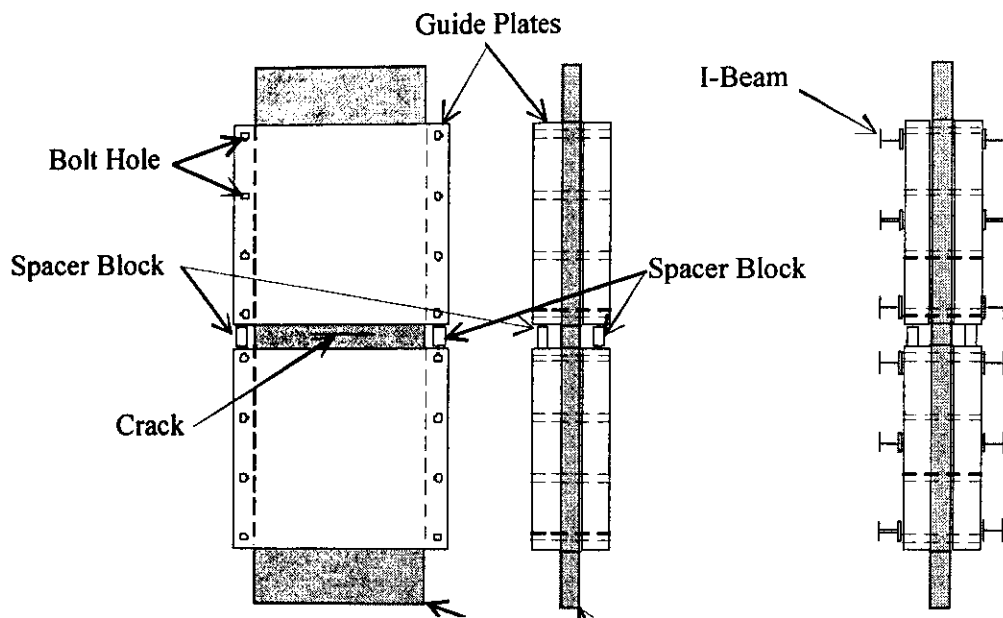


Figure 16: Suggested design for $M(T)$ anti-buckling guides.

3.4 Displacements

The fracture toughness in terms of K is evaluated from the applied force F . The force can be measured relative to either the load-point displacement q , or the crack mouth opening displacement V .

The fracture resistance J is evaluated from either the load-point displacement q or the CMOD. The crack tip opening displacement δ_5 is obtained explicitly in this Procedure.

3.4.1 Load-Point Displacement

When testing compact specimens, usually, the load-line displacement measured between knife edges placed between the pin holes, Fig. 6, is taken as a measure of load-point displacement. For compact specimens which do not permit measurement of the load-line displacement, Fig. 5, the relationship between the measured displacement and the load-line displacement must be established so that load-line values can be inferred.

When testing single edge cracked bend specimens, it is important to exclude extraneous displacements arising from system compliance and load-point indentations. Suitable methods for measuring load-point displacements without extraneous displacements are referenced in Appendix 2. Other methods can be used provided the extraneous displacement arising from indentation effects and elastic deformation on the fixture are determined and subtracted from the measured displacement.

When testing middle cracked tension specimens the load-point displacement is measured between two points close to the grip attachment area, Fig. A4.3. The fracture resistance J can also be determined from CMOD, Appendix 3.

3.4.2 Crack Mouth Opening Displacement (CMOD)

For the step notched compact specimen shown in **Fig. 6**, the CMOD corresponds to the load-point displacement. If the knife edges are not located at the load-line, the CMOD is measured between knife edges at a distance z from the load-line in the direction away from the crack tip, **Fig. 5**.

In the case of the single edge cracked bend specimen, the CMOD can be measured between knife edges at a distance z from the specimen surfaces, **Fig. 17**.

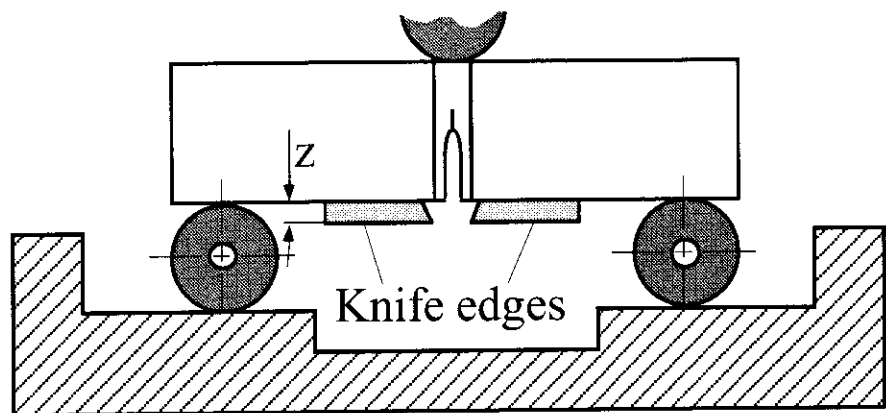


Figure 17: Position of knife edges for measuring mouth opening displacement on the SE(B) specimen.

For the middle cracked tension specimen, the CMOD can be measured between the circular knife edge in the countersunk hole shown in **Fig. 8**. Further details are given in **Appendix 3**.

3.4.3 Crack Tip Opening Displacement, CTOD (δ_5)

The crack tip opening displacement, δ_5 , is measured directly between two points at the surface of the specimen close to the crack tip. The points are located 5 mm apart across the crack plane and normal to the tip position. Further details are given in **Appendix 4**.

3.5 Accuracy of Transducers

The force and displacement transducer accuracy and reproducibility must be within ± 1 percent of the measured value or 0.2 percent of the range encountered during the test, whichever is the greater. Linearity must be within ± 0.5 percent of the transducer range encountered during the tests. Accuracy, reproducibility and linearity should be evaluated at the temperatures experienced by the transducers during the test.

3.6 Test Temperature

Specimen test temperature shall be controlled and recorded to an accuracy of ± 2 °C. For this purpose, a thermocouple or platinum resistance thermometer shall be placed in contact with the surface of the specimen in a region not further than 5 mm from the crack tip. Tests shall be made in situ in suitable low or high temperature media. Before testing in a liquid medium, the specimen shall be retained in the liquid for at least 30 s/mm of thickness B after the specimen surface has reached the test temperature. When using a gaseous medium, a soaking time of at least 60 s/mm of thickness shall be employed. Minimum soaking time at the test temperature shall be 15 min.

Throughout the test the temperature must also remain within this limit. Report the time at test temperature as required in **Section 9.3**.

3.7 Specimen and Fixture Alignment

For compact specimen testing, the centre-lines of the upper and lower clevises must be within the smaller of 0.03B or 1 mm of each other and within the smaller of 0.03B or 1 mm of both the specimen hole centre-line and the specimen mid-thickness centre-line.

For single edge cracked bend specimen testing under three-point bending, the centre-line of the upper roller must be midway between the centre-lines of the lower rollers to within 0.5 percent of the distance between the lower rollers. The axes of the rollers must be parallel to within 1 degree of each other. The specimen must be aligned in the testing fixture so that the fatigue pre-crack is midway between the centre-lines of the lower rollers to within 1 percent of the distance between the lower rollers. In addition, the length of the specimen must be within 2 degrees perpendicular to the axes of the rollers. Similar requirements apply for four-point bending accordingly.

For middle cracked tension specimen testing, the centre lines of the upper and lower loading shackle, **Fig. 14**, must be within the smaller of 0.03B or 1 mm of each other and within the smaller of 0.03B or 1 mm of the specimen mid-thickness centre line. To avoid load being transferred via the anti-buckling guides to the specimen, the rods must not be rigidly fixed to the grips.

4 TEST PROCEDURE

The test shall be carried out under either crack mouth opening, load-line or cross-head displacement control. The force-displacement data and the amount of crack extension are required to evaluate the fracture behaviour of a specimen.

4.1 Test Method

4.1.1 Measure and record the force displacement behaviour of the specimen at a rate such that the rate of the initial increase of the stress intensity is in the range 0.55 to 2.75 MPa m^{1/2}/s. Use the stress intensity factor defined in **Section 2.3.1.3** of this Procedure to determine the rate.

4.1.2 Continue the test until unstable fracture occurs or the specimen reaches a pre-determined amount of displacement.

4.1.3 If unstable fracture occurs, measure the initial crack length and stable crack extension as described in **Section 4.2**. Evaluate the fracture parameters, as appropriate, using the procedures given in **Sections 5** and **6**.

4.1.4 If only stable crack extension occurs, then the crack extension must be measured as described in **Section 4.3**, or inferred from single specimen methods described in **Appendix 5**. Evaluate the fracture parameters using the procedure given in **Section 7**. Additional specimens may be tested using the multiple specimen method.

4.2 Crack Length Measurements

Measurements of crack length are made using multi-point weighted average methods. Difficulties may arise in measuring highly irregular crack fronts such as spikes or regions of disconnected crack extension. For these situations, it may only be practicable to estimate the crack length by ignoring the spikes or subjectively averaging the crack extension regions. These irregularities must be noted in the report.

The method used to measure crack length and irregular crack fronts must be reported in **Section 9.3**.

4.2.1 In compact specimens, the initial crack length a_0 corresponds to the distance between the centre-line of the loading-pin holes and the end of the fatigue pre-cracked zone, **Fig. 18**. In the single edge cracked bend specimen, the initial crack length a_0 corresponds to the distance between the front surface and the end of the fatigue pre-cracked zone, **Fig. 19**.

In middle cracked tension specimens the initial crack length a_0 corresponds to half of the distance between the ends of the two fatigue pre-cracked zones, **Fig. 20**.

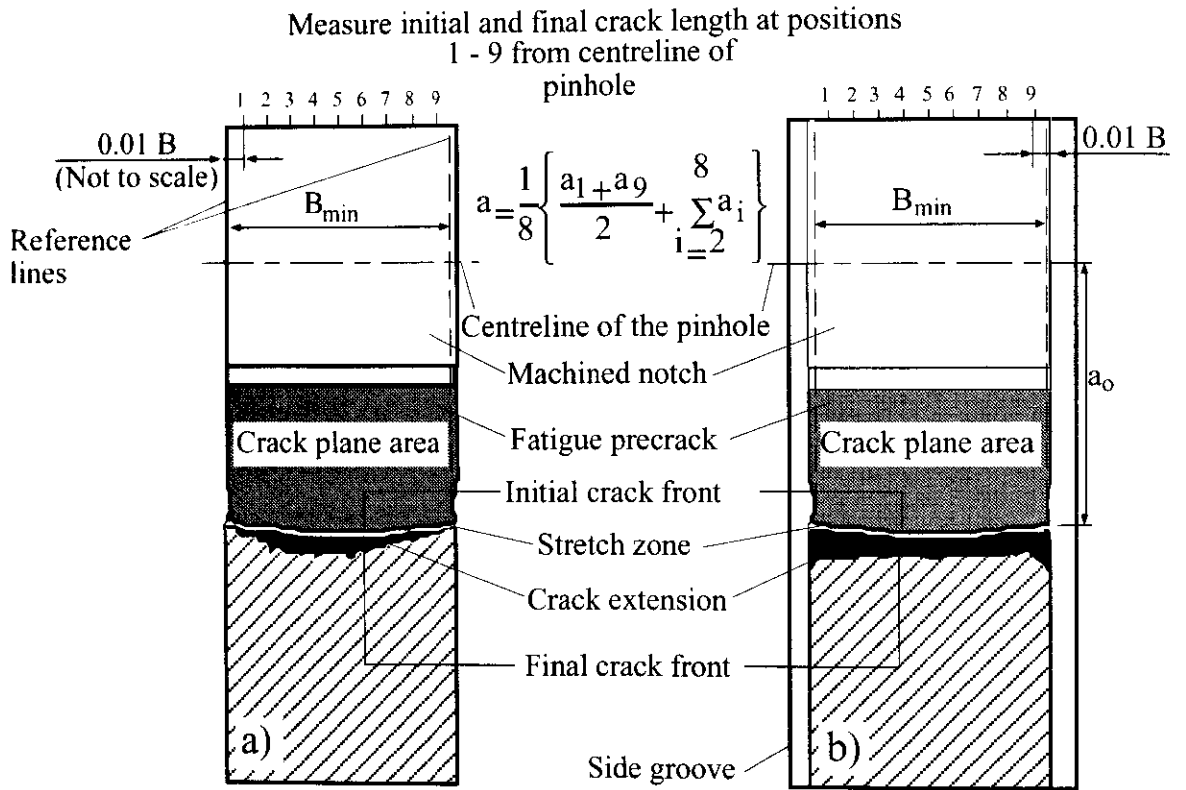


Figure 18: Measurement of crack lengths on C(T) specimens:
a) Plane sided specimens; b) Side grooved specimens.

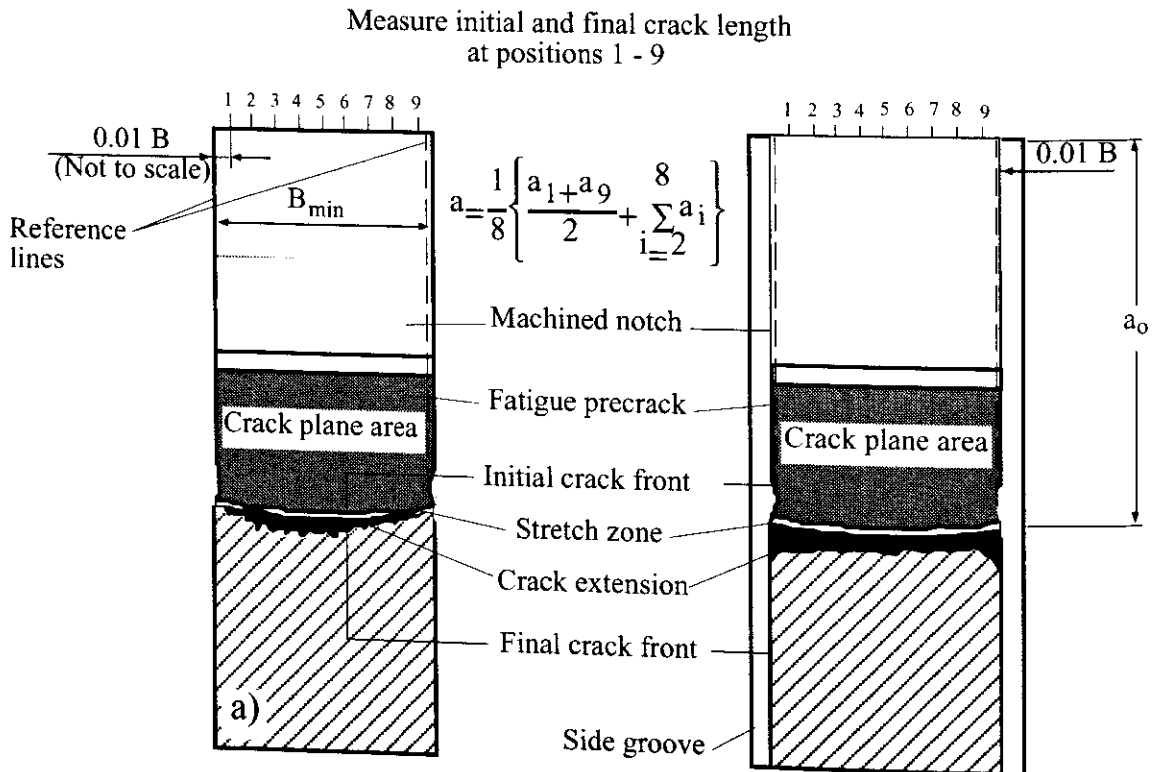


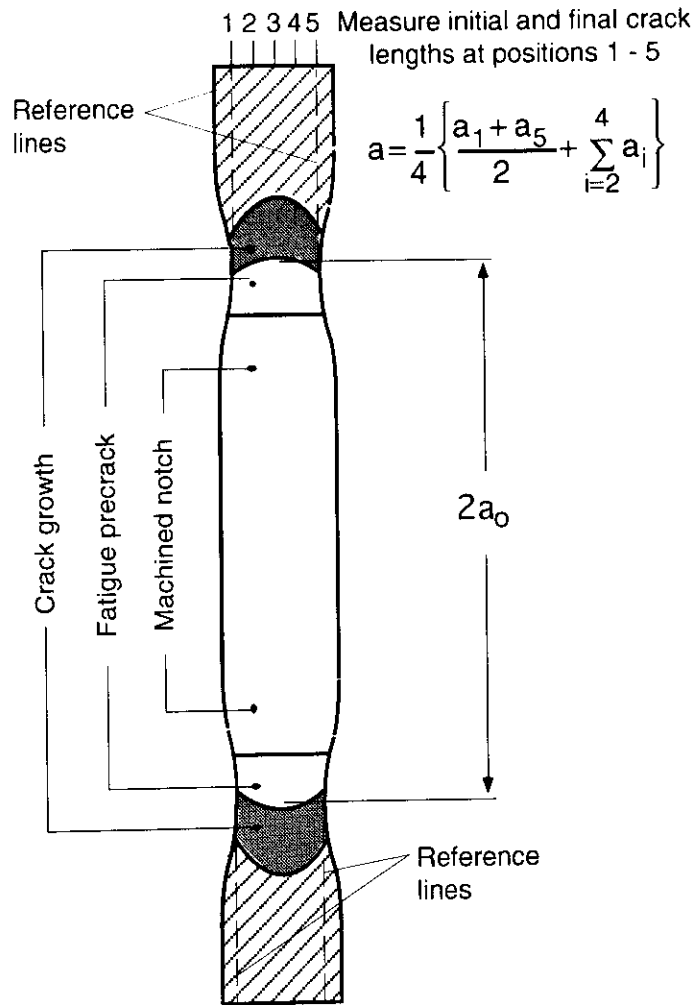
Figure 19: Measurement of crack lengths on SE(B) specimens:
a) Plane sided specimens; b) Side grooved specimens.

Figure 20:

Measurement of crack length on M(T) specimens.

The same procedure is used as outlined in **Figs. 18 and 19**.

The average of both cracks represents the crack length of the M(T) specimen.



4.2.2 Initial crack length is measured to an accuracy of 0.25 percent or 0.05 mm, whichever is the greater, between two reference lines defined at the minimum thickness positions as shown in **Figs. 14 to 16**. The measurements are made at 9 equi-spaced points where the outer points are located at 0.01B from the reference lines. The value of a_0 is obtained by firstly averaging the two measurements at 0.01B from the surfaces and then averaging this value with the 7 inner measurement points. If the difference between a_0 and any of the individual measurement points contributing to a_0 exceeds ± 10 percent, then report non-uniform fatigue pre-crack extension as required in **Section 9.3**.

4.2.3 Measure to an accuracy of 0.25 percent or 0.05 mm, whichever is the greater, the minimum difference between the initial crack length and the start of each fatigue pre-cracked zone, as appropriate. If a zone does not exceed the larger of 0.05 a_0 or 1.5 mm, then report insufficient fatigue pre-crack extension as required in **Section 9.3**. For middle cracked tension specimens, if the difference between the two zones exceeds the larger of 0.05 a_0 or 1.5 mm, then report non-symmetric fatigue pre-crack extension as required in **Section 9.3**.

4.2.4 If appropriate measure the total crack extension Δa between the initial and final crack fronts to an accuracy of 0.05 mm using the averaging procedure described in **Section 4.2.2**. For the middle cracked tension specimen the crack extension Δa is the average value obtained ahead of both initial crack fronts. If the difference between the extension ahead of the crack fronts exceeds 30 %, then report non-symmetric crack extension in **Section 9.3**.

4.2.5 Measure the maximum and minimum crack extension between measurement positions 1 to 9, **Figs. 18 to 20**. If the difference is greater than 20 percent of the average crack extension Δa , or 0.15 mm, whichever is the greater, then report non-uniform crack extension as required in **Section 9.3**. For the middle cracked tension specimen, treat the extension ahead of each crack front separately.

4.2.6 Examine the fracture surfaces for evidence of arrested unstable crack extension regions ahead of the fatigue pre-crack and any other unusual features on the fracture surfaces. Record the number of regions and associated fracture appearance as required in **Section 9.3**.

4.3 Multiple Specimen Method

The multiple specimen method the testing of several nominally identical specimens to provide the data distribution specified in **Sections 7.4, 7.8, and 7.9**, as appropriate. Usually one specimen is required to give an indication of the displacement needed to obtain the maximum crack extension allowed by this Procedure.

4.3.1 Load a specimen to a displacement just beyond the maximum force attainable, then reduce the force to zero allowing no further increase in displacement. It may not always be possible to use the result from this specimen in the data analysis.

4.3.2 Mark the extent of ductile crack extension by either post test heat tinting or fatigue cracking. The fatigue cracking should be performed at an R-ratio greater than 0.6 to avoid damage to the fracture surfaces from crack closure effects. The maximum fatigue force should not exceed three quarters of the final force measured during the test.

4.3.3 Break open the specimen at or below room temperature to reveal the fracture surfaces. Measure the crack extension as described in **Section 4.2** and evaluate J, if required, using the procedure given in **Section 7.2**.

4.3.4 Repeat the test procedure with further specimens terminating each test at the displacement judged to give crack extension satisfying the requirement given in **Sections 7.4, 7.8, and 7.9**, as appropriate.

4.3.5 Only data satisfying the crack extension criteria, Δa_{\max} , given in **Section 7.3**, can be used in subsequent analysis of the data.

5 FRACTURE TOUGHNESS K_{Ic} UNDER LINEAR ELASTIC CONDITIONS

The procedure to evaluate the linear elastic fracture toughness K_{Ic} from compact and single edge cracked bend specimens which exhibit an essentially linear force-displacement record, **Fig. 4a**, prior to unstable fracture is described in this section. An equivalent requirement for the middle cracked tension specimen has not yet been established. Consequently, the middle cracked tension specimen cannot be used to evaluate K_{Ic} of a material.

5.1 Interpretation of Test Record

Examples of three typical force-displacement records are shown in **Fig. 21**.

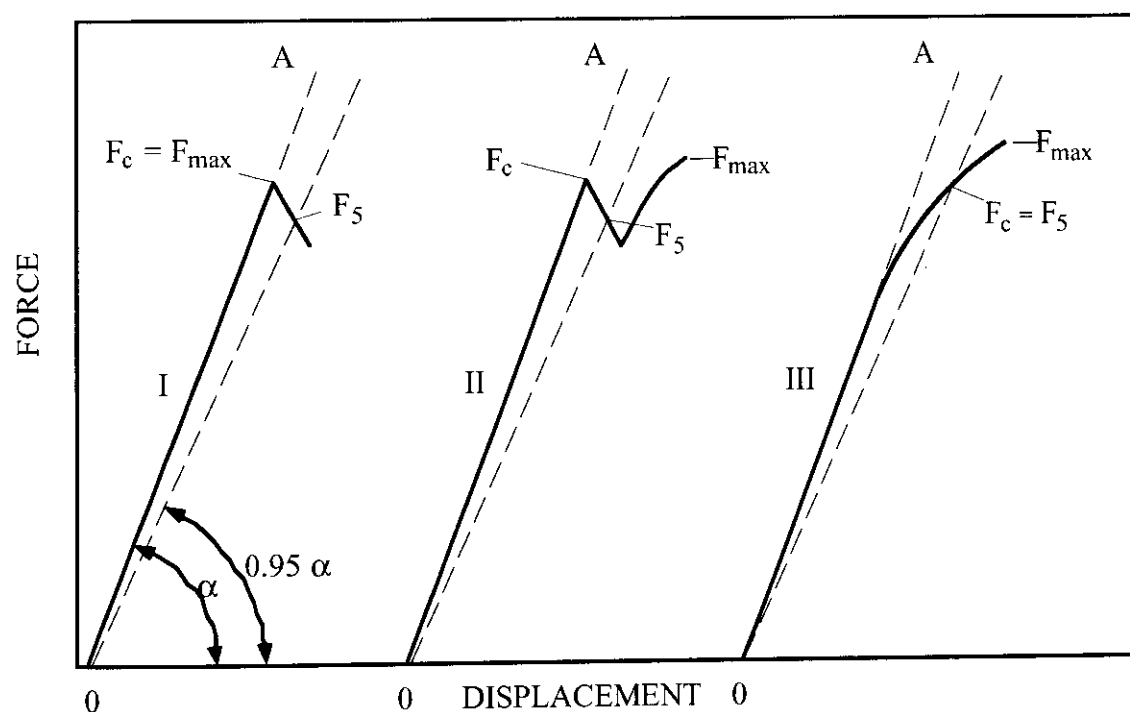


Figure 21: Typical force-displacement records.

5.1.1 Construct a tangent OA to the linear portion of the force-displacement record, ignoring any slight initial non-linearity, and measure the slope, m , of OA. Construct a line of reduced slope $0.95 m$ through the intercept of the tangent and the displacement axis. The intercept of the tangent with the test record is defined as F_5 , **Fig. 21**.

5.1.2 The force F_c used to evaluate K_c is defined in relation to F_5 depending on the type of test record, **Fig. 21**. For type I and II test records, F_c is the highest force that precedes F_5 . For type III record F_c equals F_5 .

5.1.3 Calculate the ratio F_{max}/F_c where F_{max} is the maximum sustained force, **Fig. 21**. If the ratio exceeds 1.10, then the test record is considered non-linear and either the fracture parameters δ_{5c} , δ_{5u} , δ_{5uc} or J_c , J_u , J_{uc} should be evaluated, **Section 6**.

5.2 Parameter K_c

If F_{\max}/F_c is less than or equal to 1.10, then calculate K_c from

$$K_c = \frac{F_c}{B\sqrt{W}} f(a_o/W)$$

where the stress intensity function $f(a_o/W)$ is defined in **Appendix 1**. For side grooved specimens replace B with $\sqrt{BB_n}$ where B_n is the net section thickness.

5.3 Validity Requirement

The validity requirement can only be applied to K_c values obtained from compact and single edge cracked bend specimens.

5.3.1 Calculate K_{\max} from the smaller of

$$K_{\max} = R_{p0.2} \sqrt{\frac{a_o}{2.5}}$$

$$K_{\max} = R_{p0.2} \sqrt{\frac{W - a_o}{2.5}}$$

and

$$K_{\max} = R_{p0.2} \sqrt{\frac{B}{2.5}}$$

where $R_{p0.2}$ is the yield strength at test temperature.

5.3.2 If K_c is less than K_{\max} , then K_c can be designated K_{Ic} , the linear elastic fracture toughness.

5.3.3 Guidance for statistical treatment of scattered data is provided in **Appendix 10**.

5.3.4 If K_c is greater than K_{\max} , then a fracture parameter according to **Section 6** can be determined.

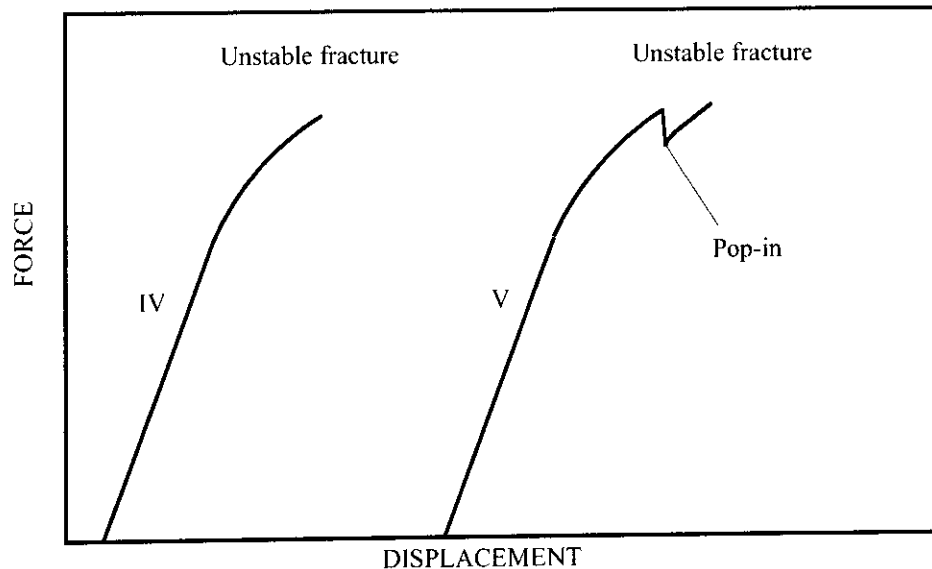
6 FRACTURE PARAMETERS δ_{5c} , J_c , δ_{5u} , J_u AND δ_{5uc} , J_{uc}

The procedure to evaluate δ_{5c} , J_c ; δ_{5u} , J_u and δ_{5uc} , J_{uc} from specimens which exhibit a non-linear force-displacement record, **Fig. 4b**, prior to unstable fracture, is described in this

section. This type of test record is usually exhibited by materials in the ductile-brittle transition region.

Examples of typical test records are shown in **Fig. 18**. Type V has a pop-in step in the force-displacement record prior to unstable fracture. The pop-in is usually characterized by either an abrupt force drop or sudden increase in displacement. The behaviour is associated with the initiation and arrest of a rapidly moving crack during unstable crack extension which often appears as a distinct brittle thumbnailed region on the fracture surface of a specimen. In order to interpret type V test records, **Fig. 22**, it is necessary to assess the significance of a pop-in and relate the number of pop-in steps to the number of thumbnailed regions on the fracture surface, **Section 4.2.6**.

Figure 22:
Typical force-displacement records.



For those cases where the amount of stable crack extension cannot be measured prior to unstable fracture, δ_5 and J are designated δ_{5uc} and J_{uc} , respectively. The subscript uc means the parameter is evaluated for an unknown amount of crack extension. Fracture in this regime may result in large scatter. Guidance for statistical treatment is given in **Appendix 10**.

6.1 Significance of a Pop-in

6.1.1 Evaluate the load drop f_i/F_i and displacement increase d_i/D_i , **Fig. 23**, at each pop-in. If both the force drop and displacement increase are less than 1 percent, then the pop-in step is considered insignificant.

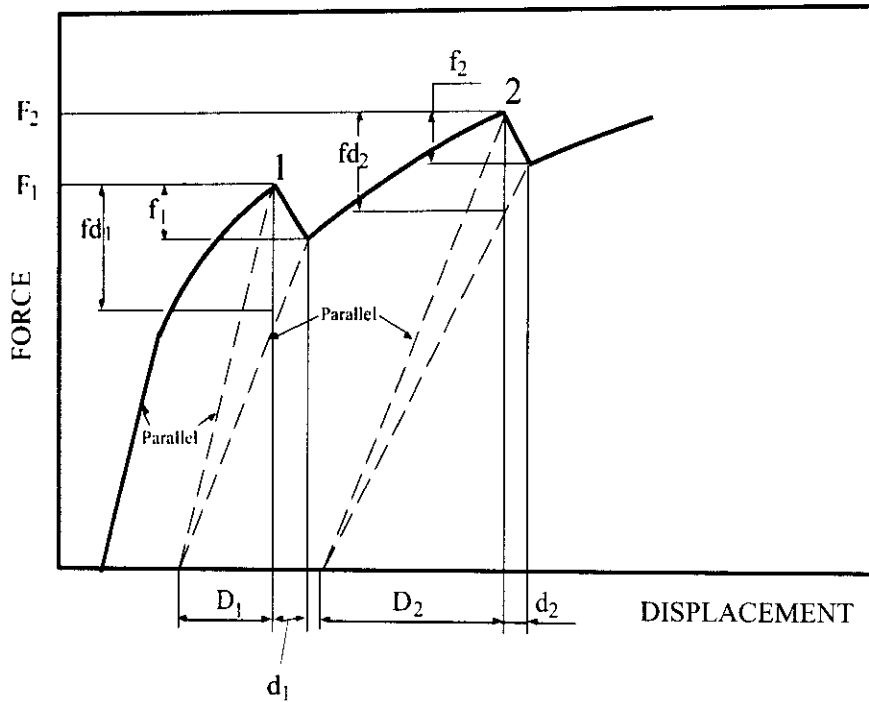


Figure 23:
Assessment of pop-in step behaviour.

6.1.2 For those pop-in steps not satisfying the requirement given in Section 6.1.1, calculate the percentage force drop at the i^{th} pop-in using the equation

$$\frac{fd_i}{F_i} = 1 - \frac{D_i}{F_i} \left\{ \frac{F_i - f_i}{D_i + d_i} \right\}$$

where the terms are defined in Fig. 23. If fd_i/F_i exceeds 5 percent then the pop-in step is considered significant. Then at this point the fracture parameter has to be evaluated as per Section 6.4.

6.1.3 Record the number of insignificant and significant pop-in steps as required in Section 8.3.

6.2 Fracture Parameter δ_5

6.2.1 The crack tip opening displacement, δ_5 is measured directly in this Procedure, Section 3.4.3. Measure δ_5 at either the unstable fracture point or the first significant pop-in step.

6.2.2 Calculate $\delta_{5,\text{max}}$ from the smaller of

$$\delta_{5,\text{max}} = \frac{(W - a_0)}{30}$$

and $\delta_{5,\text{max}} = \frac{B}{30}$.

6.2.3 If δ_5 does not exceed $\delta_{5,max}$, then δ_5 characterises the fracture process for the specimen tested.

6.3 Fracture Parameter J

6.3.1 C(T) and SE(B) specimens

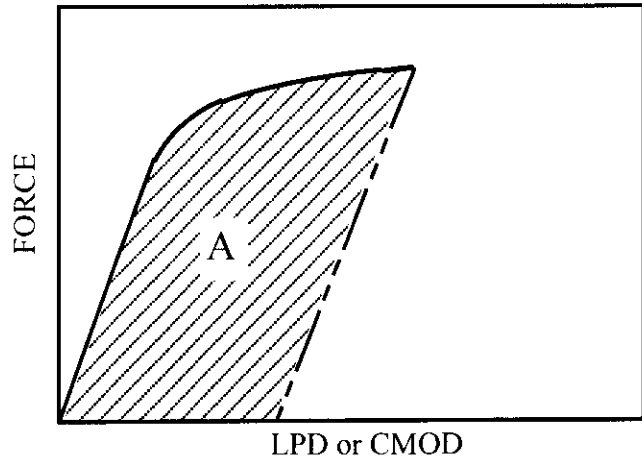


Figure 24: Definition of A.

6.3.1.1

- (i) Measure the area A under the force versus load point displacement (LPD) or crack mouth opening displacement record up to a line parallel to the initial slope, **Fig. 24**, corresponding to either the unstable fracture point or the first significant pop-in step.
- (ii) Calculate J_o using the relationship

$$J_o = \frac{K^2}{E(1-\nu^2)} + \frac{\eta_{pl}}{B(W-a_o)} A$$

where

$$\eta_{pl} = \begin{cases} 2 + 0.522 \left(1 - \frac{a_o}{W}\right) & \text{for C(T) specimens} \\ 2, & \text{for SE(B) specimens} \end{cases}$$

when the LPD is used for determining A,

$$\begin{aligned} &= 3.724 - 2.244 \frac{a_o}{W} + 0.408 \left(\frac{a_o}{W}\right)^2 && \text{for SE(B) specimens} \\ & && \text{under three-point bending} \\ &= 4.81 - 4.78 \frac{a_o}{W} + 2.03 \left(\frac{a_o}{W}\right)^2 && \text{for SE(B) specimens} \\ & && \text{under four-point bending} \end{aligned}$$

when the CMOD is used for determining A.

For sidegrooved specimens replace B with the net section thickness B_n .

6.3.1.2 Calculate J_{\max} from the smaller of

$$J_{\max} = (W - a_0) \frac{R_f}{20}$$

and $J_{\max} = \frac{BR_f}{20}$,

where R_f the flow stress is $(R_{p0.2} + R_m)/2$.

6.3.1.4 If J_0 does not exceed J_{\max} , then J_0 characterizes the fracture process for the thickness tested.

6.3.2 M(T) specimens

6.3.2.1 Measure the area A^* under the force versus load-point displacement or CMOD record up to the point corresponding to either unstable fracture or the first significant pop-in step, Fig. 25.

NOTE: *The CMOD is much easier to measure than the load-point displacement.*

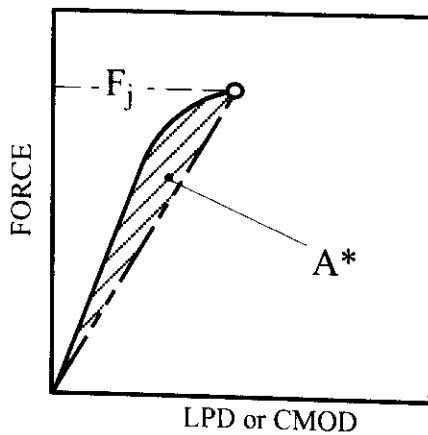


Figure 25:
Determination of A^ from force-CMOD diagram.*

6.3.2.2 Calculate J_0 using the relationship

$$J_0 = \frac{K^2}{E} + \frac{A^*}{B(W - a_0)}$$

where

$$K = \frac{F_j}{B\sqrt{W}} f(a_0/W)$$

and F_j is the force at unstable fracture or the first significant pop-in, **Fig. 25**, $f(a_0/W)$ is the stress intensity function defined in **Appendix 1**, E is Young's modulus. J_0 should only be evaluated from this relationship if $F_j < 1.8 R_{p0.2} BW$. If F_j exceeds this limit, then J_0 may be severely overestimated and is therefore regarded as invalid.

6.4 δ_{5c} , J_c ; δ_{5u} , J_u and δ_{5uc} , J_{uc}

6.4.1 If the total measured stable crack extension prior to unstable fracture or to the first significant pop-in is less than $0.2 \text{ mm} + (\delta_5/1,87) (R_{p0.2}/R_m)$ or $0.2 \text{ mm} + (J/3.75 R_m)$, then δ_5 and J_0 are designated δ_{5c} and J_c , respectively.

NOTE: $R_{p0.2}$ and R_m , respectively, are the yield strength and ultimate tensile strength at test temperature!

6.4.2 If the total measured stable crack extension prior to unstable fracture or to the first significant pop-in is greater than or equal to the values specified in **Section 6.4.1**, then δ_5 and J_0 are designated δ_{5u} and J_u , respectively. δ_{5u} and J_u values must be reported with the corresponding Δa value as required in **Section 9.4**.

6.4.3 If the amount of stable crack extension cannot be measured prior to unstable fracture or to the first significant pop-in then δ_5 and J_0 are designated δ_{5uc} and J_{uc} , respectively.

6.4.4 If these parameters have been determined using M(T) specimens, then they must be reported with the superscript M(T), e.g. $\delta_{5c}^{M(T)}$.

7 CRACK EXTENSION RESISTANCE CURVES AND RELATED FRACTURE PARAMETERS $\delta_{5,0.2/BL}$, $J_{0.2/BL}$, $\delta_{5,0.2}$, $J_{0.2}$ UNDER HIGH CONSTRAINT CONDITIONS

Procedures to evaluate the fracture behaviour of specimens which exhibit only stable crack extension and a non-linear force-displacement record, **Fig. 4c**, under conditions of high constraint are described in this section. The specimen dimensions are described in **Clause 2.2.1.1**. The fracture behaviour is characterized in terms of either the variation in crack tip opening displacement δ_5 or fracture resistance J with crack extension, Δa . Methods are given for interpreting the δ_5 - Δa and J - Δa behaviour in terms of the fracture parameters $\delta_{5,0.2/BL}$, $J_{0.2/BL}$, $\delta_{5,0.2}$, $J_{0.2}$. The analysis procedures given in this section for determining either δ_5 or J are based on multiple specimen data, as determined in **Section 4.3**.

For structural integrity assessments, data are frequently required which are independent of test specimen size. Validity limits are applied to the data in an attempt to ensure size independence so that δ_5 and J characterise the fracture behaviour of ductile materials.

The validity limits are expressed in terms of the maximum δ_5 , J and Δa values which can be measured for a given test specimen size. Data satisfying the validity limits are regarded as a material property independent of specimen size.

If these limits are exceeded then the crack extension resistance data are only relevant to the thickness tested. In such cases, it may be possible with the use of the Δa_{max} limit together with a width-to-thickness requirement to ensure that the data are independent of the in-plane dimensions of the specimen, **Section 8**.

Three fracture parameters are described for estimating δ_5 and J close to the onset of crack initiation from crack extension resistance data.

These parameters are:

- (1) $\delta_{5,0.2/BL}$ or $J_{0.2/BL}$ which measure the fracture resistance at 0.2 mm crack extension beyond crack initiation. They provide an engineering definition of initiation and avoid the use of a scanning electron microscope. These parameters attempt to rank materials covering a wide range of crack extension resistance behaviour with respect to crack initiation.
- (2) $\delta_{5,0.2}$ or $J_{0.2}$ which measure the fracture resistance at 0.2 mm of total crack extension including crack tip blunting. In many areas these parameters provide a useful engineering estimate of initiation which are generally lower bound values compared with ($\delta_{5,0.2/B}$ and $J_{0.2/BL}$). However, high toughness materials may be ranked unduly low.
- (3) A more accurate estimate of the fracture resistance at crack initiation, δ_{5i} or J_i , requiring the use of a scanning electron microscope is given in **Appendix 6**.

NOTE: *For valid initiation parameters the data points in the construction of the R- curve fit do not have to meet the δ_{5max} or J_{max} requirements.*

The parameters δ_{5g} and J_g are defined which give the maximum fracture resistance values that can be measured from a given test specimen. Also $d\delta_5/da$ and dJ/da , which are the slopes of the δ_5 - Δa and J - Δa curves, respectively, are used to measure the material resistance to crack extension.

A flowchart of the procedure to follow in order to determine the fracture parameters described in this section is given in **Fig. 3b**.

As an alternative to J the rate of dissipated energy, R , and its determination are described in **Appendix 16**.

7.1 Fracture Resistance δ_5

The crack tip opening displacement, δ_5 , is measured directly in this Procedure, **Section 3.4.3**.

7.2 Fracture Resistance J

7.2.1 C(T) and SE(B) specimens

7.2.1.1

- (i) Measure the area A under the force versus LPD or CMOD diagram up to the line parallel to the initial slope, **Fig. 24**, corresponding to the termination of the test.
- (ii) Calculate J_0 using the relationship

$$J_0 = \frac{K^2}{E(1-\nu^2)} + \frac{\eta_{pl}}{B(W-a_0)} A$$

where

$$\eta_{pl} = 2 + 0.522 \left(1 - \frac{a_0}{W} \right)$$

$$= 2$$

for C(T) specimen

for SE(B) specimen

when the LPD is used for determining A and

$$= 3.724 - 2.244 \frac{a_0}{W} + 0.408 \left(\frac{a_0}{W} \right)^2$$

for SE(B) specimens
under three-point bending

$$= 4.81 - 4.78 \frac{a_0}{W} + 2.03 \left(\frac{a_0}{W} \right)^2$$

for SE(B) specimens
under four-point bending

when the CMOD is used for determining A.

For sidegrooved specimens replace B with B_n in the above formula.

7.2.1.2 Fracture resistance J allowing for crack extension

The J-equation used in **Clause 7.2.1.1** does not allow for crack extension during a test. The errors in the J-values are usually negligible for crack extension less than 0.1 (W- a_0). If the crack extension validity limit is extended beyond 0.1 (W- a_0) then all data points should be corrected for crack extension. A suitable approximation is

$$J = J_0 \left\{ 1 - \frac{(0.75\eta - 1)\Delta a}{(W - a_0)} \right\}$$

where η is defined in **Clause 7.2.1.1**.

7.2.2 M(T) Specimens

7.2.2.1 Measure the area A^* under the force versus LPD or CMOD record up to the point corresponding to the termination of the test, **Fig. 25**.

7.2.2.2 Calculate J_0 using the relationship

$$J_0 = \frac{K^2}{E} + \frac{A^*}{B(W - a_0)}$$

where $K = \frac{F_j}{B\sqrt{W}} f(a_0/W)$

and F_j is the force at termination of the test, **Fig. 25**,
 $f(a_0/W)$ is the stress intensity function defined in **Appendix 1**,
 E is Young's modulus.

J_0 should only be evaluated if $F_j < 1.8 R_{p0.2} BW$. If F_j exceeds this limit, then J_0 may be severely overestimated and is therefore regarded as invalid.

7.2.2.3 Fracture resistance J allowing for crack extension

The J -equation used in **Clause 7.2.2.2** does not allow for crack extension during a test. The errors in the J -values are usually negligible for crack extension less than $0.1(W - a_0)$. If crack extension is analyzed beyond this value, then all data points should be corrected for crack extension. A suitable approximation is

$$J = J_0 \left\{ 1 - \frac{(0.75\eta - 1)\Delta a}{(W - a_0)} \right\}$$

where $\eta = 0.5$.

7.3 Δa_{\max} Crack Extension Limit

7.3.1 Construct a plot of fracture resistance versus crack extension using the data obtained in **Sections 4.2, 7.1 and 7.2**.

7.3.2 C(T) and SE(B) Specimens

7.3.2.1 For each specimen, calculate Δa_{\max} from either

$$\Delta a_{\max} = 0.25(W - a_0) \quad \text{for } \delta_5$$

or

$$\Delta a_{\max} = 0.1(W - a_0) \quad \text{for } J.$$

7.3.3 M(T) Specimens

For each specimen, calculate Δa_{\max} from either

$$\Delta a_{\max} = W - a_0 - B \quad \text{for } \delta_5$$

or

$$\Delta a_{\max} = 0.4 (W - a_0) \quad \text{for J.}$$

7.3.4 Determine the slope of the blunting line as described in **Appendix 7**. Plot the blunting line on a graph containing the crack extension fracture resistance data. Report the slope of the blunting line as required in **Section 9.4**.

7.3.5 Construct the crack extension limit exclusion line parallel to the blunting line at an offset corresponding to the minimum value of Δa_{\max} calculated in either **Section 7.3.2** or **Section 7.3.3**, **Fig. 26**.

7.3.6 Construct an exclusion line parallel to the blunting line at an offset of 0.10 mm, **Fig. 26**.

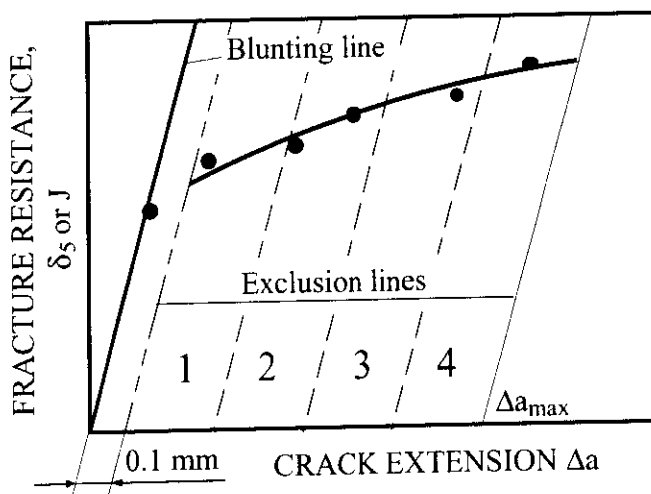


Figure 26:

Data point distribution for determining fracture parameters.

7.3.7 If only the crack extension fracture resistance curve is to be determined, the bluntingline construction can be avoided by the use of a vertical exclusion line at Δa_{\max} , **Fig. 27**.

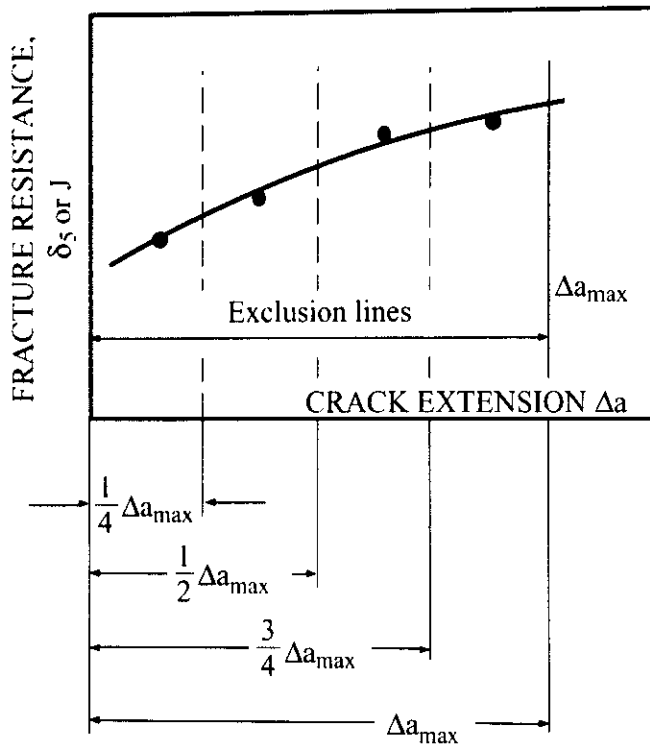


Figure 27:
Data point distribution for determining the R-curve.

7.4 Data Spacing Requirement

7.4.1 A minimum of four and preferably six data points must be used to describe the crack extension resistance behaviour. Ideally the data points should be evenly spaced. At least one data point is required in each of the four equal crack extension regions shown in **Figs. 26** and **27**. The data spacing requirement shown in **Fig. 26** must be used for the evaluation of the fracture parameters $\delta_{5,0.2/BL}$, $J_{0.2/BL}$, δ_{5i} , and $J_{i..}$. The alternative data spacing shown in **Fig. 27** can be used if only the crack extension fracture resistance curve is determined.

7.4.2 Any specimen which exhibits unstable fracture shall be reported as required in **Section 9.3**. If the amount of prior stable crack extension can be measured, then the data can be used to describe the crack extension fracture resistance curve. Any unstable fracture data points shall be clearly identified on the fracture resistance curve as required in **Section 9.4**.

7.5 Curve Fit

7.5.1 Determine the best fit curve through the data points which lie within the Δa_{max} exclusion lines shown in either **Fig. 26** or **Fig. 27**, whichever is appropriate, using the equation

$$\delta_5 \text{ or } J = A + C\Delta a^D$$

where A and $C \geq 0$ and $0 \leq D \leq 1$

A method for evaluating the constants A, C and D is given in **Appendix 9**. If A or C are less than zero the curve fit is unacceptable and additional tests or the use of single specimen test techniques, **Appendix 5**, are recommended.

The crack extension resistance curve can also be represented as the series of data points.

7.6 δ_5 Validity Limits

7.6.1 C(T) and SE(B) Specimens

7.6.1.1 For each specimen calculate $\delta_{5,\max}$ from the smaller of

$$\delta_{5,\max} = \frac{(W - a_0)}{30}$$

and

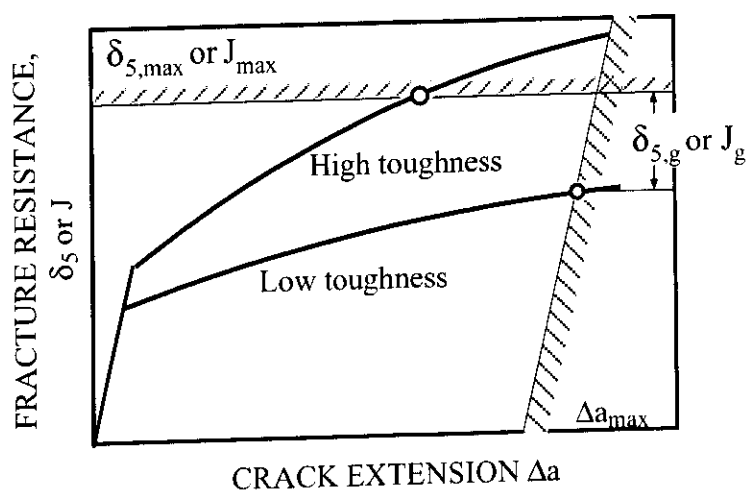
$$\delta_{5,\max} = \frac{B}{30}$$

7.6.1.2 Construct an exclusion line to the δ_5 - Δa data at the minimum calculated $\delta_{5,\max}$ value, **Fig. 28**.

7.6.1.3 The crack extension resistance curve enclosed by the $\delta_{5,\max}$ and Δa_{\max} exclusion lines may be regarded as a material property independent of specimen size.

7.6.1.4 The intersection of the curve with either the $\delta_{5,\max}$ or Δa_{\max} exclusion lines defines $\delta_{5,g}$, **Fig. 28**. $\delta_{5,g}$ is the upper limit to δ_5 -controlled crack extension behaviour for the test specimen size.

Figure 28: *Validity limits.*



7.6.2 M(T) Specimens

The crack extension resistance curve is in general size dependent. If a_0 and $(W - a_0)/B$ are equal to or greater than 4 and the δ_5 - Δa curve is within the Δa_{\max} exclusion line, then the crack

extension resistance curve is independent of the in-plane dimensions, see **Section 8.1**, however, it may be thickness dependent.

NOTE: *An established $\delta_{5,max}$ limit for M(T) specimens is not yet available.*

7.7 J Validity Limits

7.7.1 C(T) and SE(B) Specimens

7.7.1.1 For each specimen, calculate J_{max} from the smaller of

$$J_{max} = (W - a_0) \frac{R_f}{20}$$

and

$$J_{max} = B \frac{R_f}{20}.$$

where R_f the flow stress is $(R_{p0.2} + R_m)/2$.

7.7.1.2 Construct an exclusion line to the J- Δa data at the minimum calculated J_{max} value, **Fig. 28**.

7.7.1.3 The crack extension fracture resistance curve enclosed by the J_{max} and Δa_{max} exclusion lines may be regarded as a material property independent of specimen size.

7.7.1.4 The intersection of the best fit curve with either the J_{max} or Δa_{max} exclusion line defines J_g , **Fig. 28**. J_g is the upper limit to J-controlled crack extension behaviour for the test specimen size.

7.7.1.5 If J is greater than $(B \cdot R_f)/20$, then the crack extension resistance curve may be thickness dependent. If $(W - a_0)/B$ is equal to or greater than 4 and the J- Δa curve is within the Δa_{max} exclusion line, the crack extension resistance curve is independent of the in-plane dimensions.

7.7.2 M(T) Specimens

The crack extension resistance curve is in general size dependent.

NOTE: *An established J_{max} limit for M(T) specimens is not yet available. Numerical evidence suggests that J_{max} may be given by*

$$J_{max} = (W - a_0) \frac{R_{p0.2}}{100}.$$

7.8. Fracture Parameters at 0.2 mm of Ductile Tearing

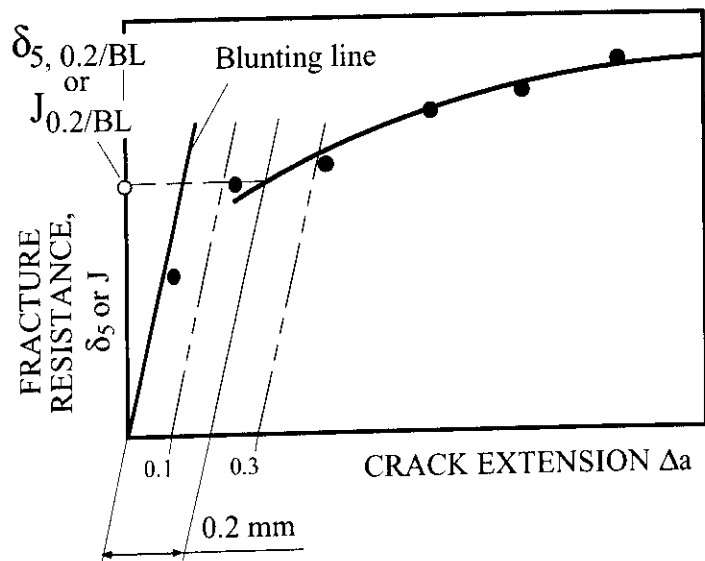
The following procedure applies to C(T) and SE(B) specimens. It can also be applied to M(T) specimens, but the resulting values of $\delta_{5,0.2/BL}$ and $J_{0.2/BL}$ may be thickness dependent.

7.8.1 $\delta_{5,0.2/BL}$

7.8.1.1 Construct a plot of the blunting line, **Section 7.3.4**, and the best fit curve, **Section 7.5.1**, through the δ_5 - Δa data.

7.8.1.2 Construct a parallel line offset to the blunting line at 0.2 mm crack extension, **Fig. 29**. The intersection of the best fit curve with the offset line defines $\delta_{5,0.2/BL}$. At least one δ_5 - Δa data point should be within 0.1 mm of the parallel offset line.

Figure 29:
Determination of $\delta_{5,0.2/BL}$
and $J_{0.2/BL}$



7.8.1.3 If $\delta_{5,0.2/BL}$ exceeds $\delta_{5,max}$ determined in **Section 7.6.1**, then $\delta_{5,0.2/BL}$ is invalid according to this Procedure.

7.8.1.4 Evaluate the slope of the δ_5 - Δa curve, $\left(\frac{d\delta_5}{da}\right)_{0.2/BL}$ at the intersection point from the equation determined in **Clause 7.8.1.1**. If the slope of the blunting line

$$\left(\frac{d\delta_5}{da}\right)_{BL} < 2\left(\frac{d\delta_5}{da}\right)_{0.2/BL},$$

then $\delta_{5,0.2/BL}$ is invalid according to this Procedure.

7.8.2 $J_{0.2/BL}$

7.8.2.1 Construct a plot of the blunting line, **Section 7.3.4**, and the best fit curve, **Section 7.5.1** through the J- Δa data.

7.8.2.2 Construct a parallel line offset to the blunting line at 0.2 mm crack extension, **Fig. 29**. The intersection of the best fit curve with the offset line defines $J_{0.2/BL}$. At least one J- Δa point should be within 0.1 mm of the offset line.

7.8.2.3 If $J_{0.2/BL}$ exceeds J_{max} determined in **Section 7.7.1** then $J_{0.2/BL}$ is invalid according to this Procedure.

7.8.2.4 Evaluate the slope of the J- Δa curve, $(dJ/da)_{0.2/BL}$, at the intersection point from the equation determined in **Clause 7.8.1.1**. If the slope of the blunting line

$$\left(\frac{dJ}{da}\right)_{BL} < 2\left(\frac{dJ}{da}\right)_{0.2/BL},$$

then $J_{0.2/BL}$ is invalid according to this Procedure.

7.9 Fracture Parameters at 0.2 mm of Crack Extension Including Blunting

The following procedure applies to C(T) and SE(B) specimens. It can also be applied to M(T) specimens, but the resulting values of $\delta_{5,0.2}$ and $J_{0.2}$ may be thickness dependent.

7.9.1 $\delta_{5,0.2}$

7.9.1.1 Construct a line corresponding to constant total crack extension of 0.2 mm on a plot of the δ_5 - Δa data. The intersection of this line with the best fit curve through the data obtained in **Section 7.5.1** defines $\delta_{5,0.2}$, **Fig. 30**. At least one data point should be between within 0.2 and 0.4 mm.

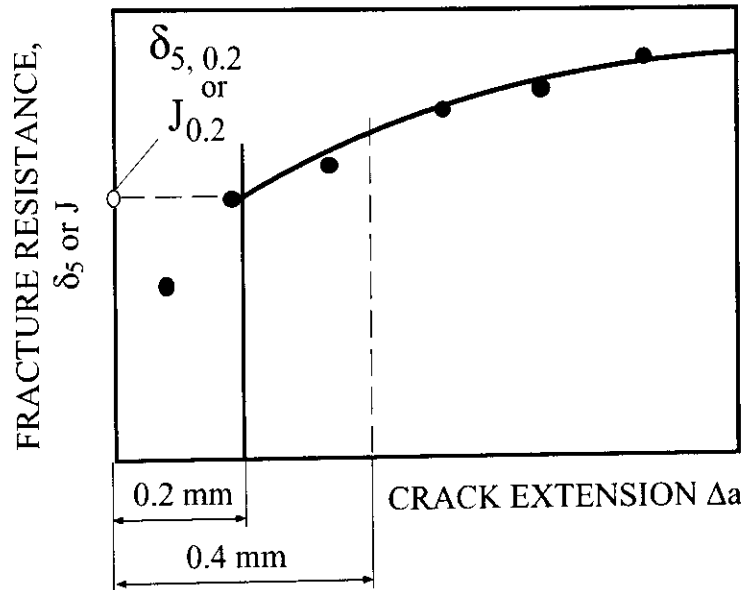
7.9.1.2 If $\delta_{5,0.2}$ exceeds $\delta_{5,max}$ determined in **Section 7.6.1**, then $\delta_{5,0.2}$ is invalid according to this Procedure.

7.9.2 $J_{0.2}$

7.9.2.1 Construct a line corresponding to constant total crack extension of 0.2 mm on a plot of the J- Δa data. The intersection of this line with the best fit curve through the data obtained in **Section 7.5.1** defines $J_{0.2}$, **Fig. 30**. At least one data point should be between 0.2 and 0.4 mm crack extension.

7.9.2.2 If $J_{0.2}$ exceeds J_{max} determined in **Section 7.7.1**, then $J_{0.2}$ is invalid according to this Procedure.

Figure 30:
Determination of $\delta_{5,0.2}$ and $J_{0.2}$.



8 CRACK EXTENSION RESISTANCE UNDER LOW CONSTRAINT CONDITIONS

Procedures to evaluate the stable crack extension in compact and middle cracked tension specimens under low constraint conditions as specified in **Clause 2.2.1.2** are described in this section [16]. The crack extension behaviour is described in terms of either the variation in crack tip opening displacement, δ_5 , with crack extension, Δa , or a critical value of the crack tip opening angle, ψ_c . In **Appendix 11** a method is described for determining K-based R-curves for high strength materials.

Requirements are given to ensure that the crack extension resistance is independent of the in-plane dimensions of the specimen. It is, however, dependent on the specimen type and thickness.

8.1 Determination of δ_5 - Δa Resistance Curve

8.1.1 Fracture Resistance δ_5

The crack tip opening displacement, δ_5 , is measured directly, **Section 3.4.3**.

8.1.2 Δa_{\max} Crack Extension Limit

8.1.2.1 For each C(T) specimen, calculate Δa_{\max} from

$$\Delta a_{\max} = 0.25 (W - a_0)$$

8.1.2.2 For each M(T) specimen, calculate Δa_{\max} from

$$\Delta a_{\max} = W - a_0 - B$$

8.1.3 R-Curve Plot

8.1.3.1 Data spacing requirement

A minimum of six data points must be used to describe the R-curve. Ideally the data points should be evenly spaced. At least one data point is required in each of the four equal crack extension regions shown in **Fig. 27**.

Any specimen which exhibits unstable fracture shall be reported as required in **Section 9.3**. If the amount of prior stable crack extension can be measured, then the data can be used to describe the R-curve. Any unstable fracture data point shall be clearly identified on the R-curve as required in **Section 9.4**.

8.1.4 Significance of Result

The R-curve thus obtained characterises the material in the thickness and specimen geometry tested, and is independent of the in-plane dimensions of either C(T) or M(T) specimens.

8.1.5 Determination of $\delta_{5,0.2/BL}$, $\delta_{5,0.2}$ and $\delta_{5,i}$

The parameters close to initiation of crack extension, $\delta_{5,0.2/BL}$, $\delta_{5,0.2}$ and $\delta_{5,i}$, respectively, are determined using the procedures described in **Clauses 7.8.1, 7.9.1, and Appendix 6**, respectively. As the validity requirements of these procedures are not applicable here, the δ_5 values thus determined may be thickness dependent and shall be reported together with the material thickness tested.

8.2 Determination of Critical CTOA

After some amount of crack extension the CTOA reaches a steady state value, Ψ_c .

8.2.1 Crack Tip Opening Angle ψ

The crack tip, opening angle is determined using the methods described in **Appendix 15**.

8.2.2 Δa_{max} Crack Extension Limit

8.2.2.1 For each specimen tested, a maximum amount of crack extension, Δa_{max} , is calculated from

$$\Delta a_{max} = W - a_0 - B$$

and a minimum amount of crack extension, Δa_{min} , is that value of Δa where ψ in **Fig. 31** attains a constant value. These serve as upper and lower bounds for the crack extension over which the critical CTOA, Ψ_c , is evaluated.

NOTE: *Due to the developing nature of the CTOA method, the Δa limits are based on limited experience.*

8.2.2.2 Measurements of ψ are made at any amount of crack extension, in particular between the crack extension limits. ψ values measured outside the crack extension limits are for informational purposes only. Plot ψ versus Δa as shown in Fig. 31. ψ_c is determined from the ψ - Δa plot between Δa_{min} and Δa_{max} .

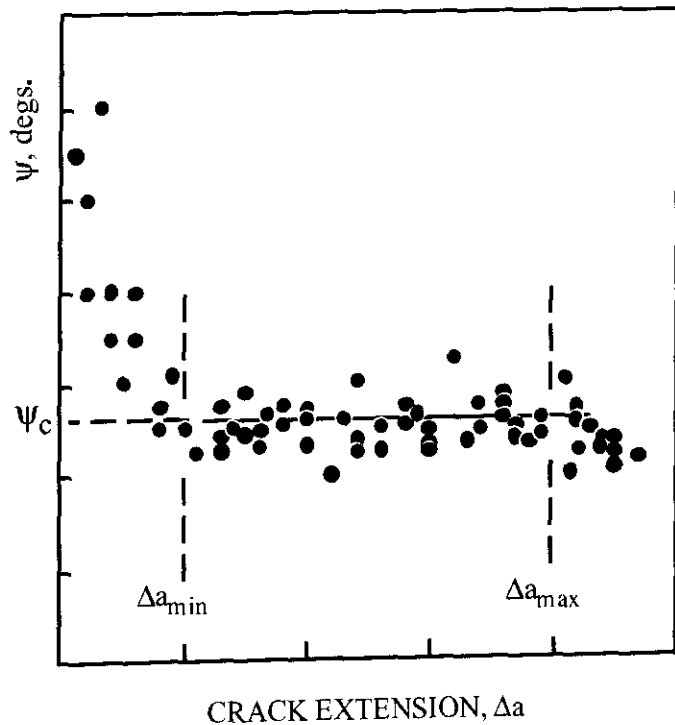
NOTE: Crack tip opening angles measured on the surface of a specimen in the initial phase of crack extension exhibit large values due to crack tip blunting and crack tunnelling. But in the interior region, which is under high local constraint, the ψ values are generally lower than the surface values, see Fig. 31.

8.2.2.3 The critical value of ψ_c is evaluated as

$$\psi_c = (\sum \psi_n) / N$$

where ψ_c is the point value and N is the total number of measured values satisfying the Δa_{min} and Δa_{max} requirements.

Figure 31:
Determination of the critical
CTOA, ψ_c .



9 PRESENTATION OF RESULTS

When reporting the test results the following information should be presented:

9.1 **Material** – specification, yield strength, tensile strength and assumed value of Young's modulus at test temperature. These properties should be measured normal to the crack plane. If available, chemical composition and heat treatment.

9.2 Specimen Geometry – type, width, thickness, net thickness of sidegrooved specimens, if applicable, and crack plane orientation from either a drawing or the notation given in Fig. 32.

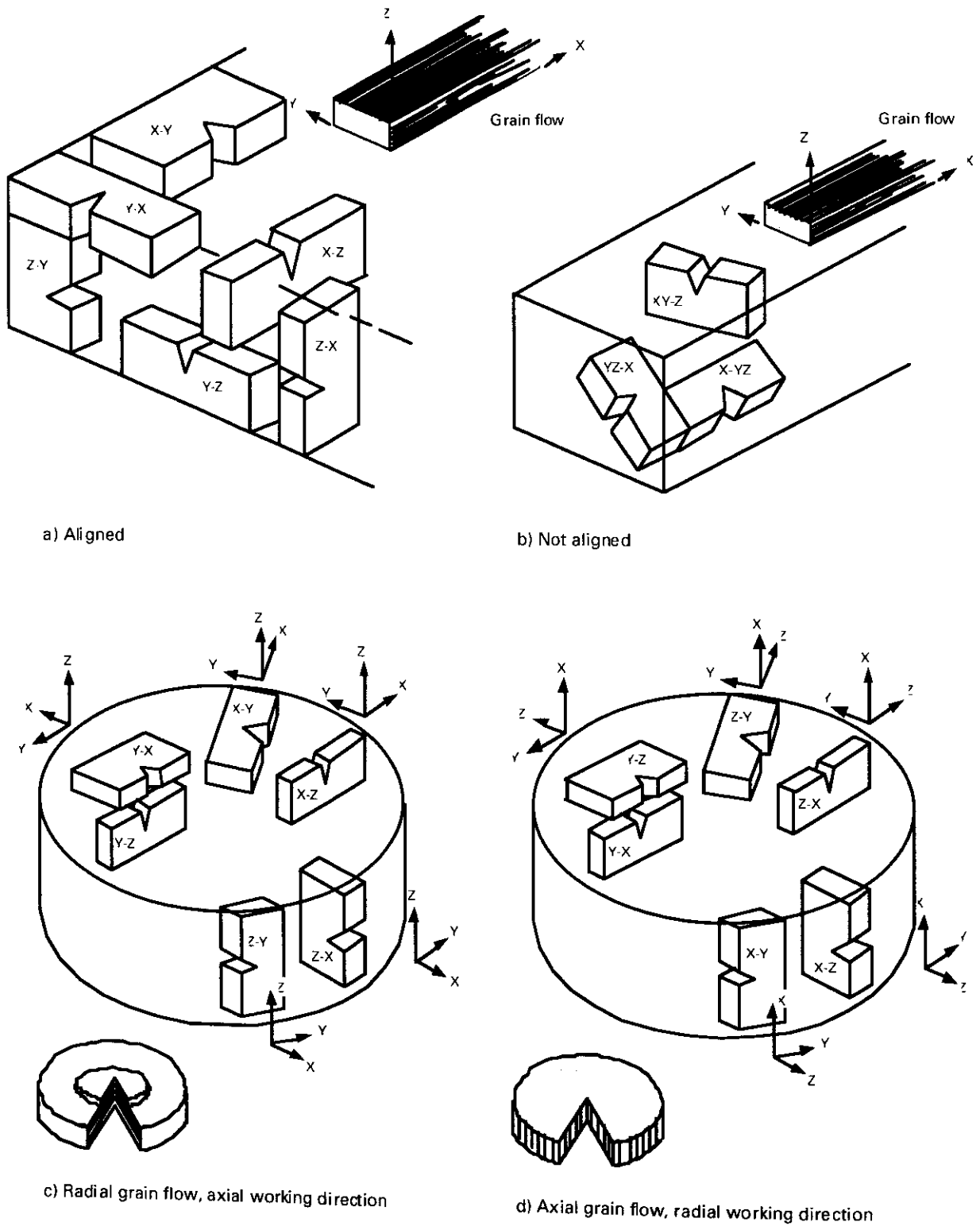


Figure 32: Fracture Plane Identification.

9.3 Test Details

- Maximum stress intensity factor and force during final stages of fatigue pre-cracking, temperature, single or multiple specimen method, loading rate and machine control.
- If applicable, total number of significant and insignificant pop-in steps on the load-displacement test record.
- Time at test temperature.
- Method of measuring initial crack length and, if applicable, crack extension.
- Measured initial crack length.
- If the multiple specimen method is used, the initial crack length range.
- If applicable, non-uniform, non-symmetric and insufficient fatigue pre-crack extension.
- Stable or unstable crack extension.
- Non-symmetric crack extension.
- Specimens exhibiting cleavage fracture.
- If applicable, number of brittle thumbnailed regions ahead of the fatigue pre-crack.
- If non-uniform or non-symmetric crack extension is exhibited, the resulting data must be clearly identified in all subsequent use.
- Any unusual features on the fracture surfaces.
- If applicable, alternative method of defining a_i the estimated initial crack length.

9.4 Results

- Force versus load-point displacement or CMOD, as appropriate.
- Record K_c , K_{Ic} , F_{max}/F_c , δ_{5u} , δ_{5c} , δ_{5uc} , J_c , J_u , J_{uc} , and ψ_c whichever is applicable.
- If either J_u or δ_{5u} is applicable, the corresponding crack extension Δa .
- Record either the δ_5 - Δa or J - Δa curve and all data points including details of the exclusion lines, the constructional procedure and equations used to derive the fracture parameters $\delta_{5,0.2/BL}$, $\delta_{5,0.2}$, $J_{0.2/BL}$, $J_{0.2}$, whichever is applicable.
- Identify on the curve any data points exhibiting unstable fracture.
- If applicable, report and provide justification for the use of extended validity limits.
- If applicable, report the slope of the blunting line.
- For M(T) specimens the values of the δ_5 fracture parameters, of the crack extension for δ_{5u} , δ_{5c} , J_u , and J_{uc} and the δ_5 - Δa curves should be reported for both crack tips separately.

9.5 Any departures from the recommendations of this Procedure should be reported and justified. In such circumstances, the resulting data must be clearly identified in all subsequent use.

9.6 The results obtained from this Procedure should be recorded on a report sheet.

ACKNOWLEDGEMENT

Many invaluable comments were received from members of the ESIS SC 1.4: Subcommittee on Fracture Mechanics Standards. These comments led to substantial improvement of this document and are greatly appreciated.

10 REFERENCES

- [1] ASTM Standards, 2002, E399-90, Standard Test Method for Plane-Strain Fracture Toughness of Metallic Materials, Annual Book of ASTM Standards, Section 3, Vol. 03.01, 443–473.
- [2] ASTM Standards, 2002, E1290-99, Standard Test Method for Crack-Tip Opening Displacement (CTOD) Fracture Toughness Measurement, Section 3, Vol. 03.01, 870–881.
- [3] ASTM Standards, 2002, E 1820-01, Standard Method for Measurement of Fracture Toughness, Annual Book of ASTM Standards, Section 3, Vol. 03.01, 1031–1076.
- [4] ASTM Standards, 1998, E1737-96, Standard Test Method for J-Integral Characterization of Fracture Toughness, Annual Book of ASTM Standards, Section 3, Vol. 03.01, 957–980.
- [5] BS 7448, Part 1 (1991): Fracture Mechanics Toughness Tests. Method for determination of K_{Ic} , critical CTOD and critical J values of metallic materials, British Standard Institution, London.
- [6] ESIS P1-92, 1992, ESIS Recommendations for Determining the Fracture Resistance of Ductile Materials.
- [7] ESIS P2-92, 1992, ESIS Procedure for Determining the Fracture Behaviour of Materials.
- [8] Hellmann, D., and Schwalbe, K.-H., 1986, On the Experimental Determination of CTOD Based R-curves, in *The Crack Tip Opening Displacement in Elastic-Plastic Fracture Mechanics*, edited by K.-H. Schwalbe, Springer-Verlag, Berlin, Heidelberg.
- [9] Neale, B.K., Curry, D.A., Green, G., Haigh, J.R., and Akhurst, K.N., 1985, *Int. J. of Pressure Vessels and Piping*, A Procedure for the Determination of the Fracture Resistance of Ductile Steels, 20(3), 155–179.
- [10] Schwalbe, K.-H., 1998, *The Engineering Flaw Assessment Method (EFAM)*, – Document EFAM 96, Report GKSS 98/E/40, GKSS-Forschungszentrum Geesthacht GmbH, Geesthacht, Germany.
- [11] Schwalbe, K.-H., Hayes, B., Baustian K., Cornec, A., Gordon, R., Hodayun, M., and Voss, B., 1993, Validation of the fracture mechanics test method EGF P1-87D (ESIS P1-90/ESIS P1-92), *Fatigue and Fracture of Engineering Materials and Structures*, Vol. 16, pp. 1231–1284.
- [12] Kim, Y.-J., and Schwalbe, K.-H., 2001, On the sensitivity of experimental J estimation to materials' stress-strain curves in fracture toughness testing, *Journal of Testing and Evaluation*, 29, pp. 67–71.

- [13] SINTAP, Structural integrity assessment procedure for European industry. British Steel Report, Sheffield (1999).
- [14] Draft International Standard ISO/DIS 12135: Metallic materials – Unified method of test for the determination of quasistatic fracture toughness, International Organization for Standardization, Geneva, 1998.
- [15] Schwalbe, K.-H., Newman, J.C., Jr., and Shannon, J., Jr., 2003, Fracture mechanics testing of specimens with low constraint – standardisation activities within ISO and ASTM, to be submitted for publication.

APPENDIX 1: Stress Intensity Functions

A1.1 For a C(T) specimen [A1.1]

$$f(a/W) = \frac{(2 + a/W)}{(1 - a/W)^{3/2}} \left[0.886 + 4.64(a/W) - 13.32(a/W)^2 + 14.72(a/W)^3 - 5.6(a/W)^4 \right]$$

A1.2 For a SE(B) specimen under three-point bending [A1.1]

$$f(a/W) = \frac{3(a/W)^{1/2}}{2(1 + 2(a/W))(1 - a/W)^{3/2}} \frac{S}{W} \left\{ 1.99 - (a/W)(1 - a/W) \right. \\ \left. [2.15 - 3.93(a/W) + 2.7(a/W)^2] \right\}$$

A1.3 For a SE(B) specimen under three-point bending [A1.1]

$$f(a/W) = \left[\frac{2.659(S_1 - S_2) \sqrt{a}}{W^{3/2}} (1.122 - 1.40(a/W) + 7.33(a/W)^2) \right. \\ \left. -13.08(a/W)^3 + 14.0(a/W)^4 \right]$$

A1.4 For a M(T) specimen [A1.3, A1.4]

$$f(a/W) = \frac{1}{2} \sqrt{\frac{\pi a}{W} \sec \frac{\pi a}{2W}}$$

where a is the half crack length and $2W$ is the specimen width.

REFERENCES

- [A1.1] Annual Book of ASTM Standards, E 1820-96, 1998, Standard Test Method for Measurement of Fracture Toughness, Section 3, Vol. 03.01, 981-1013.
- [A1.2] Tada, H., Paris, P.C., and Irwin, G.R., 1985, The Stress Analysis of Cracks Handbook, Paris Productions Incorporated, St. Louis
- [A1.3] Annual Book of ASTM Standards, E561-86, 1991, Standard Practice for R-Curve Determination, Section 3, Vol. 03.01, 577-588.
- [A1.4] Wheeler, C., Eastabrook, J.N., Rooke, D.P., Schwalbe, K.-H., Setz, W. and de Koning, A.U., 1982, Recommendations for the measurement of R-curves using centre cracked panels, J, Strain Analysis, Vol. 17, 205-213.

APPENDIX 2: Measurement of Load Point Displacement

A2.1 The method of calculating J requires the measurement of the area under the force versus load-point displacement record. Unlike the step notched compact specimen geometry shown in **Fig. 6** of the Procedure, the single edge cracked bend specimen, **Fig. 12**, and the straight notched compact specimen, **Fig. 5**, do not permit direct measurement of the load-point displacement. Consequently the extraneous displacements arising from indentation effects and elastic displacement in the fixture and test machine must be determined and subtracted from the measured displacement. A suitable method of measuring extraneous displacements is described in **[A2.1]**.

Alternatively the load-point displacement can be measured directly on a SE(B) specimen by attaching a comparator bar to the side of the specimen **[A2.2, A2.3]**, **Fig. A2.1** or employing a double clip gauge arrangement **[A2.4]**.

If the displacement is measured on the front face of a C(T) specimen, a suitable relationship to infer load-point displacement is given in **[A2.5]**.

REFERENCES

- [A2.1] Buzzard, R.J. and Fisher, D.M., 1978, *J. of Testing and Evaluation*, Load displacement measurement and work determination in three point bend tests of notched or precracked specimens, 6(1), 35–39.
- [A2.2] Koçak, M. und Schwalbe, K.-H., 1992, *Fracture Mechanics of Weldments: Microstructural, Experimental and Mechanical Aspects*, Proc. of the 9th European Conference on Fracture ECF 9, Reliability and Structural Integrity of Advanced Materials, Vol. II, 717–747, Varna, Bulgaria.
- [A2.3] Hellmann, D., Rohwerder, G. and Schwalbe, K.-H., 1984, *J. of Testing and Evaluation*, Development of a test set up for measuring deflection of single edge notched bend (SENB) specimens, 12(1), 62–64.
- [A2.4] Willoughby, A.A., 1981, WI Report 153/1981, On the unloading compliance method of deriving single specimen R-curves in three-point bending. The Welding Institute, Cambridge.
- [A2.5] Saxena, A. and Hudak, S.J. Jnr., 1978, *Int. J. of Fracture*, Review and extension of compliance information for common crack growth specimens, 14(5), 453–468.

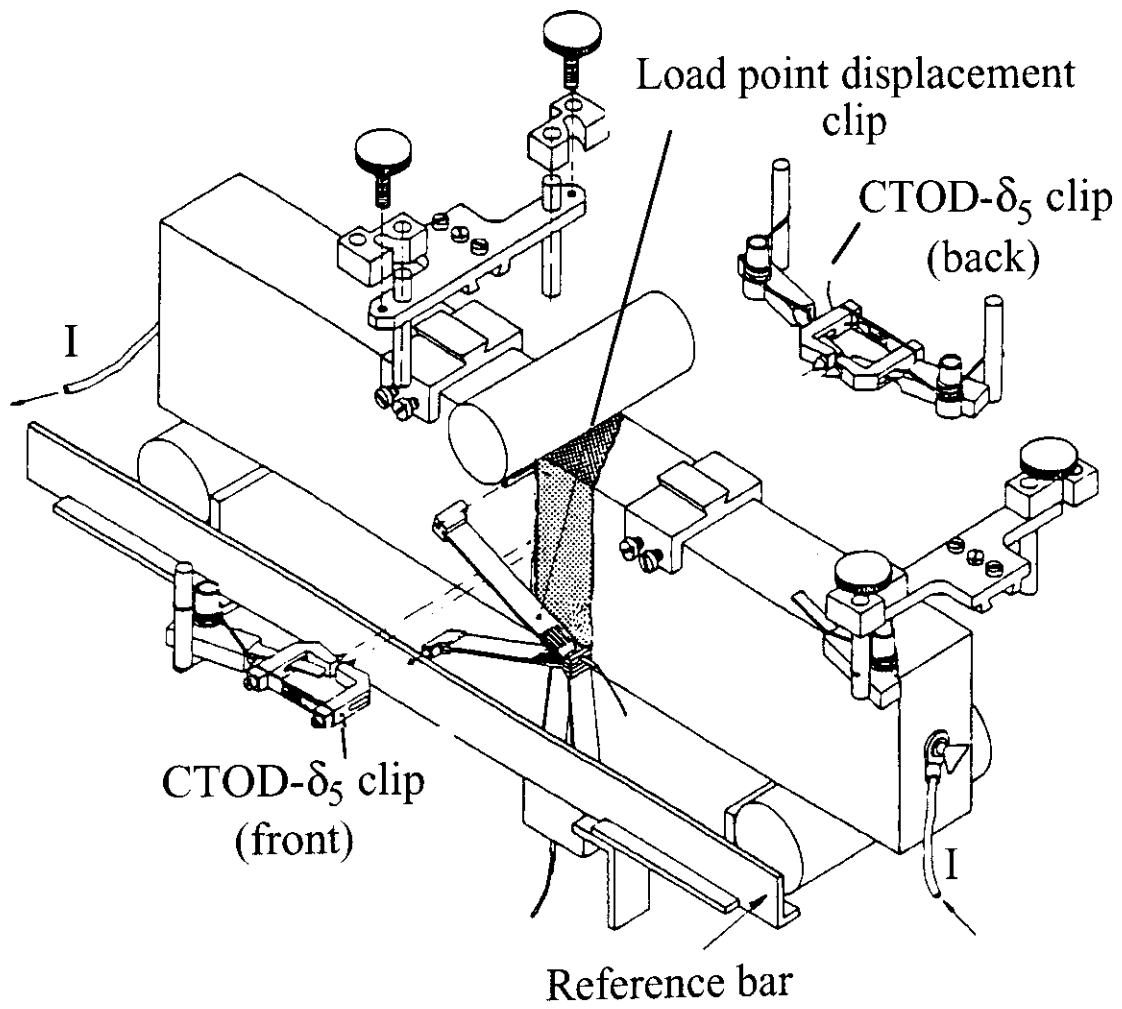


Figure A2.1: *SE(B) specimen with comparator bar for measuring the load-point displacement.
The specimen is also equipped with two δ_5 gauges and a CMOD gauge.*

APPENDIX 3: Measurement of Crack Mouth Opening Displacement on Middle Cracked Tension Specimens

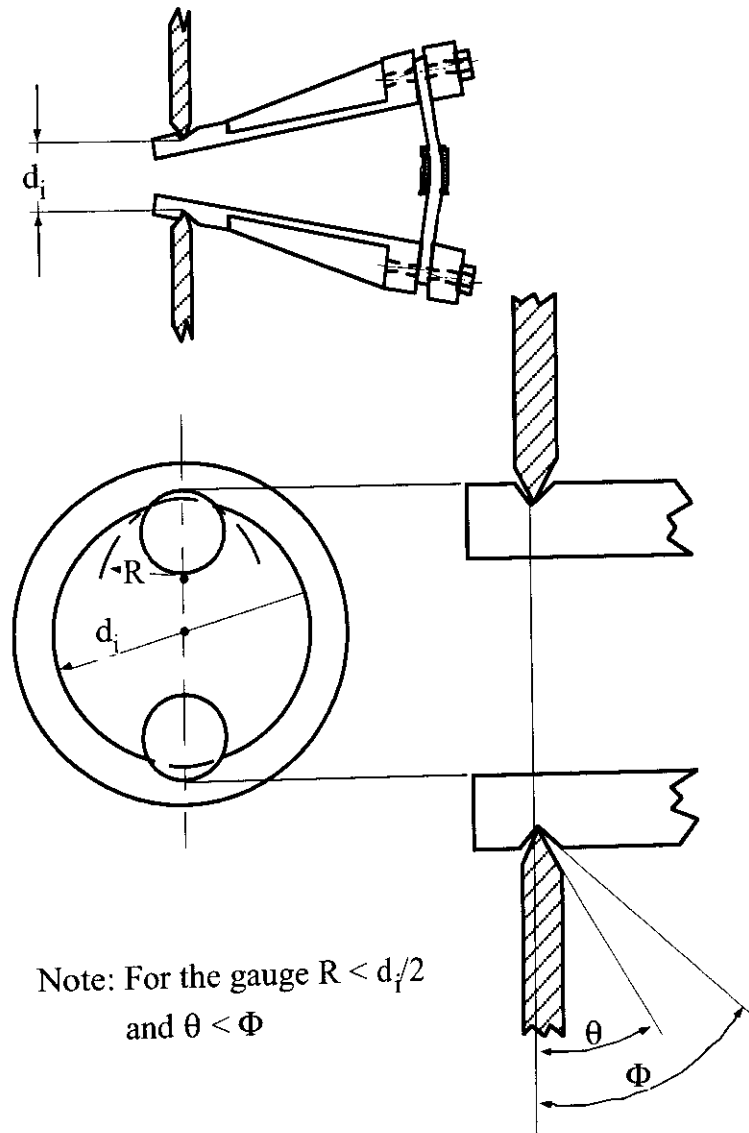
A recommended arrangement is shown in **Fig. A3.1** for the measurement of crack mouth opening displacement, V , on middle cracked tension specimens. It makes use of the circular knife edge hole detailed in **Fig. A3.2**. The gauge tips shown in **Fig. A3.1** have rounded end-pieces with a circular notch of radius R and an included angle θ . The radius R must be less, and the angle θ greater, than the corresponding dimensions of the knife-edge. In addition θ must be chosen to ensure free movement of the gauge. The rigid arms of the gauge are connected to an elastic beam, and the rotation of the beam is measured by strain gauges. Detailed drawings are given in **Fig. A3.2**.

NOTE: *The plastic portion of the crack mouth opening displacement can be used for determining the J-integral on a middle cracked tensile specimen.*

NOTE: *The diameter of the knife edge, d_i , is identical with the gauge length which appears in analytical linear elastic solutions for the crack mouth opening displacement.*

REFERENCES

- [A 3.1] Wheeler, C., Eastabrook, J.N., Rooke, D.P., Schwalbe, K.-H., Setz, W., and de Koning, A.U., 1982, Recommendations for the measurement of R-curves using centre cracked panels, *J. Strain Analysis*, Vol. 17, 205–213.
- [A 3.2] Annual Book of ASTM Standards, 1998, E561-94, Standard Practice for R-Curve Determination, Section 3, Vol. 03.01, 494–506.



Note: For the gauge $R < d_i/2$
and $\theta < \Phi$

Figure A3.1: *CMOD gauge mounting with detail of probe design [A3.1, A3.2].*

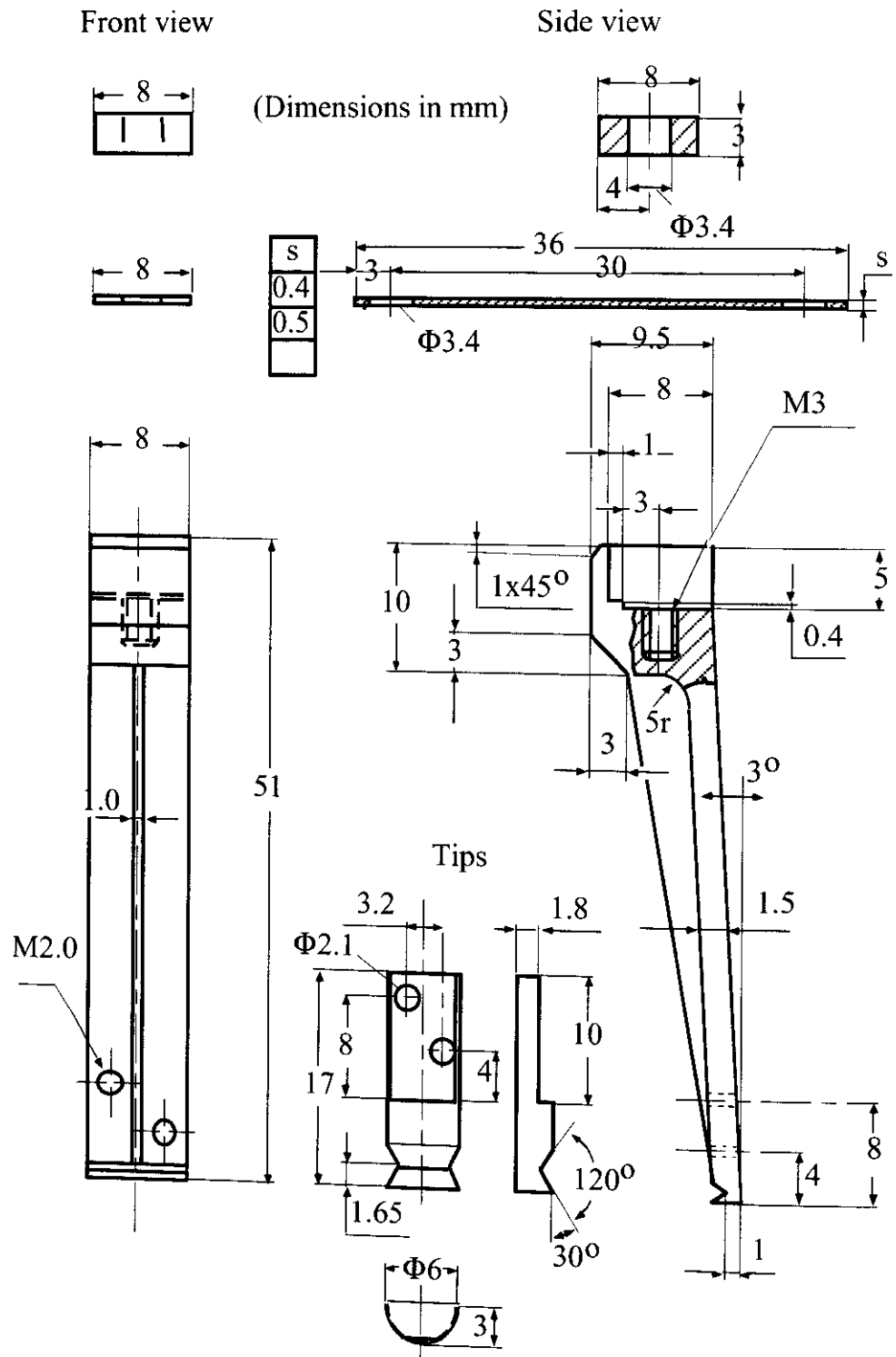


Figure A3.2: Detail drawings of CMOD gauge [A3.1, A3.2].

APPENDIX 4: Measurement of the Crack Tip Opening Displacement, δ_5 .

The basic arrangement [A4.1] for measuring δ_5 is shown in Fig. A4.1. The area around the expected fatigue crack propagation path should be polished. After fatigue pre-cracking, Vickers hardness indentations are placed ± 2.5 mm on either side of the crack tip to give a gauge length of 5 mm. A δ_5 clip gauge with needle tips is seated into the hardness indentations and attached to the specimen using the lever mechanism shown in Fig. A4.2 for a C(T) specimen. Fig. A2.1 shows a similar arrangement for an SE(B) specimen, whereas the instrumentation of a M(T) specimen is illustrated in Fig. A4.3.

δ_5 measurements on welded joints are described in Appendix 9.

Experimental evidence suggests that δ_5 values obtained from clip gauge measurements which are smaller than 0.1 mm should be discarded. Alternatively, δ_5 may be determined from field measurement techniques.

By these techniques, δ_5 is determined on the specimen surface. Appendix 14 gives hints on the behaviour of δ_5 in the centre plane of a specimen.

REFERENCES

- [A4.1] GKSS Displacement Gauge Systems for Application in Fracture Mechanics, brochure of GKSS-Forschungszentrum Geesthacht GmbH, Geesthacht, Germany, 1991.
- [A4.2] Schwalbe, K.-H., 1995, Introduction of δ_5 as an operational definition of the CTOD and its practical use, in: Reuter, W.G. et al. (Eds.): Fracture Mechanics: 26th Volume, ASTM STP 1256, American Society for Testing and Materials, West Conshohocken, 763–778.

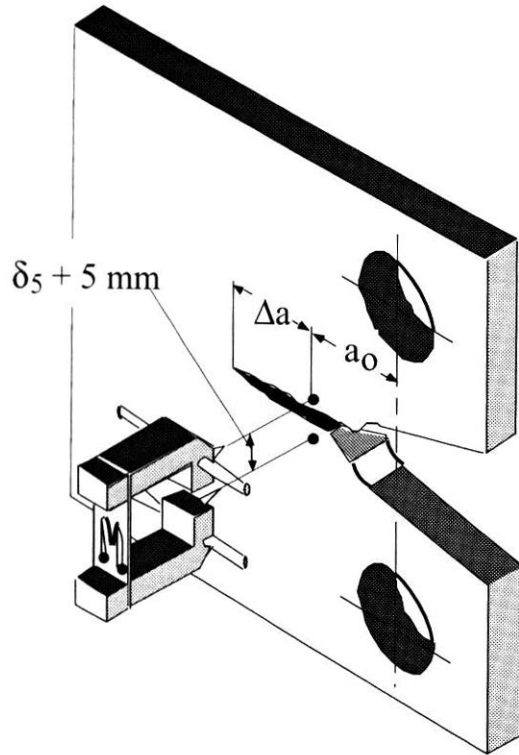


Figure A4.1: Basic arrangement for measuring δ_5 .

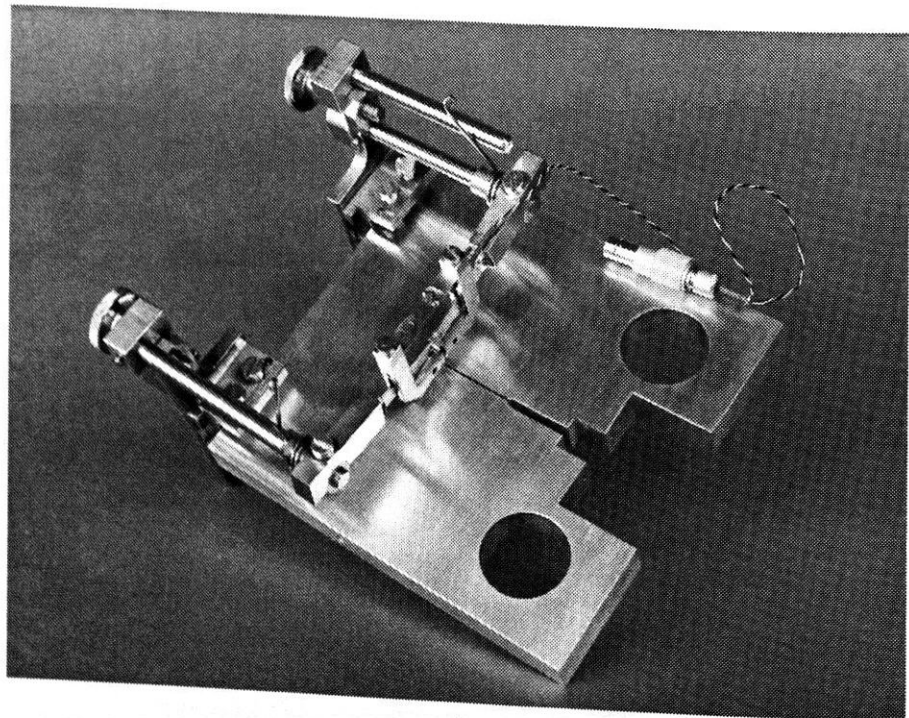


Figure A4.2: Attachment of δ_5 clip gauge to C(T) specimen.

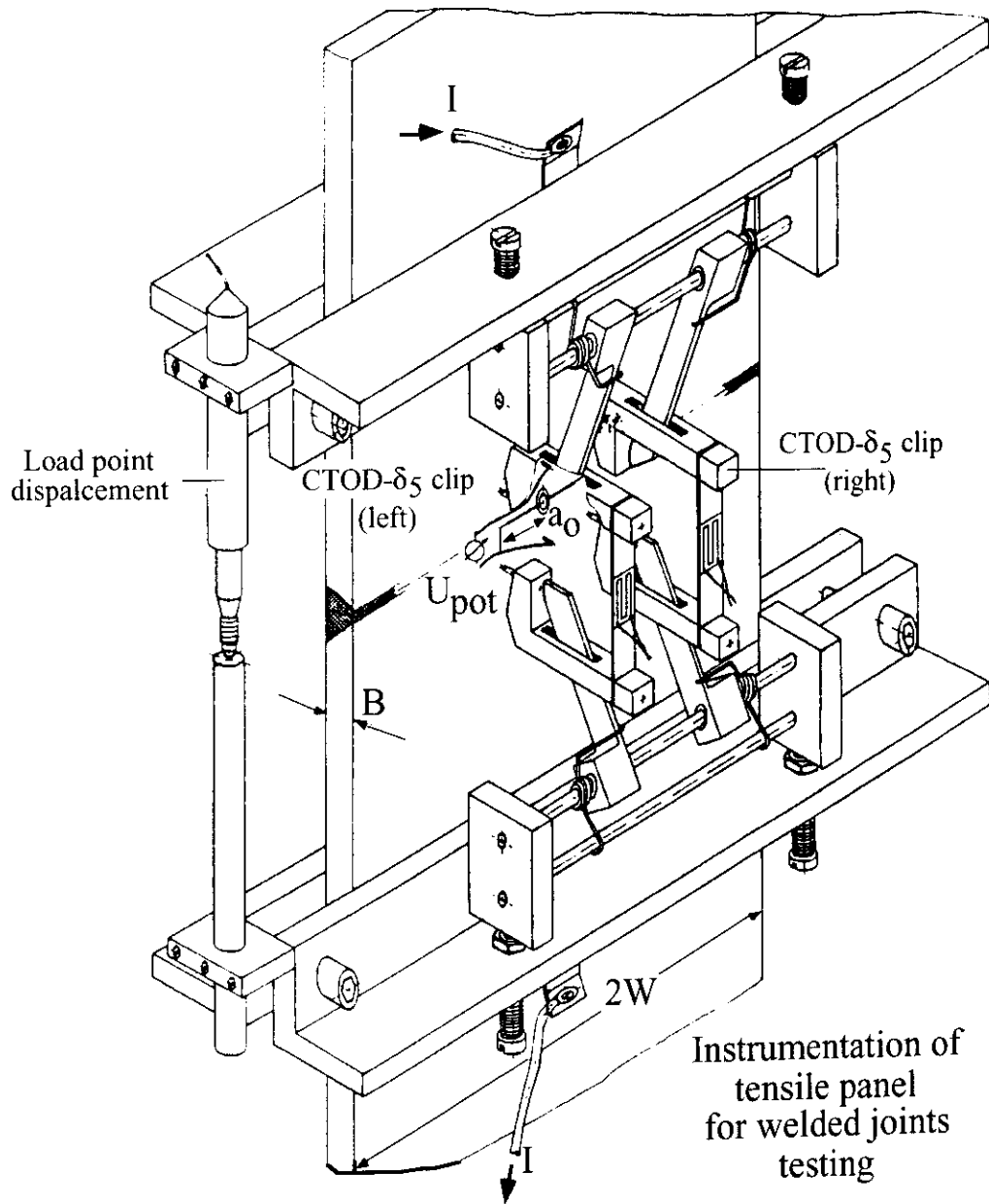


Figure A4.3: *M(T)* specimen showing instrumentation for δ_5 and load line displacement.

APPENDIX 5: Single Specimen Methods to Determine R-Curves

Any single specimen test method may be used provided sufficient accuracy can be demonstrated.

Methods are described in this Appendix for measuring crack extension in a specimen based on the unloading compliance and electrical potential drop techniques.

In the unloading compliance technique, a specimen is partially unloaded and then reloaded at specified intervals during the test. The unloading slopes, which tend to be linear and independent of prior plastic deformation, are used to estimate the crack length at each unloading from analytical elastic compliance relationships. The unloading compliance technique is not recommended for middle cracked tension specimens.

The potential drop technique relies on the fact that the potential distribution in the vicinity of a crack changes with crack extension. With suitable instrumentation, the changes in potential can be detected and calibrated to provide an estimate of increase in the crack length. The applied potential may be either direct or alternating. In this appendix, however, only direct current (DC) techniques are described.

Both techniques are ideally suited to computer control and subsequent analysis of the test data. However, it should be noted that they require careful experimentation and sophisticated test equipment in order to realise their full potential. The tests should be controlled using either the transducer monitoring mouth opening or load point displacement.

There is a fundamental difference between multiple and single specimen test methods. The multiple specimen method gives an average of the crack extension resistance behaviour and of the initiation parameters. The single specimen method gives individual results which can provide information on material inhomogeneity.

For the first crack extension fracture resistance curve measured in a series of tests using the single specimen methods, at least three specimens are needed. Two of these are required to demonstrate the accuracy of the test equipment at small and intermediate amounts of crack extension. One test should be terminated between 0.1 and 0.3 mm of ductile crack extension, **Fig. 5.1**. The other should be terminated midway between the valid crack extension range, Δa_{\max} , **Fig. A5.1**. Suitable termination points can be estimated from data for the specimen covering the Δa_{\max} range. If the difference between the estimated and measured crack extension exceeds 15 percent of the measured crack extension or 0.15 mm, whichever is the greater, then the test is invalid and the single specimen technique may require improvement.

In order to characterize the fracture behaviour of a material, all single specimen data must also satisfy the data spacing requirements, **Section 7.4**, and the appropriate validity limits, **Sections 7.6** and **7.7**.

The data points from valid tests used to demonstrate the accuracy of the test equipment can be combined to generate a single crack extension fracture resistance curve.

A5.1 Unloading Compliance Technique for C(T) and SE(B) Specimens

Several test procedures have been written for the unloading compliance technique [A5.1–A5.4]. None of these has become universally accepted although the ASTM procedures [A5.3, A5.4] are probably the most widely used. The method described here includes many aspects of the ASTM procedures. Alternative methods are allowed but any departures from the methodology described here must be given when reporting the results as required in **Section 8.5** of this procedure.

In the unloading compliance test, the elastic compliance C_k is determined at each unloading/reloading event performed during the test from

$$C_k = \left(\frac{\Delta Q}{\Delta P} \right)_k$$

where Q is the appropriate displacement or strain.

The crack length a_k at each unloading is determined from the measured compliance C_k using theoretical or experimental correlations in the form

$$(a/W)_k = f(C_k)$$

Data recording and evaluation of the partial unloadings may be accomplished with a computer or autographically with an x-y recorder. For M(T) specimens no recommendation concerning the unloading compliance technique is available.

A5.1.1 Test Requirements

The test requirements given in **Section 3** of this Procedure must be adhered to in conjunction with the following additional points.

A5.1.1.1 Specimens

Prepare sidegrooved specimens to the specification given in **Section 2** of the Procedure with an initial crack length a_0 in the range $0.45 \geq a_0/W \geq 0.65$.

A5.1.1.2 Test fixtures

For compact specimen testing, the clevis must have a flat bottomed hole, **Fig. 11**. Hardened steel inserts between the loading pin and clevis may help in minimising plastic indentation [A5.5]. Steel inserts can also be used between the single edge notch bend specimen and the outer rollers [A5.6]. Care must be taken to retain the inserts in place during a test in order to avoid accidents.

A5.1.1.3 Compliance measurement

Unloading compliance is determined from either mouth opening or load point displacements, **Section 3.4**. If the displacement is measured at an alternative point, then the appropriate compliance function must be evaluated. For bend specimens, compliance can be measured from the load-point displacement transducer used to determine J. However, it is recommended that an additional transducer should be used and be located at the mouth of the crack as for crack opening displacement.

Errors may occur in the compliance measurements as a result of transducer non-linearity. Significant improvement in accuracy is possible by curve fitting the lowest order polynomial function as possible through the calibration data [A5.7]. The maximum deviation of an individual data point to the curve fit should be within ± 0.2 percent of the calibrated range.

A5.1.1.4 Digital signal resolution

For an unloading compliance measurement, the digitised displacement resolution Δq should be better than

$$\Delta q = \frac{W' R_{p0.2}}{500E}$$

where W' is the minimum of 50 mm or the specimen width.

The corresponding digital force resolution ΔF should be better than

$$\Delta F = \frac{BW' R_{p0.2}}{15000}$$

For the duration of a test, stability of the digitised force and displacement signals should be less than $\pm 4\Delta F$ or $\pm 4\Delta q$, whichever is appropriate. The maximum signal noise should be less than $\pm 2\Delta F$ or $\pm 2\Delta q$, whichever is appropriate.

A 16 bit A-D converter will meet the requirements for most applications. It is permissible to amplify the force and displacement signals to attain a satisfactory level for digitisation.

A5.1.1.5 Autographic signal resolution

When unloading compliance measurements are derived directly from x-y plots, the pen displacement should be greater than 100 mm in both axes. Pen stability should be within ± 3 mm throughout the duration of the test.

A5.1.2 Procedure

A5.1.2.1 Pre-cycling

Before commencing the test it is recommended that the specimen be cycled several times in the elastic regime at test temperature to allow the specimen to 'bed-in'. During this operation the maximum applied force must not exceed the final fatigue force.

A5.1.2.2 Loading rate

The loading rate during unload/reload cycles should be as fast as possible to minimise time dependent effects but slow enough to ensure that sufficient data is recorded to enable the compliance of the specimen to be estimated accurately.

If possible the loading rate during the unload/reload cycles should not be less than that employed between the unloadings. It is recommended that prior to each unloading the displacement should be held constant until force relaxation caused by time dependent plasticity effects is observed to cease.

A5.1.2.3 Initial crack length measurement

At least three unloading compliance measurements should be made at a force less than the maximum allowable final fatigue force defined in **Section 2.3.1.3** of the procedure. No value of the estimated crack length shall differ from the mean by more than ± 0.1 mm. The maximum range of the unload/reload cycles should not exceed 50 percent of the actual maximum force used to measure the three initial unloadings.

Non-linear parts of the force displacement record that may occur at low forces from crack closure effects should be excluded from the compliance measurement.

A5.1.2.4 Crack length measurements

Partially unload and reload the specimens at intervals during the test. The unloadings should be performed at displacement intervals selected to ensure evenly spaced data points are obtained. Typically 30 unloadings are sufficient to define the crack extension fracture resistance behaviour and meet the data spacing requirement given in **Section 7.4**. It is recommended that the unloading range should be as small as practicable but not exceed 30 percent of the current force value. To improve the accuracy at lower forces it is permissible to exceed this limit. However, in such cases non-linear parts of the force-displacement record that may occur at low forces from crack closure effects should be excluded from the compliance measurement.

At each unloading evaluate the crack length a and δ_5 or J , as appropriate, using the formulae given in **Sections A.5.1.5**, **A5.1.3** and **A5.1.4** of the Procedure, respectively. The compliance of the specimen, C , is obtained by dividing the change in crack mouth opening or load-point displacement by the corresponding change in force. In the case of computerised test systems, the compliance is generally determined by performing a regression analysis of the recorded data.

A5.1.2.5 Termination of test

After the final unloading reduce the force to zero ensuring no further increase in displacement. Mark the extent of ductile crack growth as described in **Section 4.3.2** of the procedure. Break open the specimen at or below room temperature to reveal the fracture surfaces. Measure the initial crack length a_0 and the total crack growth using the procedure described in **Section 4.2**.

A5.1.3 Crack Tip Opening Displacement, δ_5

The crack tip opening displacement, δ_5 , is measured directly in this Procedure, **Section 3.4.3**.

A 5.1.4 Fracture Resistance J

A5.1.4.1 Calculate $J_{o,k}$ for compact and single edge cracked bend specimens at the k-th data point on the load displacement record using the relationship

$$J_{o,k} = \frac{\eta U_k}{B_n(W - a_o)}$$

where $\eta = 2 + 0.522(1 - a_o/W)$ for C(T) specimens
 $= 2$ for SE(B) specimens

and U_k is the area under the force displacement record up to the line of constant displacement at the k th data point.

A5.1.4.2 Fracture resistance J allowing for crack extension

The J equations used in **Section A5.1.4.1** do not allow for crack extension during a test. The errors in J are usually negligible for crack extension less than 0.1 (W-a_o). If crack extension is analysed beyond this value, then all data points should be corrected for crack extension. A suitable approximation for compact and single edge cracked bend specimens is given in **Clause 7.2.1.3**.

A5.1.5 Crack Tip Opening Angle, ψ

The crack tip opening angle is determined according to **Section 8.2**.

A5.1.6 Crack Length Calculation

A5.1.6.1 C(T) specimens

The crack length corresponding to a specimen compliance, C, determined from the load line displacement is given by

$$a/W = 1.000196 - 4.06319\mu + 11.242\mu^2 - 106.043\mu^3 + 464.335\mu^4 - 650.677\mu^5$$

where

$$\mu = \frac{1}{[B_{\text{eff}}E_M C]^{1/2} + 1}$$

$$B_{\text{eff}} = B - \frac{(B - B_n)^2}{B}$$

and E_M , the effective Young's Modulus, is determined from

$$E_M = \frac{1}{C_o B_{\text{eff}}} \left(\frac{W + a_o}{W - a_o} \right)^2 \left[2.163 + 12.219 \left(\frac{a_o}{W} \right) - 20.065 \left(\frac{a_o}{W} \right)^2 \right. \\ \left. 0.9925 \left(\frac{a_o}{W} \right)^3 + 20.609 \left(\frac{a_o}{W} \right)^4 - 9.9314 \left(\frac{a_o}{W} \right)^5 \right]$$

C_o is the average compliance determined from the unloadings performed in the elastic regime, **Section A5.1.2.3.**

The effective modulus E_M fits the above equation to the crack length a_o measured in **Section A5.1.2.5.** The effective modulus E_M is then used to calculate all crack lengths for the specimen under consideration. Should E_M deviate from a known value of Young's modulus, by more than 10 percent then the test is not valid.

A5.1.6.2 Rotation correction for compact specimens

To account for the change in specimen geometry that occurs from loading, the measured load-line compliance should be corrected for rotation according to

$$C_c = \frac{C}{\left[\left(\frac{h}{r} \sin \theta - \cos \theta \right) \left(\frac{D}{r} \right) \sin \theta - \cos \theta \right]}$$

- where
- C = measured compliance
 - C_c = compliance corrected for rotation
 - h = one half of the initial distance between the centres of the loading pin holes, **Fig. 6.**
 - r = radius of rotation given by $\frac{W + a}{2}$ where a is the current crack length
 - D = one half of the initial distance between the displacement measurement points.
 - θ = the angle of rotation given by $\arcsin \left[\left(\frac{q}{2} + D \right) / \left(D^2 + r^3 \right)^{1/2} \right] - \arctan \left(\frac{D}{r} \right)$
 - q = total measured load line displacement

A5.1.6.3 SE(B) specimens under three-point bending with crack mouth opening displacement measured at specimen surface

The crack length corresponding to a specimen compliance, C , determined from mouth opening displacement measured at the surface is given by

$$a/W = 0.999748 - 3.9504\mu + 2.9821\mu^2 - 3.21408\mu^3 \\ + 51.51564\mu^4 - 113.031\mu^5$$

where

$$\mu = \frac{1}{\left[\left(\frac{4W}{S} \right) B_{\text{eff}} E_M C \right]^{1/2} + 1}$$

$$B_{\text{eff}} = B - (B - B_n)^2 / B$$

and E_M , the effective Young's Modulus, is determined from:

$$E_M = \frac{6S}{B_{\text{eff}} W C_o} \left(\frac{a_o}{W} \right) \left[0.76 - 2.28 \left(\frac{a_o}{W} \right) + 3.87 \left(\frac{a_o}{W} \right)^2 \right. \\ \left. - 2.04 \left(\frac{a_o}{W} \right)^3 + \frac{0.66}{(1 - a_o / W)^2} \right]$$

C_o is the average compliance determined from the unloadings performed in the elastic regime, **Section A5.1.2.3**.

The effective modulus E_M fits the above equation to the crack length a_o measured in **Section A5.1.2.5**. The effective modulus E_M is then used to calculate all crack lengths for the specimen under consideration. Should E_M deviate from a known value of Young's Modulus by more than 10 percent then the test is invalid.

A5.1.6.4 SE(B) specimens under three-point bending with compliance based on load point displacement

The crack length corresponding to a specimen compliance, C , determined from load-point displacement for S/W of 4 is given by

$$a/W = 0.07204 + 1.25147 \times 10^{-2}\mu - 1.10295 \times 10^{-4}\mu^2 \\ + 5.28088 \times 10^{-7}\mu^3 - 1.26564 \times 10^{-9}\mu^4 + 1.18958 \times 10^{-12}\mu^5$$

where $\mu = E_M B_{\text{eff}} C$

$$B_{\text{eff}} = B - (B - B_n)^2 / B$$

and E_M , the effective Young's Modulus, is determined from

$$E_M = \frac{1}{B_{\text{eff}} C_o} \left[\left[0.24 \left(\frac{S}{W} \right)^3 (1.04 + 3.238(1 + \nu)(W/S)^2) \right] \right. \\ \left. + 2(1 - \nu^2) \left(\frac{a_o}{W} \right) \left(\frac{S}{W} \right)^2 \left[4.21 \left(\frac{a_o}{W} \right) - 8.89 \left(\frac{a_o}{W} \right)^2 + 36.9 \right. \right. \\ \left. \left(\frac{a_o}{W} \right)^3 - 83.6 \left(\frac{a_o}{W} \right)^4 + 174.3 \left(\frac{a_o}{W} \right)^5 - 284.6 \left(\frac{a_o}{W} \right)^6 \right. \\ \left. \left. + 387.6 \left(\frac{a_o}{W} \right)^7 - 322.8 \left(\frac{a_o}{W} \right)^8 + 149.8 \left(\frac{a_o}{W} \right)^9 \right] \right]$$

C_o is the average compliance determined from the unloadings performed in the elastic regime, **Section A5.1.2.3**.

The effective modulus E_M fits the above equation to the crack length, a , measured in **Section A5.1.2.5**. The effective modulus E_M is then used to calculate all crack lengths for the specimen under consideration. Should E_M deviate from a known value of Youngs Modulus by more than 10 percent then the test is not valid.

A5.1.6.5 Rotation correction for SE(B) specimens

The measured compliance should be corrected to allow for specimen rotation and changes in the test fixture which occur during a test. No explicit formula is given here because of the lack of an agreed approach although a relationship has been developed for mouth opening displacement [**A5.8**].

A5.1.7 Crack Extension Fracture Resistance

Ideal crack extension fracture resistance behaviour is characterised by monotonically increasing crack extension, **Fig. A5.2**. However, the unloading compliance often does not give this idealised behaviour. Discrepancies may include positive or negative offset from the original estimate of initial crack length, scatter in the data and apparent negative crack extension.

These effects are made worse by problems in the testing fixture, transducer gauge seating, electronic noise and signal non-linearity.

A5.1.7.1 Construction of resistance curves

Plot graphs of either δ_5 or J versus the predicted crack length.

A5.1.7.2 Estimated initial crack length

In order to determine the crack extension fracture resistance behaviour, it is necessary to define the estimated initial crack length, a_i . However, since the unloading compliance technique frequently produces anomalous data no standard method for defining a_i has yet emerged. The three most common methods are:

- (i) Defining a_i as the average crack length obtained from the elastic unloading compliance measured in **Section A5.1.2.3**.
- (ii) Defining a_i as the minimum crack length obtained in the test.
- (iii) Defining a_i in such a way that the early stages of the crack extension behaviour follow the apparent blunting line equations

$$\delta_5 = N\Delta a \text{ or } J = NR_f\Delta a$$

where $l \geq N \geq 6$.

Alternative methods of defining a_i can be used provided details of the method are reported and justified in **Section 8.3** of the Procedure.

It should be noted that the above methods of defining a_i frequently yield similar estimates. However for crack extension fracture resistance behaviour which exhibit apparent negative crack extension, the estimates can be significantly different.

A5.1.7.3 Estimated crack extension

Calculate the estimated crack extension Δa_k at the k-th unloading from

$$\Delta a_k = a_k - a_i.$$

A5.1.7.4 Crack extension resistance curves

Construct plots of δ_5 or J versus estimated crack extension Δa_k .

A5.1.7.5 At least 5 data points should remain within 0.2 mm of a_i in order to adequately describe the initial portion of the crack extension fracture resistance curve.

A5.2 Potential Drop Techniques

Two DC potential drop methods are described in this section.

A5.2.1 Method 1: Predictive Method

- (i) The preferred DC potential drop test system [A5.11-A5.14] is shown in **Fig. A5.3**.
- (ii) Load the specimen as described in **Section 4** of the Procedure and obtain records of force against displacement and potential. The general form of the load-potential test record is illustrated in **Fig. A5.4**.
- (iii) On completion of the test mark the extent of stable crack extension as described in **Section 4.3.2** before breaking the specimen open.
- (iv) Measure the initial crack length a_0 and the total crack extension, Δa , as described in **Section 4.2** of the Procedure.

A5.2.1.1 Interpretation of test records

- (i) Construct a straight line through the steeply rising part of the force potential record as shown in **Fig. A5.4**.
- (ii) For any force of interest measure ϕ_0 and $\Delta\phi$ as shown in **Fig. A5.4** and evaluate
$$\phi = \phi_0 + \Delta\phi$$
- (iii) The crack length corresponding to the selected force can be calculated using the following expression

$$a = \frac{2W}{\pi} \cos^{-1} \left\{ \frac{\cosh(\pi y / 2W)}{\cosh\left[(\phi / \phi_0) \cosh^{-1}(\cosh(\pi y / 2W) / \cos(\pi a_0 / 2W))\right]} \right\}$$

where y is defined in **Fig. A5.3**

- (iv) The corresponding crack extension Δa is given by

$$\Delta a = a - a_0.$$

A5.2.2 Method 2

- (i) An alternative DC potential drop system [A5.6] for Method 2 is shown in **Fig. A5.5**.
- (ii) Load the test specimen as described in **Section 4** of the procedure and obtain test records of both force and potential versus either load-point or mouth opening displacement. The general form of the test records is illustrated in **Fig. A5.6**.
- (iii) On completion of the test mark the extent of ductile crack extension as described in **Section 4.3.2** before breaking the specimen open.
- (iv) Measure the initial crack length, a_0 , and the total crack extension, Δa , as described in **Section 4.2** of the Procedure.

A5.2.2.1 Interpretation of test records

- (i) The abrupt change in slope of the potential displacement record is used as an estimate of the initiation of ductile tearing.
- (ii) Measure the potential difference ($\Delta\phi_{\text{end}}$) between estimated initiation of ductile tearing and the potential at the end of the test.
- (iii) Construct a graph of total crack extension versus potential difference.

- (iv) Plot the points $\Delta a_{szw}, \Delta\phi = 0$ and $\Delta a, \Delta\phi_{end}$ and draw a straight line between them. This straight line represents the calibration line for the specimen.
- (v) To determine the amount of total crack extension corresponding to a point F_x on the force-displacement record measure the potential difference between ϕ_{min} and ϕ_x as indicated in **Fig. A5.6**. The amount of total crack extension corresponding to $\Delta\phi_x$ can be estimated from the calibrated line from (iv).

A5.2.3 Crack Extension Fracture Resistance Curves

A5.2.3.1 Crack tip opening displacement, δ_5

The crack tip opening displacement, δ_5 , is measured directly in this Procedure.

A5.2.3.2 Fracture Resistance J

Determine J for compact and single edge cracked specimens at the force F_x using the equations given in **Section A5.1.4**.

For M(T) specimens use the relationship

$$J_{0,k} = \frac{K^2}{E} + \frac{U^*}{B(W - a_0)}$$

This equation does not allow for crack extension during a test. The errors in J are usually negligible for crack extension less than 0.1 (W-a₀). If crack extension is analysed beyond this value, then all data points should be corrected for crack extension. A suitable approximation is

$$J_j = J_{j-1} + \frac{2\Delta U^*}{B(b_{j-1} + b_j)} + \frac{2}{E(b_{j-1} + b_j)} [K_j^2 b_j - K_{j-1}^2 b_{j-1}]$$

where

j and j-1 indicate two consecutive points on the test record,

ΔU^* is defined in **Fig. A5.10**,

b is the current ligament length W-a,

K is the stress intensity factor.

A5.2.3.3 Construction of resistance curves

Plot graphs of either δ_5 or J versus the predicted crack length.

REFERENCES

Unloading Compliance Technique

- [A5.1] Neale, B.K., Curry, D.A., Green, G., Haigh, J.R. and Akhurst, K.N., 1985, *Int. J. Pressure Vessels and Piping*, A procedure for the determination of the fracture resistance of ductile steels, 20(3), 155–179.
- [A5.2] Gordon, J.R., 1985, WI Report 275/1985, The Welding Institute Procedure for the Determination of the Fracture Resistance of Fully Ductile Steels.
- [A5.3] ASTM Standards, 1993, E1152-87 Standard Test Method for Determining J-R Curves, Section 3, Vol. 03.01, 853–863.
- [A5.4] ASTM Standards, 1990, E813-89 J_{Ic} , A Measure of Fracture Toughness, Section 3, Vol. 03.01, 700–714.
- [A5.5] Voss, B., 1983, On the problem of 'Negative Crack Growth' and 'Load Relaxation' in single specimen partial unloading compliance tests, CSNI Workshop on Ductile Fracture Test Methods, Paris, 210–219.
- [A5.6] Hellmann, D., Rohwerder, G. and Schwalbe, K.-H., 1984, Development of a test set up for measuring the deflection of single-edge notch bend (SENB) specimens, *J. of Testing and Evaluation* 12, 42–44.
- [A5.7] Gordon, J.R., 1986, WI Report 325/1986, An assessment of the accuracy of the unloading compliance method, for measuring crack growth resistance curves.
- [A5.8] Steenkamp, P.A.J.M., 1985, J-R curve testing of three point bend specimens by the unloading compliance method, Presented at 18th National Symposium on Fracture Mechanics, Boulder, Colorado, USA, June 25–27.
- [A5.9] Futato, R.J., Aadland, J.D., Van der Sluys, W.A. and Lowe, A.L., 1985, ASTM STP 856, A sensitivity study of the unloading compliance single specimen J-test technique, 84–103.
- [A5.10] Schwalbe, K.-H., Hayes, B., Baustian K., Cornec, A., Gordon, R., Homayun, M., and Voss, B., 1993, Validation of the fracture mechanics test method EGF P1-87D (ESIS P1-90/ESIS P1-92), *Fatigue and Fracture of Engineering Materials and Structures*, Vol. 16, 1231–1284.

Potential Drop Technique

- [A5.11] Roo, de P. and Marandet, B., 1982, Application of the AC potential method to the detection of initiation in static and dynamic testing, in: *Ductile Fracture Test Methods*, Proceedings of a CSNI Workshop, OECD, Paris, 1–3 December.
- [A5.12] Schwalbe, K.-H., Hellmann, D., Heerens, J., Knaack, J. and Müller-Roos, J., 1985, Measurement of stable crack growth including detection of initiation of growth using the DC potential drop and the partial unloading methods, *ibid*, 338–362.
- [A5.13] Schwalbe, K.-H. and Hellmann, D., 1981, *J. Testing and Evaluation*, Application of the electrical potential method to crack length measurements using Johnson's formula, 9, 218–221.
- [A5.14] Dietzel, W. and Schwalbe, K.-H., 1986, Monitoring stable crack growth using a combined a.c./d.c. potential drop technique, *Materialprüfung*, 28, 368–372.

- [A5.15] Johnson, H.H., 1965, *Materials Research and Standards*, Calibrating the electric potential method for studying slow crack growth, 5, 442–445.
- [A5.16] Hollstein, T., Blauel, J.G., and Voss, B., 1985, *ASTM STP856*, On the determination of elastic-plastic fracture material parameters: A comparison of different test methods, 104–116.
- [A5.17] Okomura, K., Venkatasubramanian, T.V., Unvala, B.A. and Baker, T.J., 1981, *Engineering Fracture Mechanics*, Application of the AC potential drop technique to the determination of R-curve of tough ferritic steels, 14, 617–625.
- [A5.18] Prantl, G., 1982, Assessment of crack extension by different methods, *Proceedings of a CSNI Workshop, OECD, Paris, 1–3 December*.
- [A5.19] Berger, C. and Vahle, F., 1982, Application of the DC potential method to prediction of crack initiation, *Proceedings of a CSNI Workshop, OECD, Paris, 1–3 December*.
- [A5.20] Debel, C.P. and Adrian, F., 1982, Experience with ductile crack growth measurements applying the DC-PD technique to compact tension fracture specimens, *Proceedings of a CSNI Workshop, OECD, Paris, 1–3 December*.
- [A5.21] Schwalbe, K.-H., Hayes, B., Baustian K., Cornec, A., Gordon, R., Hodayun, M., and Voss, B., 1993, Validation of the fracture mechanics test method DGF P1-87D (ESIS P1-90/ESIS P1-92), *Fatigue and Fracture of Engineering Materials and Structures*, Vol. 16, 1231–1284.

Figure A5.1:
Single specimen crack extension termination requirement.

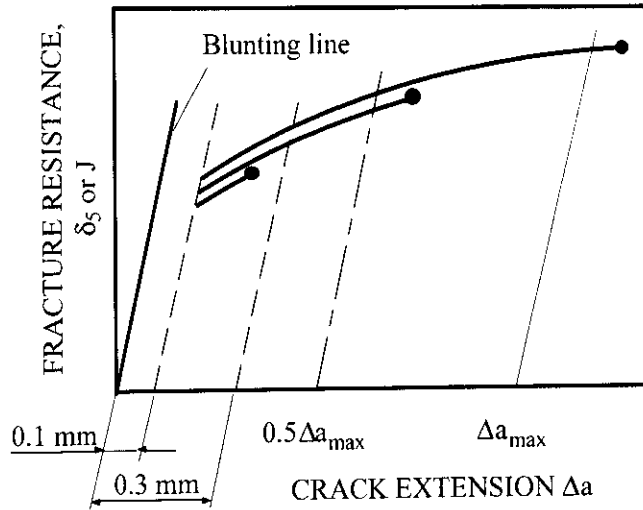


Figure A5.2:
Ideal behaviour of crack extension fracture resistance curve.

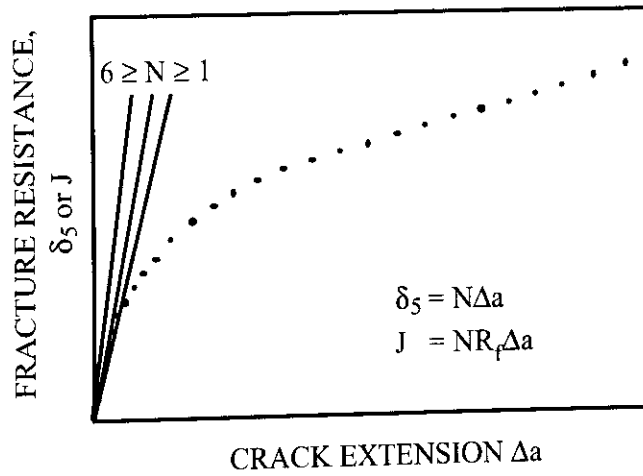
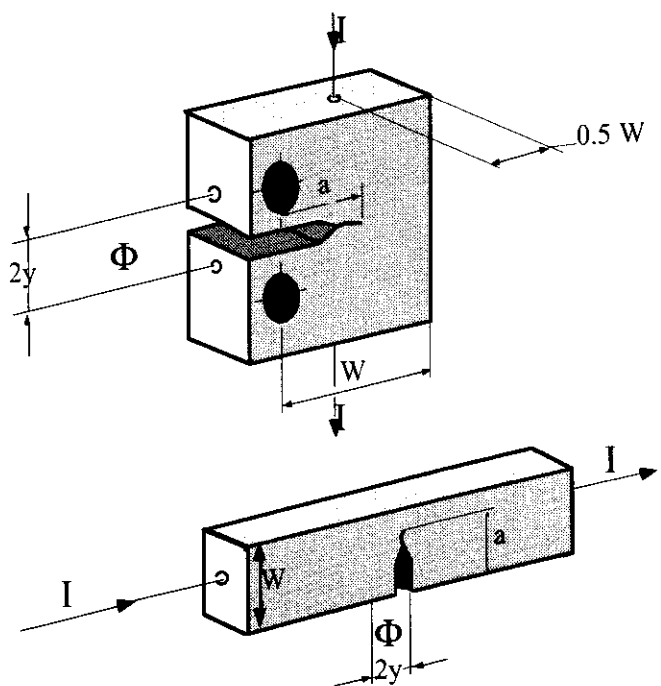


Figure A5.3:
Preferred DC potential drop test system.



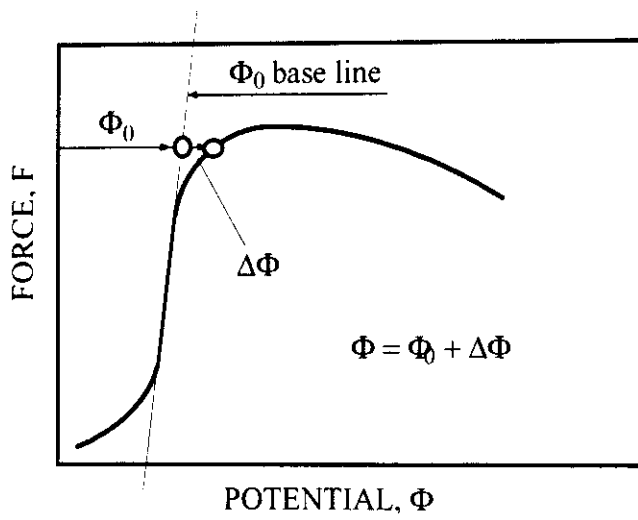


Figure A5.4:
Typical DC potential drop test record
for system shown in Fig. A5.3.

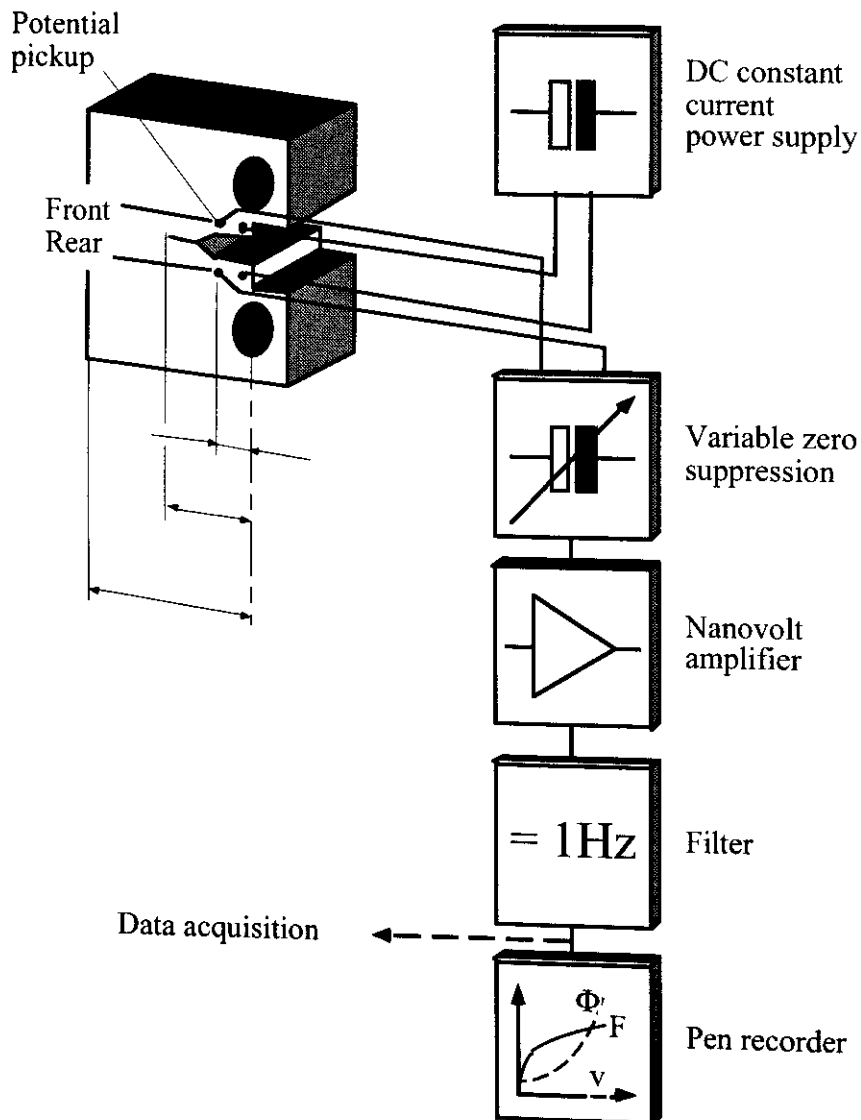


Figure A5.5:
Alternative DC potential
drop test system.

Figure A5.6:
 Typical DC potential drop test record for system shown in Fig. A5.5.

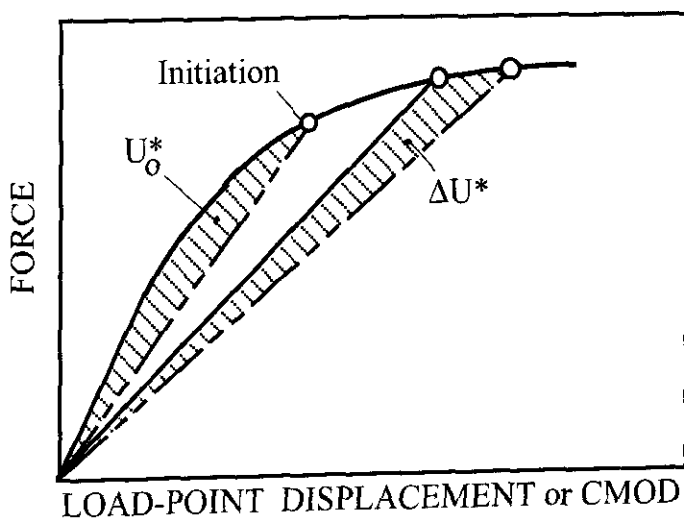
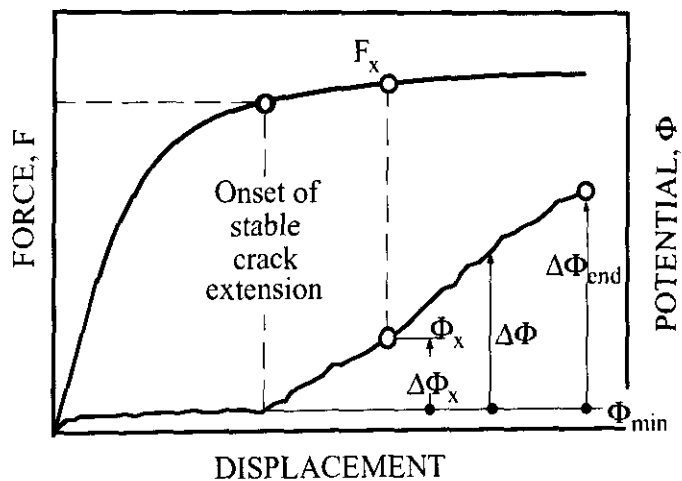


Figure A5.7: Definition of ΔU^* .

NOTE: If the force at any point of the diagram to be evaluated exceeds $1.8 R_{p0.2}BW$, then evaluate U^* and ΔU^* from a force versus CMOD record.

APPENDIX 6: δ_{5i} and J_i Determination

The determination of δ_{5i} and J_i require the use of a scanning electron microscope (SEM) to measure the stretch zone width on the fracture surfaces of the specimens. The method can produce large scatter in the values of δ_{5i} and J_i as a result of the subjective interpretation and measurement of the stretch zone width. Therefore it is desirable to have experience in interpreting SEM fractographs. If the stretch zone width cannot be distinguished from ductile crack extension, δ_{5i} and J_i cannot be determined.

A6.1 Critical Stretch Zone Width Measurement

A6.1.1 Measure the local critical stretch zone width SZW_L at the 9 positions shown in **Figs. 14 to 16** using calibrated photographs taken in a SEM. An example is shown in **Fig. A6.1**. At each location the SEM magnification should be adjusted so that both the start and end of the stretch zone are visible at the same time, **Fig. A6.2**. At least 5 measurements are required at each position giving the local stretch zone width

$$\overline{\Delta a}_{szw,L} = \frac{1}{k} \sum_{i=1}^k \Delta a_{szw,i} \quad \text{for } k \geq 5.$$

A6.1.2 Determine the critical stretch zone width of the specimen by averaging the nine local measurements

$$\overline{\Delta a}_{szw} = \frac{1}{9} \frac{1}{k} \sum_{i=1}^k \Delta a_{szw,L,i}$$

A6.1.3 For each specimen the crack extension Δa measured in **Section 4.2** must be greater than $\Delta a_{szw} + 0.2\text{mm}$. Exclude the data points which fail to meet this requirement from those used to determine the mean critical stretch zone width, $\overline{\Delta a}_{szw}$. At least three data points are required to determine $\overline{\Delta a}_{szw}$.

$$\overline{\Delta a}_{szw} = \frac{1}{j} \frac{1}{k} \sum_{i=1}^j \Delta a_{szw,i} \quad \text{providing } j \geq 3.$$

A6.1.4 For the middle cracked tension specimen, $\overline{\Delta a}_{szw}$ must be obtained from the average measurement ahead of both fatigue pre-cracks.

A6.2 δ_{5i}

A6.2.1 Construct a plot of the δ_5 - Δa data obtained in **Sections 4** and **7.1** and the critical stretch zone widths Δa_{szw} as shown in **Fig. A6.3**.

A6.2.2 Construct a line parallel to the δ_5 -axis through the mean of the stretch zone width data $\overline{\Delta a_{szw}}$ as shown in **Fig. A6.3**. Evaluate and draw the best fit curve through all the δ_5 - Δa data which exceeds $\overline{\Delta a_{szw}}$ using the Procedure given in **Section 7.5.1**. The intercept of the curve with the parallel line defines δ_{5i} . Construct a line through the intersection point and the origin. At least one δ_5 - Δa point should be within 0.2mm of this line.

A6.2.3 If δ_{5i} exceeds δ_{5max} determined in **Section 7.6**, then δ_{5i} is invalid according to this Procedure.

A6.2.4 Evaluate the slope of the δ_5 - Δa curve at the intersection point using the equation determined in **Section A6.2.2**. If the slope of the line constructed in **Section A6.2.2**

$$\left(\frac{d\delta_5}{da}\right)_L < 2\left(\frac{d\delta_5}{da}\right)_i,$$

then δ_i or δ_{5i} is invalid according to this Procedure.

A6.3 J_i

A6.3.1 Construct a plot of the J-data obtained in **Sections 4** and **7.2** and the critical stretch zone widths Δa_{szw} as shown in **Fig. A6.3**.

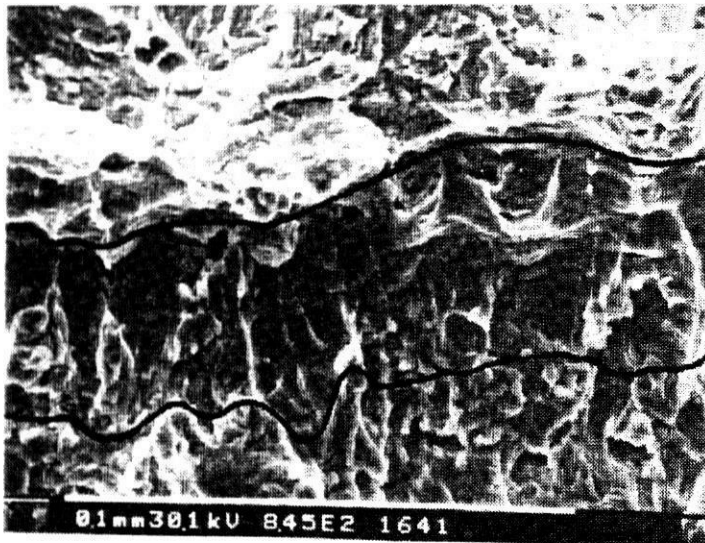
A6.3.2 Construct a line parallel to the J-axis through the mean of the critical stretch zone width data $\overline{\Delta a_{szw}}$ as shown in **Fig. A6.3**. Evaluate and draw the best fit curve through the J- Δa data which exceeds $\overline{\Delta a_{szw}}$ using the procedure given in **Section 7.5.1**. The intercept of the curve with the parallel line defines J_i . Construct a line through the intersection point and the origin. At least one J- Δa point should be within 0.2mm of this line.

A.6.3.3 If J_i exceeds J_{max} determined in **Section 7.7**, then J_i is invalid according to this procedure.

A6.3.4 Evaluate the slope of the J- Δa curve at the intersection point using the equation determined in **Section A6.3.2**. If the slope of the line constructed in **Section A6.3.2**.

$$\left(\frac{dJ}{da}\right)_L < 2\left(\frac{dJ}{da}\right)_i,$$

then J_i is invalid according to this Procedure.



- Fracture after test loading
- ↑ End
- ZW (40μm)
- ↓ Begin
- Fatigue crack

Figure A6.1: Typical stretch zone width.

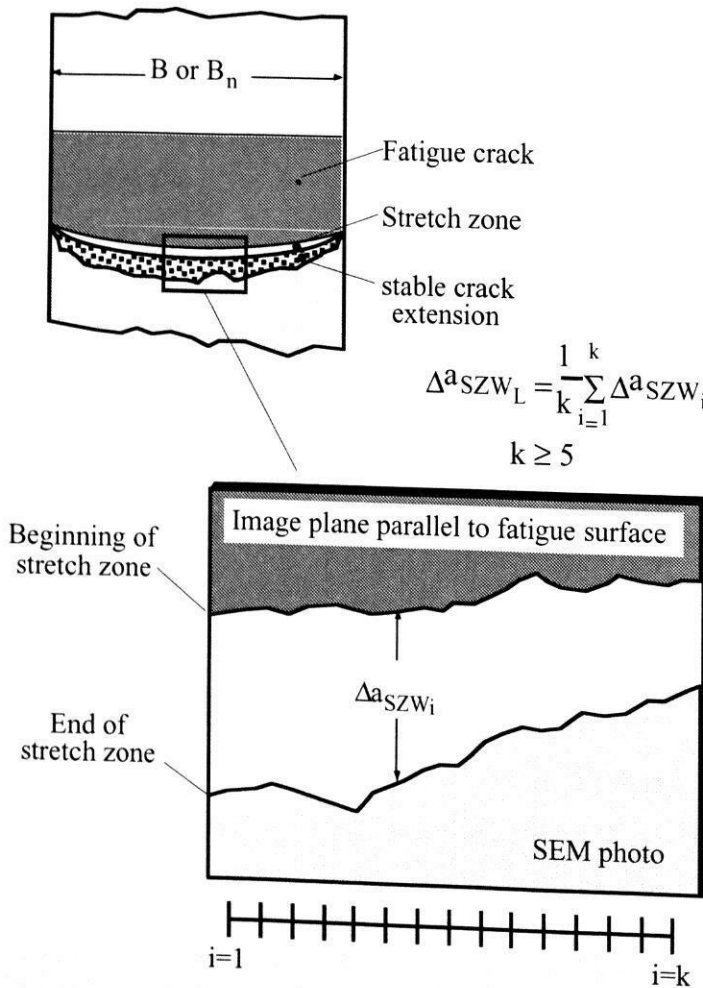
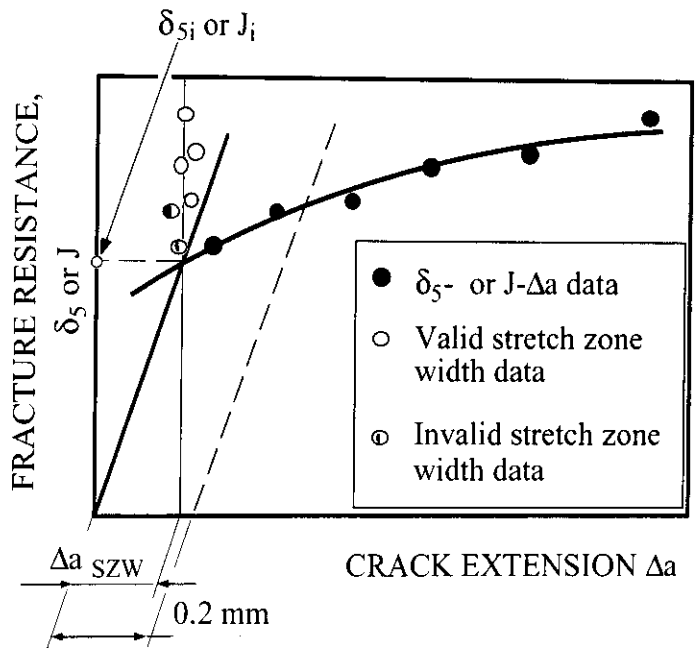


Figure A6.2:
Determination of Δa_{SZW} .

Figure A6.3:

Determination of δ_{5i} and J_i



REFERENCES

- [A6.1] Heerens, J., Cornec, A. and Schwalbe, K.-H., 1988, Results of a round robin on stretch zone width determination, *Fatigue Fract. Engng. Mater. Struct.* Vol. 11, No. 1, 19–29.
- [A6.2] Schwalbe, K.-H., Hayes, B., Baustian, K., Cornec, A., Gordon, R., Homayun, M., Voss, B., 1993, Validation of the fracture mechanics test method EGF P1-87D, (ESIS P1-90/ESIS P2-92), *Fatigue Fract. Mater. Struc.*, Vol. 16, No. 11, 1231–1284.
- [A6.3] Schwalbe, K.-H., Hayes, B., Baustian, K., Cornec, A., Gordon, R., Homayun, M., Voss, B., 1993, Validation of the fracture mechanics test method DGF P1-87D, (ESIS P1-90/ESIS P2-92), *Fatigue Fract. Engng. Mater. Struc.*, Vol. 16, No. 11, 1231–1284.

APPENDIX 7: Determination of the Blunting Line from Tensile Properties

The blunting line describes the initial behaviour of the fatigue pre-crack in a fracture specimen under monotonically increasing loads prior to ductile crack extension. The true stress-strain curve of the material is represented by the power law

$$\frac{\varepsilon}{\varepsilon_0} = \left(\frac{\sigma}{\sigma_0} \right)^{1+N} \quad \text{for } \sigma \geq \sigma_0$$

where σ_0 is the reference stress, ε_0 is the reference strain equivalent to σ_0/E , N is the strain hardening exponent and E is Young's modulus.

The slope of the blunting line is determined from

$$\Delta a_B = 0.4 d_N^* \frac{J}{E}$$

where the proportionality constant d_N^* is a function of N and σ_0/E used to describe the stress-strain curve. A method is given in this Appendix for estimating d_N^* assuming plane strain conditions prevail.

A7.1 Measure the stress-strain behaviour of the material at the same temperature as the fracture tests and determine Young's modulus E , yield strength $R_{p0.2}$ and ultimate tensile stress R_m . The longitudinal dimension of the tensile specimen must be normal to the crack plane of the specimens and be in the same material condition.

A7.2 Determine the strain hardening exponent N from

$$\frac{R_{p0.2}}{R_m} = \frac{1}{1 + \varepsilon_{p0.2}} \left\{ \frac{27181 \ln(1 + \varepsilon_{p0.2})}{N} \right\}^N$$

where

$$\varepsilon_{p0.2} = \frac{R_{p0.2}}{E} + 0.002$$

A graphical solution for n is given in **Fig. A7.1**.

A7.3 Determine the reference stress σ_0 from

$$\sigma_0 = R_{p0.2} 10^t$$

where

$$t = \frac{N \lg(E \varepsilon_{p0.2} / R_{p0.2})}{N - 1}$$

A7.4 δ_5 Blunting line

d_N^* is given graphically in Fig. A7.2 for n of 0.3. Alternatively, d_N^* can be determined using the equation

$$d_N^* = \epsilon_0^{N-1} \cdot D_n$$

where $D_N = A_0 + A_1N + A_2N^2 + A_3N^3 + A_4N^4 + A_5N^5$

N is the strain hardening exponent, and the coefficients of the polynomial are

$$\begin{aligned} A_0 &= 0.787 \\ A_1 &= 1.554 \\ A_2 &= -2.45 \\ A_3 &= 16.952 \\ A_4 &= -38.206 \\ A_5 &= 33.13 \end{aligned}$$

The slope of the blunting line is given by

$$\Delta a_B = 0.8d_N^* \left(\frac{R_{p0.2}}{E} \right) \delta_5$$

A suitable approximation is given by

$$\Delta a_B = \frac{\delta_5}{1.87(R_m / R_{p0.2})}$$

A7.5 J Blunting Line

Evaluate d_N^* as described in Section A7.4. The slope of the blunting line is given by

$$\Delta a_B = 0.4d_N^* \frac{J}{E}$$

A suitable approximation is given by

$$\Delta a_B = \frac{J}{3.75R_m}$$

REFERENCES

- [A71] Cornec, A., Heerens, J. and Schwalbe, K.-H., 1986, Bestimmung der Rispitzenaufweitung CTOD und Riabstumpfung SZW aus dem J-Integral, GKSS Report 86/E/15. GKSS-Forschungszentrum Geesthacht GmbH, Geesthacht, Germany.
- [A7.2] Schwalbe, K.-H., 1984, Crack Tip Opening Displacement for Work-Hardening Materials, *International Journal of Fracture*, 25, R49–R52.
- [A7.3] Schwalbe, K.-H., Heerens, J., Hellmann, D. and Cornec, A., 1986, Relationships Between Various Definitions of the Crack Tip Opening Displacement, published in *The Crack Tip Opening Displacement in Elastic-Plastic Fracture Mechanics*, edited by K.-H. Schwalbe, Springer-Verlag.
- [A7.4] Landes, J.D., 1995, The blunting line in elastic-plastic fracture. *Fatigue and Fracture of Engineering Materials and Structures*, V. 18, No. 11, 1289–1297.

Figure A7.1:
Determination of strain hardening exponent, N .

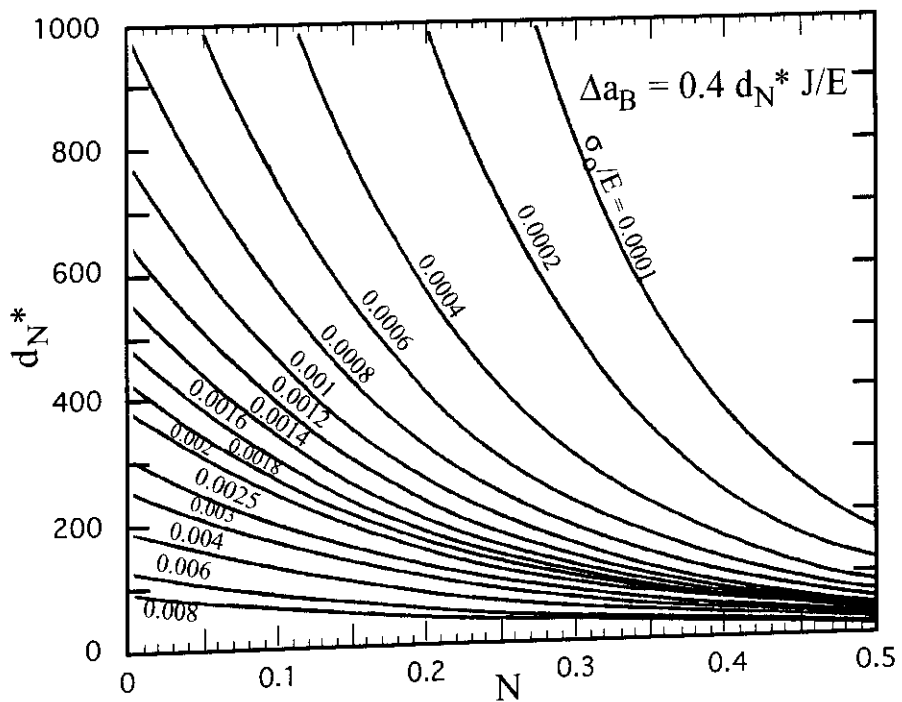
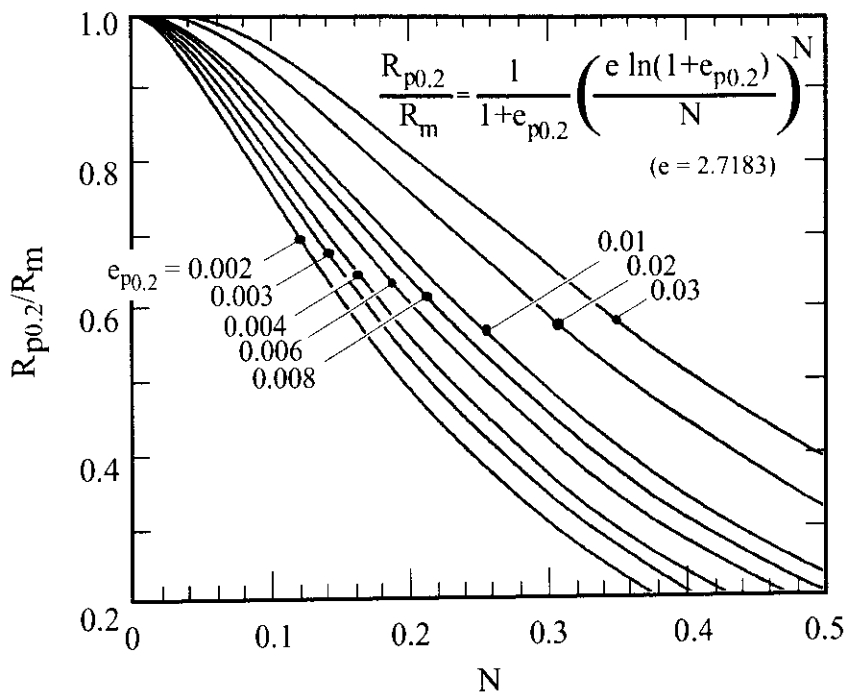


Figure A7.2:
Determination of d_N^* .

APPENDIX 8: Offset Power Law Fit to Crack Extension Fracture Resistance Data

A 8.1 The equation fitted to the crack extension data ($y_i, \Delta a_i$) is of the general form

$$y = A + C\Delta a^D$$

where y is either J or δ_5 , Δa is the crack extension, A , C and D are constants.

A 8.2 The substitution of $x = \Delta a^D$ in the equation enables A and C to be evaluated using linear regression available in statistical analysis packages or hand calculators. The value of D is then chosen so as to maximise the correlation coefficient. An approach for doing this is given below.

A 8.3 Take values of D from 0 to 1 in steps of 0.01. For each value of D calculate $x_i = \Delta a_i^D$ and the correlation coefficient r from

$$r = \frac{S_{xy}}{\sqrt{S_{xx}S_{yy}}}$$

where

$$S_{xx} = \sum x_i^2 - \frac{(\sum x_i)^2}{N}$$

$$S_{yy} = \sum y_i^2 - \frac{(\sum y_i)^2}{N}$$

$$S_{xy} = \sum x_i y_i - \frac{\sum x_i \sum y_i}{N}$$

for the N data points.

A 8.4 Select the value of D which maximises r . Evaluate the corresponding A and C from

$$C = \frac{S_{xy}}{S_{xx}} \text{ and } A = \bar{y} - C\bar{x}$$

where

$$\bar{x} = \frac{\sum x_i}{N} \text{ and } \bar{y} = \frac{\sum y_i}{N}$$

REFERENCE

- [A8.1] Neale, B. K., 1993, On the best fit curve through crack growth fracture resistance data, *Fatigue Fract. Engng. Mater. Struct.*, 16, 465–472

APPENDIX 9: Testing of Weldments

The testing and evaluation procedure outlined in this Appendix was mainly generated from the investigations in Ref. [A9.1-A9.7]. It covers the following subjects:

- Determination of tensile properties of weldments,
- Determination of fracture toughness values of weldments using SE(B) or M(T) specimens.

This Appendix provides information on the special features of weld joint testing. The following points represent the main differences to the testing of homogeneous materials:

- Determination of tensile properties,
- Fatigue precracking,
- Definition of the microstructure at the fatigue crack front,
- Evaluation of J.

Once this information has been obtained using this Appendix, fracture properties can be determined according to **Sections 1 to 8** of this Procedure.

A9.1 Terminology:

Base Metal (BM)

Metal to be welded.

Weld Metal (WM)

All melted and solidified metal as well as stirred metal (in case of friction stir weld, FSW) during welding process.

Heat Affected Zone (HAZ)

The unmelted base metal zone but metallurgically affected by the thermal cycle of the welding process.

CGHAZ

Coarse grained HAZ (a HAZ region adjacent to the fusion line).

Fusion Line (FL)

Metallurgically visible border between weld metal and heat affected zone.

Post Weld Heat Treatment (PWHT)

Heat treatment made to reduce the welding residual stresses or to improve the weld joint properties.

Weld Width (2H)

The distance between two fusion lines of the weld metal. Note the different widths of the welds at top ($2H_{top}$) and root ($2H_{root}$) sides of the welds as well as narrow mid-thickness width ($2H_{mid}$) in case of X-groove.

Strength Mis-Match Ratio (M)

The ratio of yield strength of weld metal to base metal ($M = R_{p0.2}^W / R_{p0.2}^B$).

$M > 1$ Overmatching

$M < 1$ Undermatching

Target Area

The specific weld region intended to be tested (e.g. CGHAZ), weld centre line etc.). The target area shall be defined by pre-test metallography including hardness test and shall suitably be covered by the central thickness of the specimen.

Fracture Path Deviation (FPD)

Deviation of stable or unstable fracture path from targeted zone into neighbouring material of different strength due to strength mis-match.

Post Test Metallography and Fractography

Metallurgical examination on one half of the broken specimen for the purpose of identifying fracture location or final fatigue crack tip microstructure with respect to target area. Fractographic examination may be needed to identify the fracture initiation location.

A9.2 Scope

A weld joint comprises the weld metal (WM), the heat affected zone (HAZ) and the base metal (BM) parts, each having different properties. The microstructures and mechanical properties of the WM and HAZ are closely related to the materials (base and consumable) as well as the welding process and procedure used.

The determination of the tensile properties and fracture toughness values of the various parts of a weld presents particular problems due to the heterogeneous nature of the joints, the narrow width of the HAZ, and its microstructural complexity. Therefore, the use of present procedures and standards for mechanical testing of metallic materials require some modifications of specimen preparation, testing, and interpretation of the data of structural weldments. For example, the “micro flat tensile specimen” technique may be used to determine the local tensile properties of the HAZ and narrow power beam weld joints.

The aim of a fracture mechanics testing method is to determine the fracture parameter value which characterizes the resistance to fracture (initiation or crack extension) of a target area of a welded joint. Fracture mechanics tests on weldments can serve two purposes:

- Material selection and welding procedure (incl. PWHT) qualification,
- Defect assessment.

The aim of the first group is to obtain lower bound fracture values. SE(B) or C(T) specimens shall be used, see **Section 2**. The thickness, **B**, should be equal to the full plate thickness. The specimens can have surface cracks or through-thickness cracks, **Fig. A9.1**.

In order to obtain lower bound fracture values for the HAZ, the fatigue crack tip should sample

a maximum amount of lower toughness zones of the HAZ. For this reason, K or 1/2K weld preparations in thick section welds should be used, **Fig. A9.2**.

If the purpose is to assess the significance of a particular defect in a structure, then the notch position and size should simulate the defect of interest. Consequently, a/W can be varied between 0.1 and 0.65. This is because the measured fracture toughness value is dependent on the microstructural and strength gradients in the vicinity of the fatigue crack.

The methods described in this Appendix apply to arc, laser and electron beam welded joints as well as to newly emerging friction stir welds where some new terminology to describe the weld regions needs to be used.

A9.3 Determination of Tensile Properties of Weldments

A9.3.1 All-weld-metal properties

The tensile properties within the weld volume of the multi-pass structural weld metal or of fusion zone of laser and electron beam welds and nugget area of friction stir welds shall be determined using *all-weld-metal* tensile specimens. Standard round tensile specimens parallel to the weld direction should be prepared to determine the local variations in mechanical properties within the multi-pass weld deposit. The root passes or cosmetic top passes of many structural welds may exhibit different strength than the top side of the weld deposit. The average yield and tensile strengths from several round tensile specimens extracted from various locations of the weld metal shall be designated as $R_{p0.2}^W$ and R_m^W , respectively.

If the aim of the tensile test is to determine the strength mis-match ratio (M), this shall be done by obtaining the full stress-strain curves of the base and weld metals. Determining the strain hardening exponents of the base (N_B) and weld metals (N_w) is useful for structural assessment using the ETM-MM [A9.17] or the European SINTAP procedure [A9.18].

A9.3.2 Use of micro-flat tensile specimens for weld and HAZ regions

When tensile properties of thin section welds (e.g laser or electron beam welds as well as friction stir welded materials) or of the HAZ of thick multipass weldments are to be determined, the standard sized round tensile specimens may not be extracted due to the small size of the target area. Micro-flat tensile specimens shall be extracted from the weld and loaded as shown in **Fig. A9.4**.

A9.4 Determination of Fracture Parameter Values of Weldments

A9.4.1 General Aspects

Weldment specimens should as much as possible be representative of the service structure of interest. Factors which affect the toughness of weld metals and heat affected zones (HAZ) are [A9.8]:

- Welding process including the consumable,
- Base metal composition,
- Joint thickness and joint configuration,
- Preheat and interpass temperatures,
- Heat input,
- Welding position and detailed welding procedure,
- Restraint against distortion,
- Post weld heat treatment,
- Other post weld treatments such as plastic deformation,
- Environment, and
- Test temperature.

Also of importance, but in many cases hard to realise is the requirement that the time between welding and testing in the specimen should be identical to the time the component is already in service. Because diffusible hydrogen can reduce the toughness of the weld significantly, it may be necessary to perform a hydrogen release heat treatment. Other post weld heat treatments are not allowed, except when they have been carried out on the component, too.

An overview on the steps in testing a weldment are provided in **Fig. A9.4**.

A9.4.2 Macrosections

The weldments to be tested should represent the base metal, weld consumable, welding procedure and heat treatment. Macro-sections of welds should be prepared to conduct hardness testing and to identify the notch positions (i.e target area) prior to extracting the fracture toughness specimens from the welded plates.

A9.4.3 Specimen type and dimensions

SE(B), C(T), or M(T) specimens as per **Section 2** can be used. It is recommended to use full thickness specimens (B equal to the full thickness of the original welded plate) for weldment testing.

A9.4.4 Preparation of specimen blanks and notch placement

Weld overfill should be removed flush with the original plate surface. In order to minimise any straightening procedure for the specimen blanks extracted from curved or distorted sections, the compact specimen type can be a practical option compared to the single edge cracked bend specimen. Where significant straightening of SE(B) specimens is necessary, the weld region should be kept free of any plastic deformation.

The surfaces of the specimen blank to be notched should be ground and etched to reveal the weld metal and HAZ. After identifying the area of interest, a line should be scribed onto the surface to mark the notch location. The machine notching procedure and dimensional requirements shall be as described in **Section 2.3** of this Procedure. However, a narrow notch width (N) should be selected for narrow welds. For laser and electron beam welds electro-discharge machining with thin wire diameter should be used.

The ratios of weld metal width perpendicular to the weld axis to plate thickness ($2H/B$) and to uncracked ligament ($2H/(W-a)$) affect weldment deformation and fracture behaviour. Therefore, the values of both ratios for each specimen shall be measured from etched specimen blanks and recorded.

A9.4.5 Fatigue precracking

Fatigue precracking shall be performed with the weld specimen to be tested i.e. no intermediate mechanical and/or heat treatment between fatigue precracking and fracture testing is allowed.

Requirements concerning precracking force for the three specimen configurations are given in **Section 2.3.1.3**.

For weld metal notched specimens the value of $R_{p0.2}$ should be taken for the weld metal.

For HAZ notched specimens the lower yield strength of base or weld metal shall be used to avoid any plasticity at the weaker side of the weldment. This also applies for laser and electron beam welds with higher fusion zone strength in case of C-Mn steels and Ti-alloys. In case of Al-alloy welds, presence of lower strength fusion zone, nugget area or HAZ region need to be taken into consideration by using the $R_{p0.2}$ -value of the respective region.

Fracture toughness testing procedures require fatigue precracked specimens with restrictions on the fatigue crack front shape. Therefore, a special precracking procedure may need to be used to obtain uniform fatigue precrack extension across the weld thickness for specimen blanks containing welding residual stresses (as-welded and partially stress relieved specimens).

NOTE: *The through-thickness pattern of the welding residual stresses transverse to the weld length changes from tensile stresses near the surfaces to compression as balancing stress at about midthickness. These residual stress components act as additive stresses to the applied stresses during the cyclic loading. Therefore, during fatigue precracking, compressive stresses normal to the crack plane can counteract to the applied cyclic stresses and thereby decrease the magnitude of effective stress intensity range, thus inhibiting crack extension in that region. However, near the side surfaces extensive crack extension occurs due to the summation of the tensile applied stress and the residual stress component in tension. The development of such irregular fatigue cracks does not meet the test standard requirements for valid CTOD specimen preparation for characterization of welds in the as-welded condition.*

The process of cutting the specimen blanks from a larger weld plate redistributes the residual stresses in the individual blanks and reduces the magnitude of the residual stresses. The as-welded specimens shall be precracked and tested in this condition.

The “stepwise high-R ratio” procedure is recommended for fatigue pre-cracking. The basic principles of this technique are schematically shown in **Fig. A9.5**.

Step I (R=0.1) :

This first step is used to initiate and propagate the fatigue crack to a length of about 1.0 mm at $R = 0.1$. During this step little or no crack extension will occur at midthickness of the specimen.

Step II (R=0.7) :

The R-ratio of the cyclic loading is increased to 0.7 by keeping the same allowable maximum force as in step I.

NOTE: *The increased level of the mean force for a given maximum load will prevent a possible crack tip closure in the compressive residual stress region of the specimen. The applied mean force should be high enough to keep the crack tip open in the midthickness region of the specimen by balancing the compressive stresses. Experience has shown that in most cases using the R-ratio of 0.5 may not provide a high enough mean load to prevent the retardation of crack extension in the compressive residual stress region. Therefore, a higher mean force is required and an R-ratio of 0.7 is recommended in Step II.*

NOTE: *The local compression or reverse bending techniques can not practically be used for highly strength mis-matched welds, thick section high strength steels, dissimilar joints, laser and electron beam welds in an identical manner as well as middle cracked tension specimens. Experience also indicates that the local compression technique can result in extensive fatigue crack extension at mid-thickness of the specimens for 1%B total deformation for some welds. For each weld, time consuming trials are always necessary to establish the optimum degree of deformation.*

NOTE: *Experience indicates that surface crack SE(B) specimens do not exhibit non-uniform fatigue crack front and therefore no special precracking procedure is needed.*

A9.5 Instrumentation and Testing Procedure

Instrumentation and testing for K_{Ic} , δ_5 , and J, requirements, testing procedures and evaluation are basically given in **Sections 3 to 6** of this Procedure.

However, the procedure for evaluating J for welded specimens which exhibit strength mismatch should be modified to take into account the mis-match effects.

A9.5.1 Fracture Parameter δ_5

The δ_5 technique is used as described in **Appendix 4**. **Fig. A9.6** shows the gauge points used for determining δ_5 for M(T) specimens and SE(B) specimens with various notch locations.

A9.5.2 Fracture Parameter J

A9.5.2.1 SE(B) specimens

- (i) Measure the area A between the force versus CMOD record and a straight line parallel to the initial linear slope of the record and intersecting the record at the point to be evaluated, **Fig. 24**.

(ii) Calculate J_o using the relationship

$$J_o = \frac{K^2}{E} + \frac{\eta_{pl}^{CMOD}}{B(W-a)} A$$

where

$$\eta_{pl}^{CMOD} = 3.724 - 2.244 \frac{a}{W} + 0.408 \left(\frac{a}{W} \right)^2$$

for all $H/(W-a)$ ratios for weld metal cracks

$$\text{if } 0.1 \leq \frac{a}{W} \leq 0.5$$

$$0.9 \leq M \leq 1.25$$

where

$$M = R_{p0.2}^W / R_{p0.2}^B$$

and for HAZ cracks

$$0.1 \leq \frac{a}{W} \leq 0.7$$

$$0.9 \geq M.$$

Within these conditions, the error in J is less than 10 %. Outside these conditions, **Fig. A9.7** provides guidance for appropriate η_{pl} values. The parameter H on the abscissa in **Fig. A9.7** is defined in **Figs. A9.8** and **A9.9**.

A9.5.2.2 M(T) specimens

(i) Determine A as per **9.4.2.1(i)**.

(ii) Calculate J_o using the relationship

$$J_o = \frac{K^2}{E} + \frac{\eta_{pl}}{B(W-a)} A$$

where

$$\eta_{pl} = 1$$

$$\text{for } 0.125 \leq \frac{a}{W} \leq 0.5$$

if for weld metal cracks

$$0.9 \leq M \leq 1.1 \quad \text{plane strain and plane stress}$$

or if for HAZ cracks

$0.9 \leq M \leq 2$	plane strain
all M values	plane stress

Within these conditions, the error in J is less than 10 %. Outside these conditions, **Figs. A9.10** and **A9.11** provide guidance for appropriate η_{pl} values.

A9.5.2.3 Post test examination procedures

The tested HAZ as well as narrow laser and electron beam weld metal specimens shall be examined for validation of the test. The weld metal half of the broken HAZ specimen shall be sectioned and metallographically prepared to identify the microstructure at the fatigue crack front, as shown in **Fig. A9.12**. Sectioning perpendicular to the fracture surface across the thickness should aim the tip of the fatigue crack. An optical microscope shall be used for measuring the aimed brittle zone size(s) across the specimen thickness. Visual or microscopic examination of the fracture surfaces should be conducted on the second half of the broken specimen.

Significant fracture path deviation (FPD) may occur towards the softer part (weld or base metal depending on the mis-match level) of the specimens notched in the HAZ of conventional welds as well as for narrow laser or electron beam welds. Such an event should be examined and included into the test report.

A9.6 Validity Requirements

Requirements have to be met for K_{Ic} and δ_5 or J fracture parameters to be valid according to this Procedure. These requirements have the flow stress R_f as an input quantity.

If

$$0.9 \leq M \leq 1,$$

then the flow stress of the base material can be used for the validity requirements of **Sections 5, 6** and **7**.

Appropriate solutions for M outside this range pending, it is recommended to take

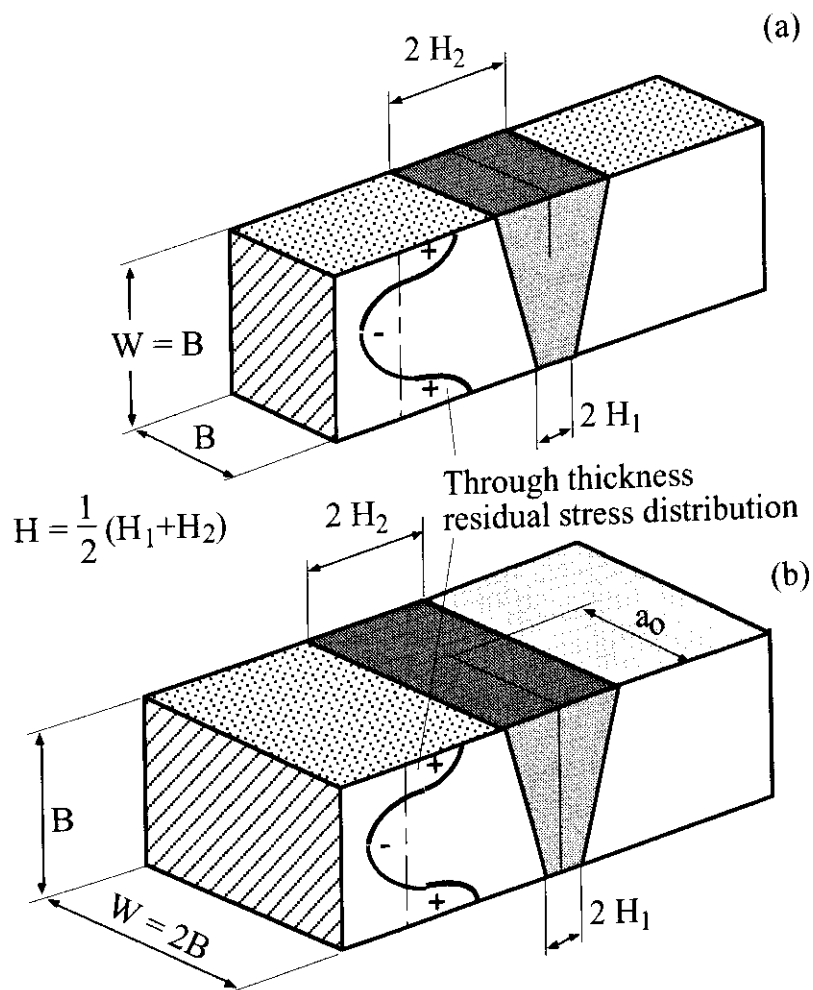
$$R_f = \min(R_f^{\text{base plate}}, R_f^{\text{weld metal}}, R_f^{\text{HAZ}})$$

Post test sectioning and metallographic examination shall provide information for the validity of the specimens with respect to the targeted zone.

A9.7 Test Report

The test report shall include the following information for tensile and fracture testing (if appropriate), in addition to items in **Section 8**:

- Weld macro section photograph and pre-test metallography,
- Weld width, $2H$,
- Original plate and weld region thicknesses,
- Specimen geometry and dimensions and crack orientation,
- Designated target area (microstructure),
- Tensile properties of weld and base metals and procedure used to obtain these values,
- Fatigue pre-cracking procedure
- Post test metallography qualification of test result.



Note:

For case (a): No need to use special fatigue precracking procedure (i.e. $R = 0.1$)

For case (b): Use step wise high R-ratio procedure (i.e. $R = 0.1$ and $R = 0.7$)

Figure A9.1: Crack orientation in a welded specimen: a) Surface crack; b) Through thickness crack.

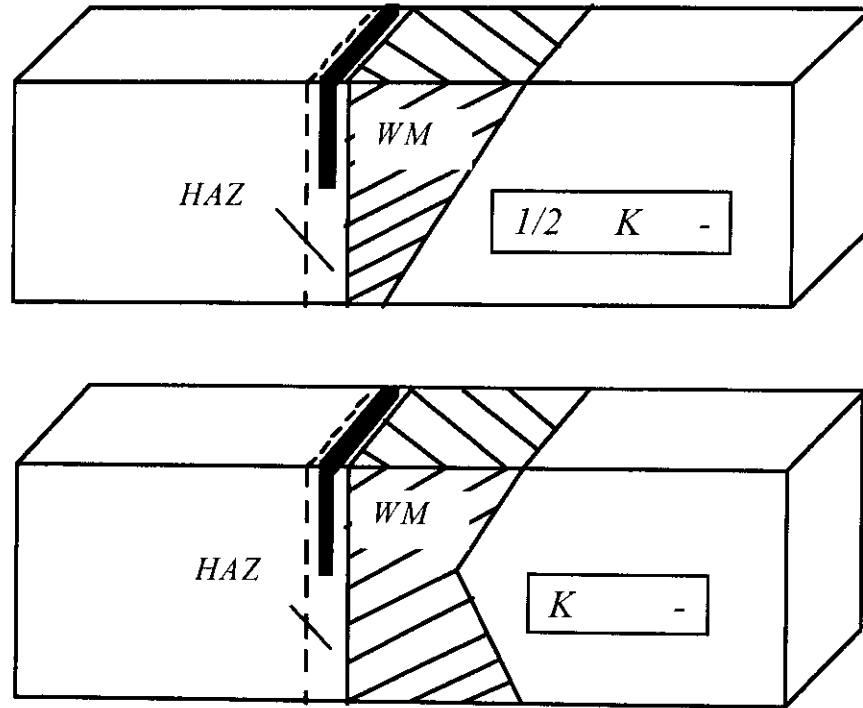


Figure A9.2: *1/2 K and K-joint preparation for HAZ crack testing.*

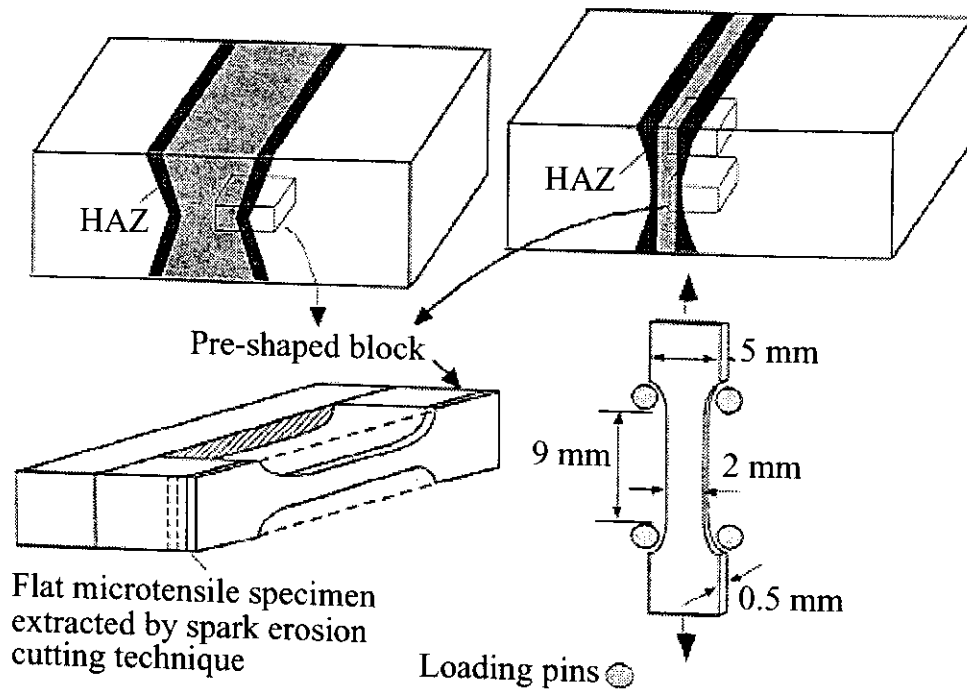


Figure A9.3: *Micro-flat tensile specimen extracted from weld.*

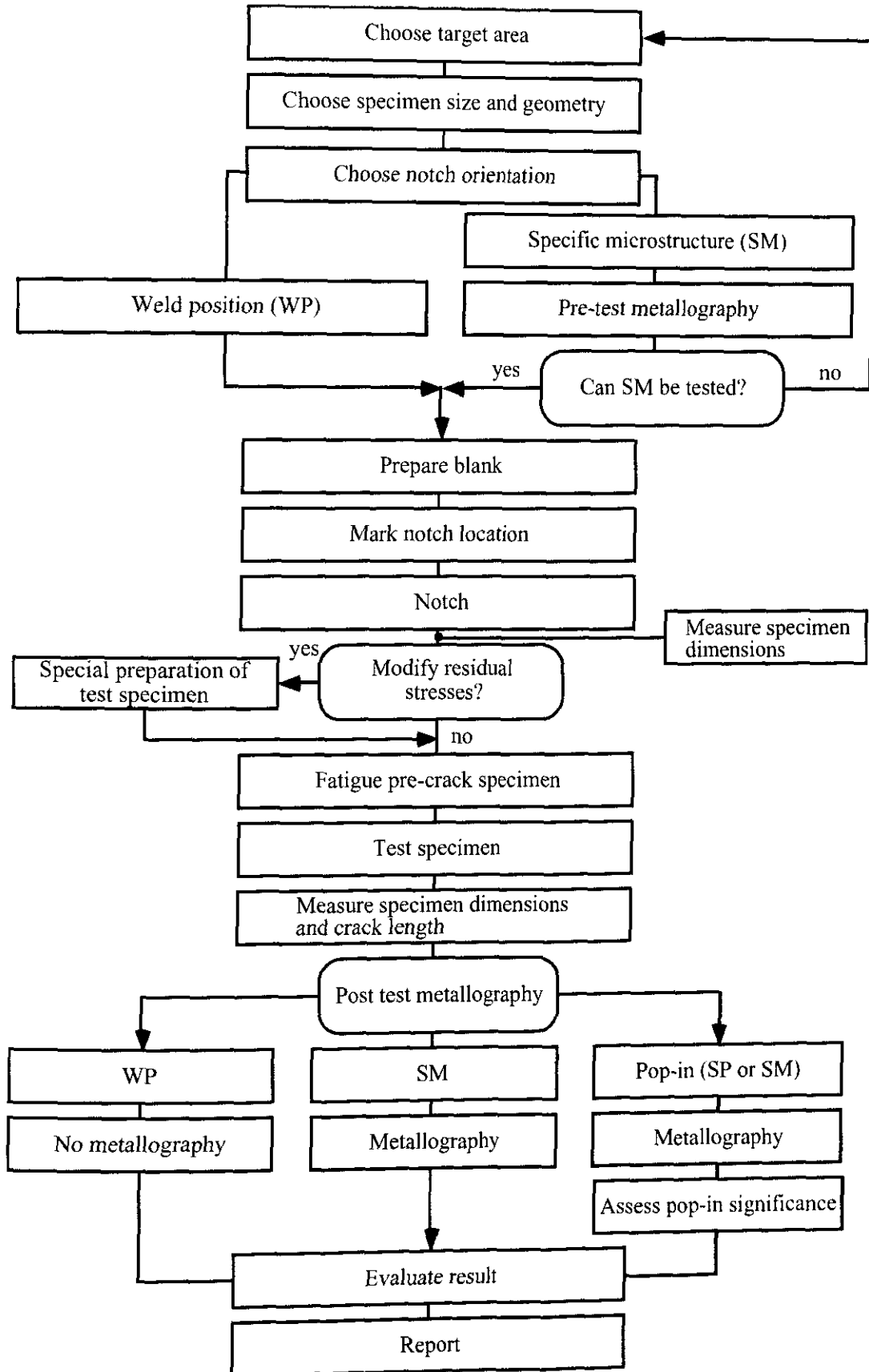


Figure A9.4: Test flow chart according to [A9.9, A9.10].

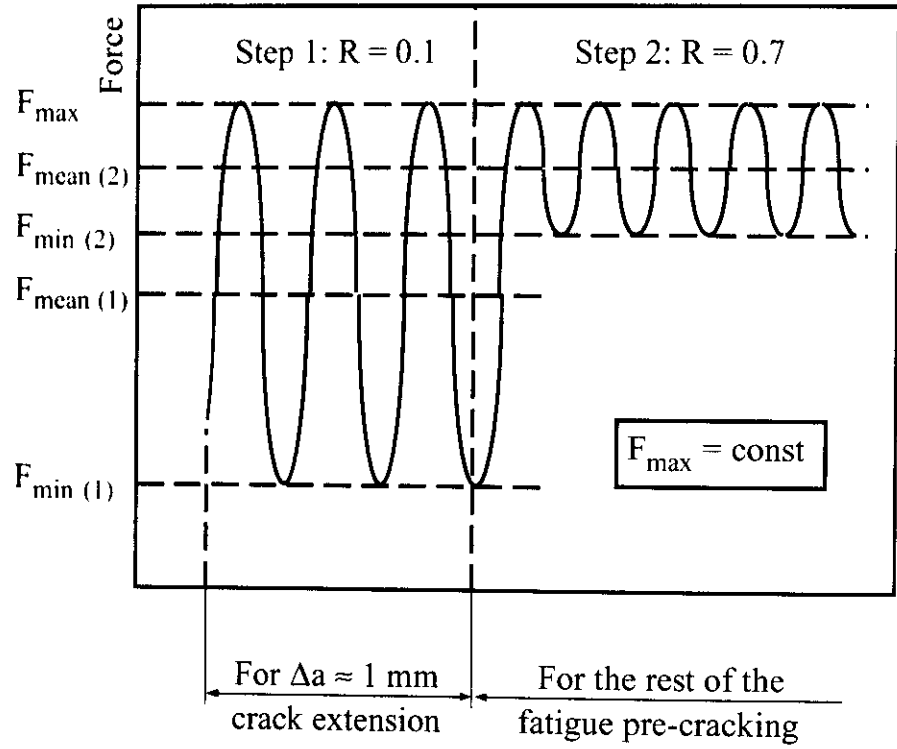


Figure A9.5: Step-wise high R-ratio pre-cracking procedure.

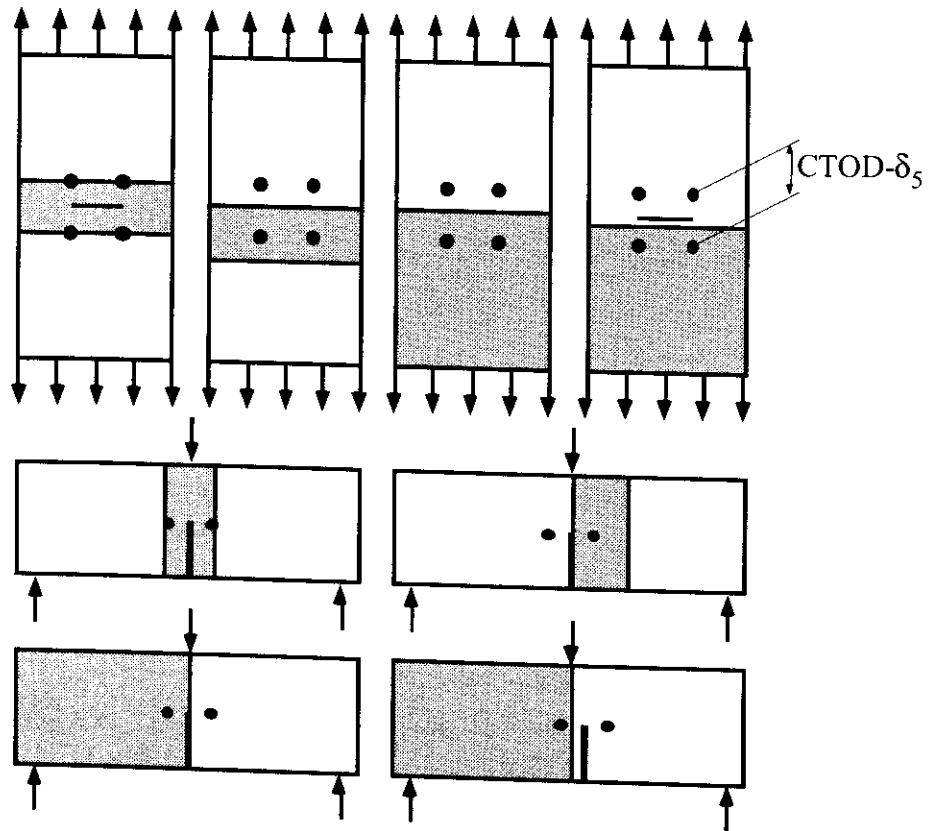


Figure A9.6: Location of δ_5 gauge points on welded specimens.

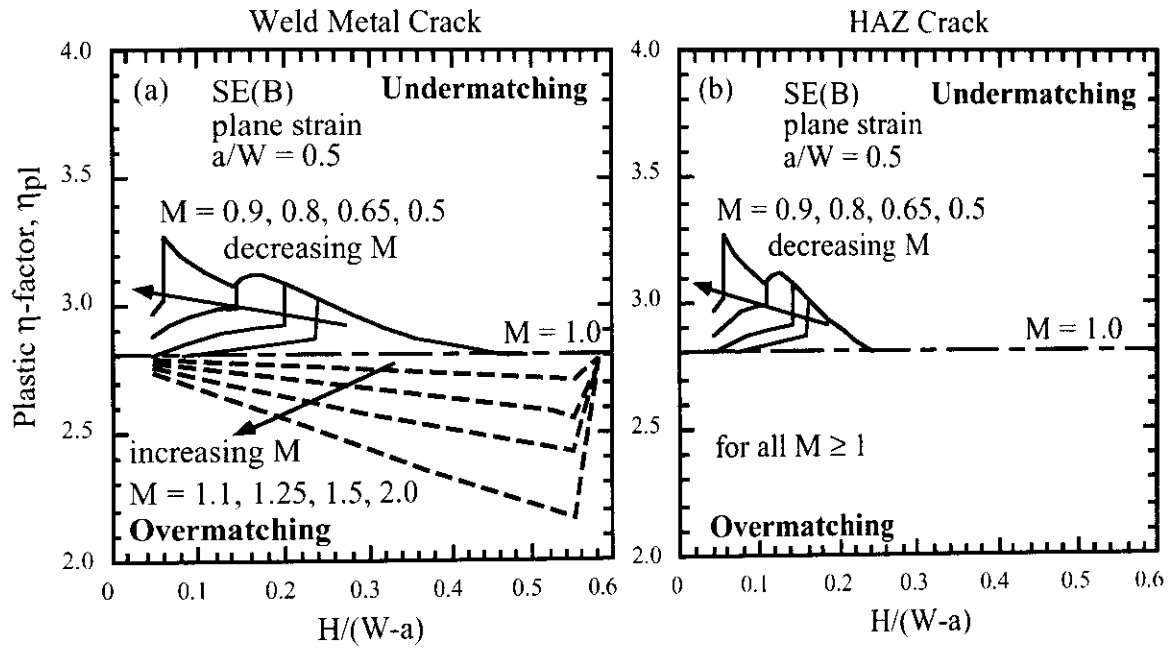


Figure A9.7: η_{pl} factor for cracks in bend specimens [A9.15],
 a) for weld metal cracks, b) for HAZ cracks.

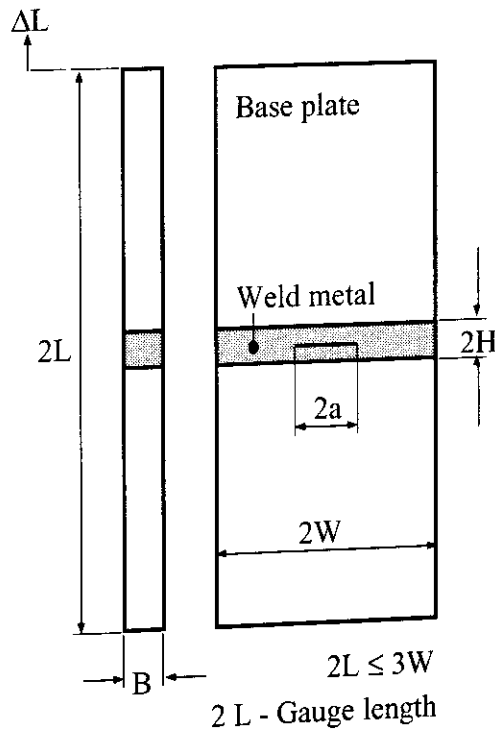


Figure A9.8: Definition of geometrical parameters of a weld specimen;
 Rectangular cross section of the weld metal.

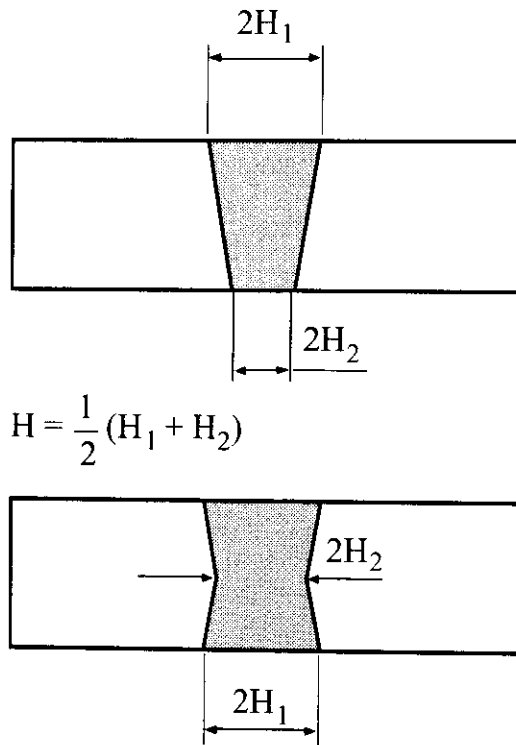


Figure A9.9: Definition of geometrical parameters of a weld specimen:
Non-rectangular cross section of the weld metal.

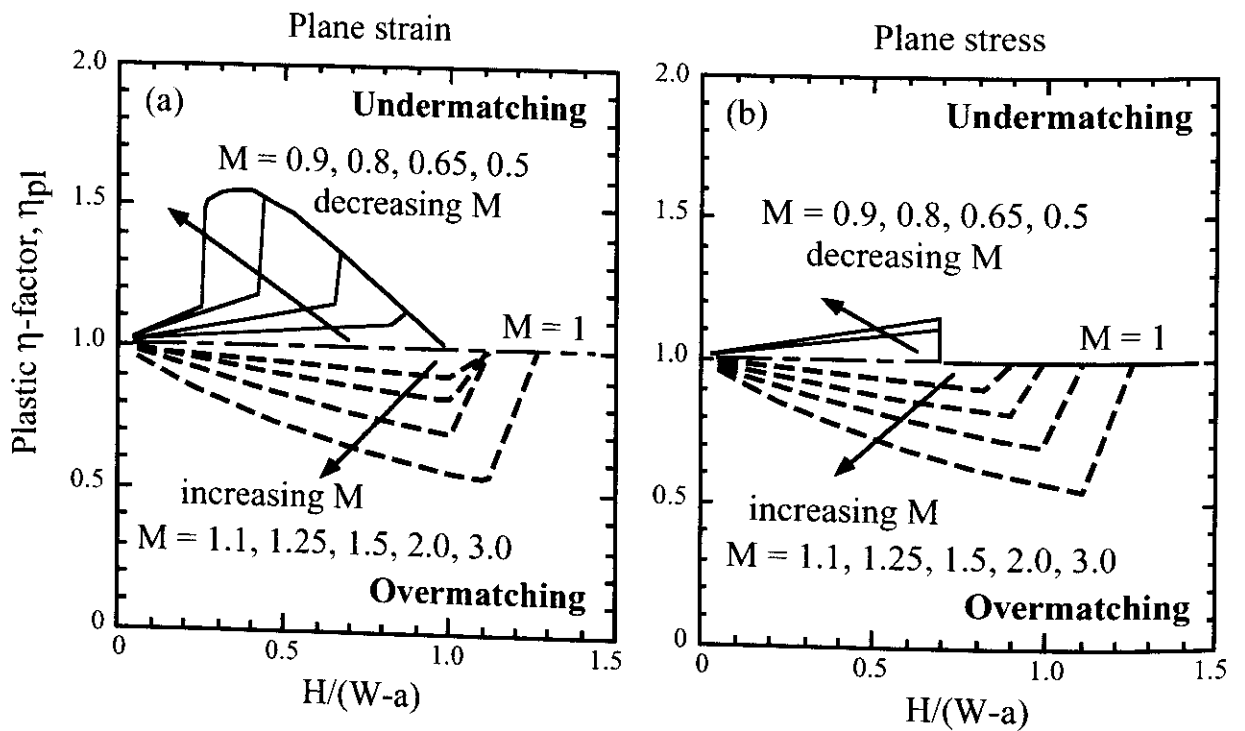


Figure A9.10: η_{pl} factor for weld metal cracks in $M(T)$ specimens made of mismatched welded joints [A9.15], a) plane strain, b) plane stress.

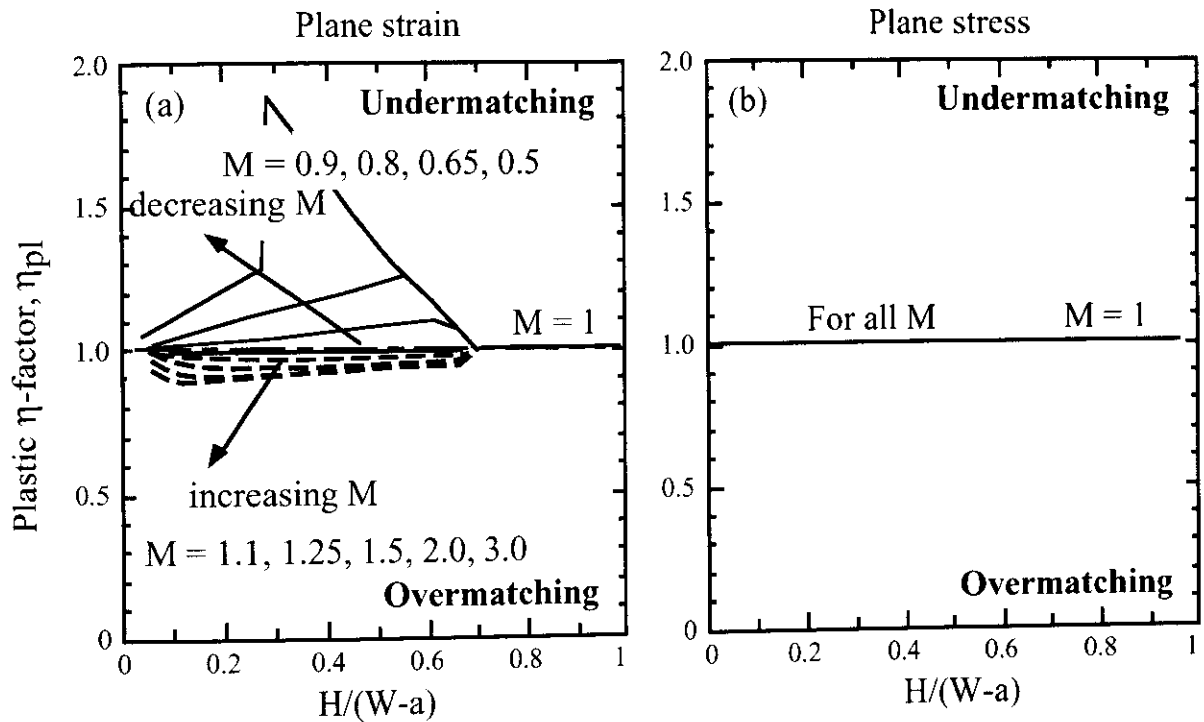


Figure A9.11: η_{pl} factor for HAZ cracks in $M(T)$ specimens [A9.15],
 a) plane strain , b) plane stress.

REFERENCES

- [A9.1] Koçak, M., Yao, S., and Schwalbe, K.-H., 1989, Effect of Welding Residual Stresses on Fatigue Precracking of CTOD Specimens Metal Behaviour & Surface Engineering, IITT Technology Transfer Series, France, 249–254.
- [A9.2] Koçak, M, Schwalbe, K.-H., Chen, L. and Gnirss, G., 1988, Effects of notch position and weld metal matching on CTOD of HAZ, Proc. of the Int. Conf. on Weld Failures", TWI, 21-24 Nov. 1988, P7.
- [A9.3] Koçak,, M., Es-Souni,M., Chen, L., Schwalbe, K.-H., 1989, Microstructure and weld metal matching effects on heat affected zone toughness, Proc. of the 8th Int. Conf. OMAE-ASME, The Hague, Netherlands, March 19-23, 623–633.

- [A9.4] Koçak, M., Knaack, J., and Schwalbe, K.-H., 1990, Fracture behaviour of undermatched weld joint, Proc. of the 9th Int. Conf. on Offshore Mech., and Arctic Eng., ASME, Houston, Texas, Feb. 18-23, Volume III - Part B, 453–459.
- [A9.5] Tschegg, E., Kirchner, H.O.K., and Koçak, M., 1990, Cracks at the Ferrite-Austenite Interface, *Acta metall. mater.*, Vol. 38, No. 3, 469–478.
- [A9.6] Tschegg, E., Kirchner, H.N.O., and Koçak, M., 1991, Interfacial and subinterfacial cracks in the copper-ferrite system, *Engineering Fracture Mechanics*, Vol. 39, No. 4, 739–750.
- [A9.7] Mis-matching of Welds, Proceedings of the International Conference MIS-MATCH'93, ESIS 17 (Ed. by Schwalbe, K.-H. and Koçak, M.) 1994, Mechanical Eng. Publications, London, U.K.
- [A9.8] Dawes, M.G., Pisarski, H.G., Squirell, S.J., 1989, Fracture mechanics tests on welded joints, ASTM STP 995, 191–213.
- [A9.9] BS 7448, Part 2, 1997, Fracture Mechanics Toughness Tests. Method for Determination of K_{Ic} , Critical CTOD and Critical J Values of Welds in Metallic Materials. British Standard Institution (BSI), London.
- [A9.10] ISO CD 15653, 1997, Metallic Materials – Unified Method of Test for the Determination of Quasistatic Fracture Toughness of Welds. International Standard Organisation (ISO), Geneva.
- [A9.11] Hornet, P. and Koçak, M., April 1994, Fracture of bimaterial joints: effect of strength mismatch on crack resistance curves, IIW Doc. X-F-001-94.
- [A9.12] Hornet, P. and Koçak, M. et al, Sept. 1994, Fracture of bi-material joints: effect of strength mis-match on crack resistance curves, 10th European Conference on Fracture, ECF 10, Berlin, FRG.
- [A9.13] Gordon, J.R. and Wang, Y.-Y., The effect of weld metal mis-match on fracture toughness testing and analysis procedures, *ibid*, ref. 7, 351–368.
- [A9.14] Joch, J. and Ainsworth, R.A, et al, Fracture parameters and fracture assessment for welded structures, *ibid*, ref. 7, 609-622.
- [A9.15] Koçak, M., Kim, Y.-J. and Hornet, P., 1997, Recommendations for J and CTOD testing of strength mis-matched weldments: GKSS and EDF view; IIW Doc. X-F 056-97, GKSS-Forschungszentrum Geesthacht GmbH, Geesthacht, Germany.
- [A9.16] Kirk, M.T., and Dodds, R.H., Jr., 1993, J and CTOD estimation equations for shallow cracks in single edge notch bend specimens, *Journal of Testing and Evaluation* 21, 228–238.
- [A9.17] Schwalbe, K.-H., Kim, Y.-J., Hao, S., Cornec, A., and Koçak, M., 1997, EFAM ETM-MM96 - The ETM method for assessing the significance of crack-like defects in joints with mechanical heterogeneity (strength mismatch), GKSS Report 97/E/9, GKSS-Forschungszentrum Geesthacht GmbH, Geesthacht, Germany.
- [A9.18] SINTAP. Structural integrity assessment procedures for European industry, British Steel Report, Sheffield (1999).
- [A9.19] Kim, Y.-J., 2002, Experimental J estimation equations for single-edge-cracked bars in four-point bend: homogeneous and bi-material specimens, *Engineering Fracture Mechanics* 69; 793–811.

APPENDIX 10: Statistical Analysis of Fracture Resistance Data

A10.1 Scatter of Cleavage Fracture Toughness in the Ductile-to-Brittle Transition Regime

In the ductile-to-brittle transition regime (DBTR) fracture toughness exhibits large scatter and specimen size effects, which makes it difficult to characterise material properties. This section provides statistical procedures, that can be used to analyse the scatter of toughness data for material characterisation purposes or failure assessment routines.

Three procedures for statistical small specimen toughness data treatment are presented in this Appendix. They have been derived from the investigations outlined in Refs. [A10.1-A10.3]

These procedures are:

- Assessment of the cleavage fracture probability of specimens [A10.1],
- Engineering estimation of lower bound toughness [A10.1-A10.3].

A10.1.1 Assessment of the Cleavage Fracture Probability of Specimens

When loading a specimen in the transition regime, the probability that it will fail due to the initiation of cleavage increases. The cumulative failure probability can be assessed using the following failure probability function, which is a three-parameter Weibull distribution, Fig. A10.1:

$$P_f = 1 - \exp\left\{-\left(\frac{K_J - K_{\min}}{K_0 - K_{\min}}\right)^4\right\}$$

In this equation, P_f is the cumulative failure probability, K_J is the cleavage fracture toughness, K_{\min} is a fixed quantity of 20 MPa \sqrt{m} [A10.1]. In order to determine the P_f -function for the material, K_0 has to be determined experimentally. This can be done using a set of fracture toughness values generated at a single temperature in the DBTR using C(T) or SE(B) specimens.

NOTE: *To date, the P_f -function has been mainly validated in the regime $P_f \geq 3\%$. No advice can be given regarding the reliability of the P_f -function in the regime $P_f < 3\%$.*

The K_0 -value of the probability function is determined as follows:

Step 1: Data Selection

Select a toughness data set which was generated by testing identical specimens at a given test temperature in the DBTR. The data set may consist of data points that are related to both cleavage fracture and fully ductile fracture. Both types of toughness data have to be included in the subsequent analysis.

Not included are values marking stable crack initiation such as δ_{5i} , $\delta_{5,0.2BL}$, $\delta_{5,0.2}$; J_i , $J_{0.2BL}$ and $J_{0.2}$ (Sections 6 and 7). Usually in the DBTR a specimen will fail by cleavage after a certain amount of stable tearing. In cases where a specimen exhibits fully ductile fracture (without cleavage), the toughness value at the end of the test, J_{end} , is used in the analysis. It must, however, not be smaller than the $K_{J,max}$ of Step 3 below.

NOTE: J_{end} characterizes a test which has been terminated after a substantial amount of ductile crack extension, usually far beyond maximum force.

Step 2: Data Conversion

Convert each toughness value into K_J . If toughness is measured in terms of J use the following transformation formula:

$$K_J = \sqrt{\frac{J E}{(1 - \nu^2)}}$$

If toughness is measured in terms of δ_5 , use the GKSS Java applet to convert δ_5 data into J and apply the previous equation to calculate K_J . The GKSS Java applet is available at the world wide web address: www.gkss.de/Themen/W/WME.

Step 3: Data Censoring

Both toughness values, J_{end} , related to fully ductile fracture and cleavage toughness values greater than $K_{J,max}$ shall be replaced by $K_{J,max}$ that is defined as follows:

$$K_{J,max} = \sqrt{\frac{1}{30} \frac{E}{(1 - \nu^2)}} b_0 R_e.$$

NOTE: Toughness data which are related to fully ductile fracture but smaller than $K_{J,max}$ have to be eliminated from the data set and must not be used in the subsequent analysis. These tests belong to a different statistical distribution due to the fact that the test was stopped before $K_{J,max}$ was reached.

At the end of the censoring procedure, the remaining data set has two populations: the original K_J -data from the tests and a censored population of $K_{J,max}$ -values. Both data populations are used in Step 4. The total number of data points at the end of Step 3 is N (eliminated data are not included).

Step 4: Estimation of K_0

The data set derived from Step 3 is used to calculate K_0 :

$$K_0 = \left[\frac{\left(\sum_{i=1}^N (K_{Ji} - K_{\min})^4 \right)}{N \sum_{i=1}^N \delta_i - 1 + \ln 2} \right]^{0.25} + K_{\min} \quad (\text{MPa}\sqrt{\text{m}})$$

The uncensored data (K_J -values) are designated $\delta_i = 1$ and the censored data ($K_{J,\max}$) are designated $\delta_i = 0$.

The standard deviation of K_0 is approximately given by

$$\sigma_{K_0} = \frac{0.28}{\sqrt{r}} (K_0 - K_{\min}) \quad (\text{MPa}\sqrt{\text{m}})$$

where r is the number of uncensored data (K_J -values) in the data set.

A 10.1.1.1 Assessment of Specimen Size Effects and Transferability of the Probability Function

The probability function is specimen size dependent. According to the weakest link theory an increase of the crack front length increases the probability of activating cleavage in the specimen. This crack front length effect can be assessed by adjusting the K_0 -value of the probability function:

$$K_{0,B_X} = K_{\min} + [K_{0,B} - K_{\min}] \times \left[\frac{B}{B_X} \right]^{0.25} \quad (\text{MPa}\sqrt{\text{m}})$$

K_{0,B_X} corresponds to the specimen thickness B_X and $K_{0,B}$ corresponds to the specimen thickness B . In case of side grooved specimens it is recommended to use the nominal thickness B of the specimen.

NOTE: *This crack front length correction can formally be used to convert failure probability functions of specimens to the failure probability function related to cracks in components, by converting the K_{0B} -value of the standardised specimens into a $K_{0,l}$ -value which corresponds to the crack front length of a crack in the component:*

$$K_{0,l} = K_{\min} + [K_{0,B} - K_{\min}] \times \left[\frac{B}{l} \right]^{0.25} \quad (\text{MPa}\sqrt{\text{m}})$$

where l is the actual crack front length of the crack in the component and B is the thickness of the specimen.

Little experience with using this P_f -function in structural assessment is available and therefore, no information regarding the reliability of this concept can be given yet.

A10.1.2 Assessment of the Temperature Dependence of Cleavage Fracture Probability

The temperature dependence of failure probability is determined by assessing the temperature dependence of the K_0 -value in the probability function given in **Section A10.1.1**. In case of 25 mm thick specimens the temperature dependence of K_0 is given by the following Master Curve [**A10.1**]:

$$K_{0,B=25\text{mm}} = 31 + 77 \exp[0.019(T - T_0)] \quad (\text{MPa}\sqrt{\text{m}})$$

T_0 is the reference temperature. It determines the position of the Master Curve in the toughness temperature diagram of 25 mm thick reference specimens, **Fig. A10.2**. The reference temperature is a material dependent quantity. The Master Curve gives good results at temperatures in the range $T_0 - 50^\circ\text{C} < T < T_0 + 50^\circ\text{C}$. Below this range it tends to overestimate K_0 , at temperatures greater than $(T_0 + 50^\circ\text{C})$ it tends to underestimate toughness. Therefore, care must be taken in applying the Master Curve outside this range.

The Master Curve provides the temperature dependence of the K_0 -value for 25 mm thick specimens directly. For other specimen thicknesses the temperature effect can also be assessed. This is done using the thickness correction formula given in **Section A10.1.1.1**, which allows to convert the $K_{0,B=25\text{mm}}$ -values as given by the Master Curve into K_0 -values of other specimen thickness.

The reference temperature, T_0 , needed for the application of the Master Curve concept, is determined as outlined in the following.

A10.1.2.1 T_0 determined from single temperature data set

For the determination of $K_{0,B=25\text{mm}}$ follow *Step 1* to *Step 4* of **Section A10.1.1** and then continue with *Step 5*:

Step 5: Estimation of $K_{0,B=25\text{mm}}$

If the toughness data set used for the K_0 determination in *Step 4* does not correspond to a specimen thickness of 25 mm, use the following specimen size adjustment to convert K_0 into $K_{0,B=25\text{mm}}$:

$$K_{0,B=25\text{mm}} = K_{\min} + [K_{0,B} - K_{\min}] \times \left[\frac{B}{25\text{mm}} \right]^{0.25} \quad (\text{MPa}\sqrt{\text{m}})$$

where B is the thickness of the specimens used for the calculation of $K_{0,B}$.

In case of side grooved specimens the nominal thickness, B , is used in the calculations.

Step 6: Calculation of T_0

The reference temperature, T_0 , can be calculated using:

$$T_o = T_t - \frac{1}{0.019} \ln \left[\frac{K_{0,B=25\text{mm}} - 31}{77} \right]$$

$K_{0,B}$ in MPa $\sqrt{\text{m}}$; T_o and T_t in °C

were T_t is the test temperature corresponding to the data set.

The uncertainty margin of T_o can be assessed from the standard deviation of K_o which is defined in *Step 4* of **Section A10.1.1**.

A10.1.2 Methods for Estimating Engineering Lower Bound Toughness in the Ductile-to-Brittle Transition [A10.2, A10.3]

A cumulative failure probability of 3 % is defined as engineering lower bound toughness (ELB). Such ELB may be used to characterize the cleavage susceptibility of materials. It may also be a useful input parameter in failure assessment routines.

NOTE: *The relevance of such engineering lower bound toughness in failure assessment routines has not yet been fully elaborated. This is a subject of current research.*

Two methods of determining an ELB are outlined below. One is based on the failure probability function given in **Section A10.1.1**. The ELB is assessed by a 3% cut-off of the failure probability function. The second procedure uses a modified probability function with the advantage of an easy application.

A10.1.2.1 Method A

In cases where the P_f -function of a single temperature data set is known, engineering lower bound, K_{LB} , related to a failure probability of $P_f = 3\%$ can be estimated as follows:

$$P_f = 1 - \exp \left\{ - \left(\frac{K_{LB} - K_{\min}}{K_o - K_{\min}} \right)^4 \right\} = 0.03$$

The uncertainty margin of the ELB results from the uncertainty in K_o . Therefore, it can be assessed using the K_o -standard deviation shown in *Step 4* of **Section A10.1.1**.

A10.1.2.2 Method B

This method of deriving an ELB is based on the probability function shown in **Fig. A10.3**, using a straight line fit in the low probability regime. The ELB is obtained by extrapolating the straight line down to a failure probability level of „zero“.

NOTE: *Although the method provides engineering lower bounds which are formally related to a failure probability of „zero“, recent investigations [A10.2] of very large data sets seem to indicate that the ELB as determined with this method corresponds to a cumulative failure probability of 3 % or less.*

The lower bound method can be easily applied to single temperature toughness data sets as outlined in the following steps:

Step 1: Data Selection

Select the toughness data set for which it is intended to estimate ELB. The data set must be derived from tests performed at a single temperature using one specimen size. The data set may consist of data points, which are related to cleavage fracture as well as fully ductile fracture behaviour. Both types of data have to be included in the subsequent analysis. In case of fully ductile fracture behaviour of a specimen, the toughness value at the end of the test, J_{end} , is used in the analysis.

Step 2: Data Conversion

All toughness data shall be converted into J:

$$J = \frac{1}{E} K^2 (1 - \nu^2).$$

If toughness is quantified in terms of δ_5 , it shall be converted into J using the GKSS Java applet which is available at the world wide web address: www.gkss.de/Themen/W/WME.

Step 3: Data Censoring

All J_{end} data lower than J_{max} have to be considered as „non existing tests“ and must be *eliminated* from the data set. These tests belong to a different statistical distribution due to the fact that the test was stopped before J_{max} was reached.

J_{max} is defined as:

$$J_{max} = \frac{\sigma_Y(W - a_0)}{30}.$$

All toughness values, which are greater than J_{max} shall be indicated as censored toughness data points.

Step 4: Calculation of the Lower Bound Toughness

The data set as derived in *Step 3* is used to estimate the toughness lower bound by:

$$J_{LB} = 0.26 \left(\frac{\sum_{i=1}^r J_i}{N} \right) \times \left[1 + 1.286 \frac{(N-r)}{N} \right]$$

where r is the number of *uncensored* data points without eliminated data and N is the total number of data points of the data set.

The standard deviation of the lower bound, J_{LB} , is then assessed by

$$\sigma_{LB} = \frac{0.13}{\sqrt{r}} \left(\sum_{i=1}^r J_i \right).$$

A10.2 Scatter of Crack Extension Fracture Resistance (R Curve)

The scatter in crack extension fracture resistance has been found to be broadly independent of the level of crack extension. Therefore, the standard deviation of δ_s or J at a fixed Δa -value may be used to estimate scatter at other values of δ_s or J . The scatter of R curves is known to be best described as a *normal distributed absolute scatter* of δ_s or J . For a range of materials, the scatter has been found to be typically less than 10 % of the mean value corresponding to a crack extension of 1mm. Depending on the number of tests available, two ways of assessing scatter will be given:

Limited number of tests:

For a limited number of tests, between 3 to 9, the lowest R curve may be used to assess a lower bound to crack extension fracture resistance.

Large number of tests:

For 10 or more tests, a full statistical analysis assuming normally distributed absolute scatter in δ_s or in J is recommended. The mean value of n J -values of crack extension resistance at initiation or at a specific Δa is given by:

$$\bar{J} = \frac{\sum_{i=1}^n J_i}{n}$$

if the experimental data was determined in J .

The variance S of the J -data is defined as:

$$S^2 = \frac{\sum_{i=1}^n (J_i - \bar{J})^2}{(n-1)}$$

and the confidence limits of the data are given by

$$J_{\infty} = \bar{J} \pm t_{\infty} S$$

where ∞ is the confidence limit and t_{∞} is the corresponding value of the Student's distribution at $(n-1)$ degrees of freedom. If there is a difference between individual R curves of more than 20 % in terms of J or δ_5 this is considered as an indication of material inhomogeneity.

The scatter of δ_5 is determined by the same procedure.

REFERENCES

- [A10.1] Wallin, K., Master Curve analysis of the Euro fracture toughness dataset, to be published in *Engineering Fracture Mechanics*,
- [A10.2] Heerens, J., Pfuff M., Hellmann, D., Zerbst, U., 2002, The lower bound fracture toughness procedure applied to the Euro fracture toughness data set, *Engineering Fracture Mechanics*, 69, 483 – 495.
- [A10.3] Zerbst, U., Heerens, J., Pfuff, M., Wittkowsky, B., Schwalbe, K.-H., 1998, Engineering estimation of the lower bound toughness in the ductile to brittle transition regime, *Fatigue and Fracture of Engineering Structures*, 21, 1273–1278.

Figure A10.1:
 Three-parameter Weibull distribution used to assess the cumulative failure probability P_f of cleavage initiation in specimens.

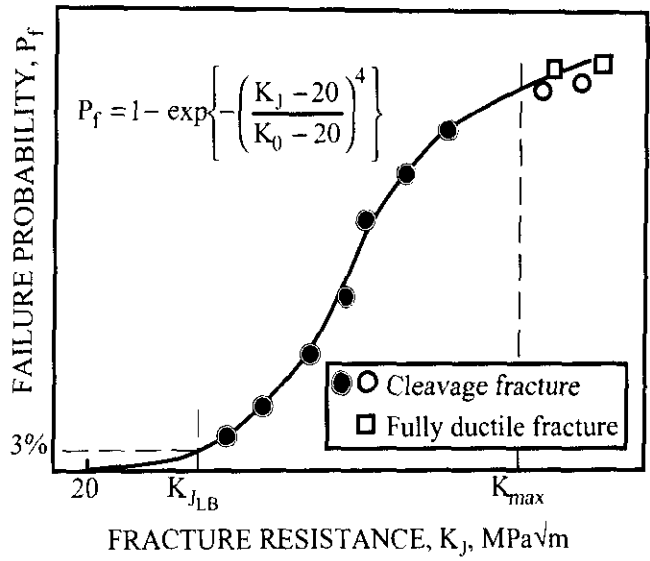


Figure A10.2:
 The Master Curve provides the influence of temperature on K_0 of 25 mm thick specimens.

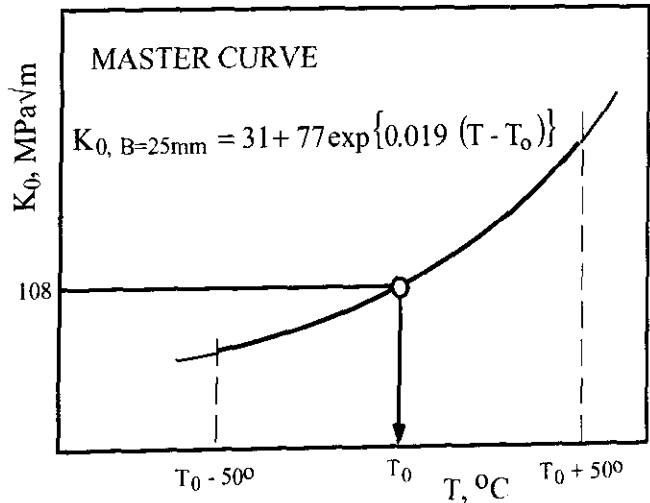
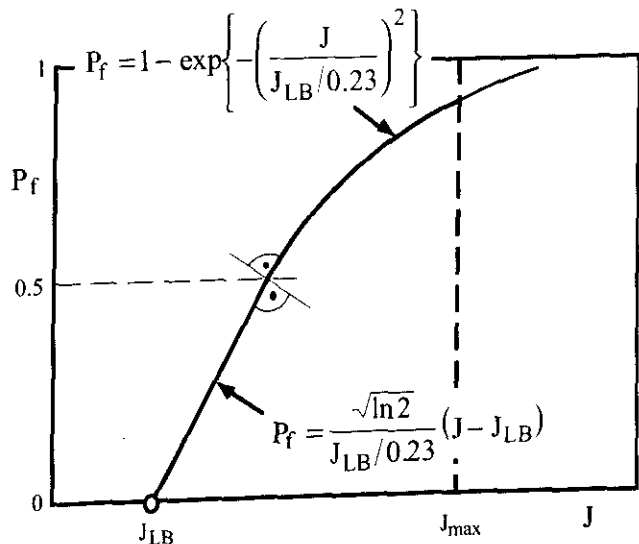


Figure A10.3:
 Determination of J_{LB} (engineering lower bound toughness) based on method B: In the regime $P_f < 0.5$ a linear relationship between P_f and J is assumed. The engineering lower bound value, J_{LB} , is obtained by extrapolating the straight line down to a failure probability $P_f = 0$.



APPENDIX 11: K-Based Fracture Resistance Curves For Middle Cracked Tension Panels

High strength materials such as aerospace materials are frequently tested in the form of M(T) specimens fabricated from thin sheets. In these cases the crack extension resistance curve can often be expressed as the variation in the plasticity adjusted stress intensity factor, K_{eff} , with crack extension, Δa .

A11.1 The option described in this Appendix can be used if

$$F_j \leq 1.8 R_{p0.2} (W-a)B$$

where F_j is either the force at termination of the test when using the multiple specimen method or the last point to be evaluated in a single specimen test.

A11.2 The specimens should satisfy the requirement

$$(W-a_0)/B \geq 4.$$

A11.3 Calculate the fracture resistance

$$K_{\text{eff}} = \frac{F}{B\sqrt{W}} f(a_{\text{eff}} / W)$$

where

$$a_{\text{eff}} = a + \frac{K^2}{2\pi R_{p0.2}^2}$$

F = applied force

$$K = \frac{F}{B\sqrt{W}} f(a / W)$$

and $f(a/W)$ is the stress intensity function given in **Appendix 1**.

A11.4 Determine Δa_{max} from either the crack extension associated with

$$F = 1.8 R_{p0.2} (W-a)B$$

or $\Delta a_{\text{max}} = 0.5 (W-a_0)$, whichever is the smaller.

A11.5 The plot of ΔK_{eff} versus Δa represents the crack extension resistance curve for a given thickness, B, provided the data spacing requirements of **Section 7.4** are met.

A11.6 The crack extension resistance curve is either represented by the curve fit of **Section 7.5.1** or as the series of data points.

A 11.7 For the presentation of the results, the requirements of **Section 8** shall be met as appropriate.

REFERENCES

- [A11.1] Schwalbe, K.-H., and Setz, W., 1981, R-curve and fracture toughness of thin sheet materials, *Journal of Testing and Evaluation*, Vol. 9, 182–194.
- [A11.2] Schwalbe, K.-H., and Hellmann, D., 1984, Correlation of stable crack growth with the J-integral and the crack tip opening displacement, effects of geometry, size, and material. GKSS Report 84/E/37, GKSS-Forschungszentrum Geesthacht GmbH, Geesthacht, Germany.

APPENDIX 12: Testing Specimens With Shallow Cracks

The initial crack length ratio $0.45 \leq a_0/W \leq 0.65$ required for compact and single edge cracked bend specimens ensures high constraint and hence lower bound fracture resistance. However, in many structural applications the cracks are shallow, i.e. the crack length ratio is substantially smaller than 0.45. This leads to a loss of constraint and hence to increased fracture resistance which can be beneficial if the crack length ratio of the test specimen models the structural situation.

Tests of this kind can be carried out using this Procedure considering the following suggestions:

- Only SE(B) specimens should be used because C(T) specimens containing shallow cracks tend to fail at the pin holes or at the machined steps.
- The J formula in **Section 7.2.1.3** can be used for cracks down to $a_0/W = 0.1$. The δ_5 technique can be used for any crack length.
- The validity criteria outlined in this Procedure should not be applied to the test results.
- The test results should be reported together with the a_0/W value used in the test.

APPENDIX 13: Relationship Between δ_5 and other Fracture Parameters

A13.1 Tests With Stable Crack Extension Less Than 0.1 mm

3D finite element and experimental studies [A13.1] show that within a window which covers frequently used configurations of C(T) and SE(B) specimens, δ_5 can be set equal to $CTOD_{standard}$ or $J/(2\sigma_Y)$, **Fig. A13.1**. $CTOD_{standard}$ is defined in test standards [A13.2-A13.5], σ_Y stands for $R_{p0.2}$ or R_{eL} , as appropriate.

For configurations outside this window, correlations between δ_5 and $CTOD_{standard}$ or $J/(2\sigma_Y)$ are available on the internet page www.gkss.de/Themen/W/WME/delta5.html.

NOTE: Although the findings shown in **Fig. A13.1** were derived from SE(B) specimens under three-point bending it is assumed that they are also valid for four-point bending.

A13.2 R-Curve Testing

In R-curve testing, δ_5 is in good agreement with $CTOD_{standard}$ [A13.6], provided that the $CTOD_{standard}$ version with correction for crack extension [A13.3-A13.5] is used.

Furthermore, during stable crack extension δ_5 is approximately related to the CTOA, ψ , [A13.7] according to

$$\psi \approx \frac{d\delta_5}{da}$$

and

$$\frac{dJ}{da} \approx \frac{dJ}{d\delta_5} \psi$$

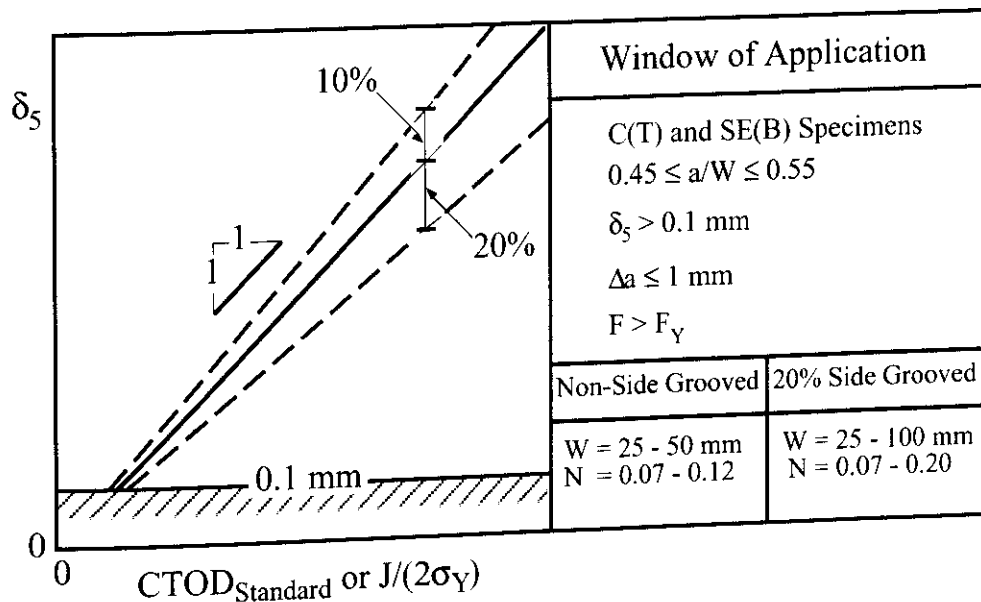


Figure A13.1: Window where the parameters δ_5 , $CTOD_{standard}$ and $J/(2\sigma_Y)$ are roughly equal.

REFERENCES

- [A13.1] Nikishkov, G.P., Heerens, J., Schwalbe, K.-H., 1999, Transformation of CTOD δ_5 to CTOD δ_{BS} and J-integral for 3PB and CT specimens, submitted to Engng. Fracture Mech. 63, 573-589.
- [A13.2] BS 57662: 1979, Methods for crack opening displacement (COD) testing, The British Standards Institution, 1979.
- [A13.3] ESIS P2-92, ESIS procedure for determining the fracture behaviour of materials, 1992.
- [A13.4] ASTM E 1820-96, Standard Test Method for Measurement of Fracture Toughness, American Society for Testing and Materials, 1996.
- [A13.5] ISO 12135, 1998, Metallic Materials - Unified Method of Test for the Determination of Quasistatic Fracture Toughness, International Standard Organisation.
- [A13.6] Hellmann, D., Schwalbe, K.-H., 1986, On the experimental determination of CTOD based R-curves, in: Schwalbe, K.-H. (Ed): The Crack Tip Opening Displacement in Elastic-Plastic Fracture Mechanics, Springer-Verlag Berlin Heidelberg New York Tokyo.
- [A13.7] Brocks, W., and Yuan, H., 1990, FE-Analysen des Risswachstumsverhaltens dünner Proben bei großem Risswachstum, Research Report BAM-1.01, 90/4, Bundesanstalt für Materialforschung und -prüfung, Berlin.

APPENDIX 14: Determination of δ_5 and J in the Centreplane of SE(B) and C(T) Specimens

The δ_5 or J fracture parameters determined in this Procedure represent values averaged across the specimen thickness and hence along the crack front or measured on the side surface of the specimen. In reality, these values vary along the crack front. For structural assessment, it may be more appropriate to determine the value a fracture parameter attains in the centreplane of a specimen where the constraint is highest. The recommendations given in the following have been derived from three-dimensional finite element analyses for stationary cracks.

They are valid for

- SE(B) and C(T) specimens,
- $a/W = 0.55$,
- δ_{5i} , J_i , δ_{5c} , J_c , δ_{5u} , J_u , δ_{5uc} , J_{uc} , $\delta_{5,0.2}$, $J_{0.2}$, $\delta_{5,0.2/BL}$, $J_{0.2/BL}$.

The ratio of δ_5 in the centreplane, δ_5^c , to δ_5 determined according to **Appendix 4** and the value of η^c in the equation

$$J_o^c = \eta^c \frac{U}{B_n(W - a_o)}$$

depend on

- Specimen type,
- Presence of sidegrooves,
- F/F_Y ,
- Strain hardening exponent of the material,
- Crack front curvature

$$\alpha = \frac{a(o) - a(B/2)}{W}$$

where $a(o)$ is the crack length at the surface and $a(B/2)$ is the crack length in the centreplane.

Values for δ_5^c / δ_5 and η^c are shown in **Figs. A14.1 to A14.4**.

REFERENCE

- [A14.1] Nikishkov, G.P., Heerens, J., and Schwalbe, K.-H., 1999, Effect of crack front curvature and sidegrooving on CTOD δ_5 and J-integral in CT and 3PB specimens, *Journal of Testing and Evaluation*, 27, No.5, 312-319.

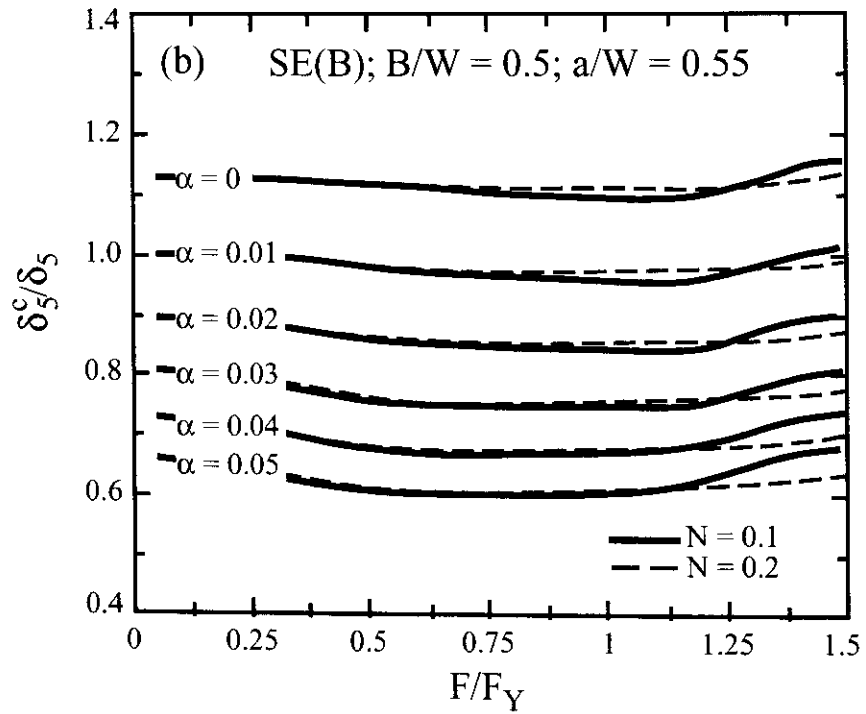
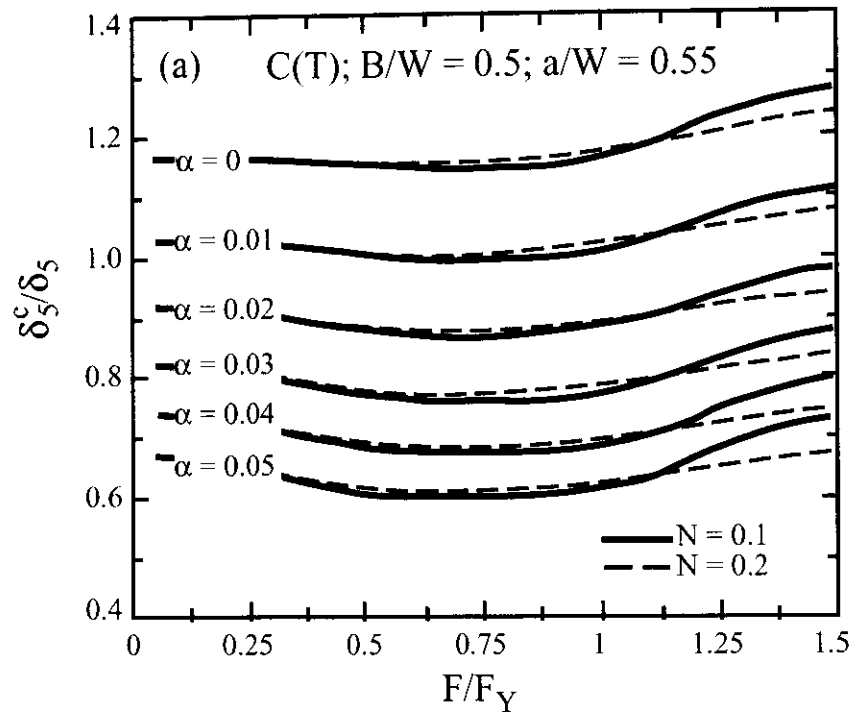


Figure A14.1: δ_5^c/δ_5 for non-sidegrooved specimens
a) C(T) specimens,
b) SE(B) specimens.

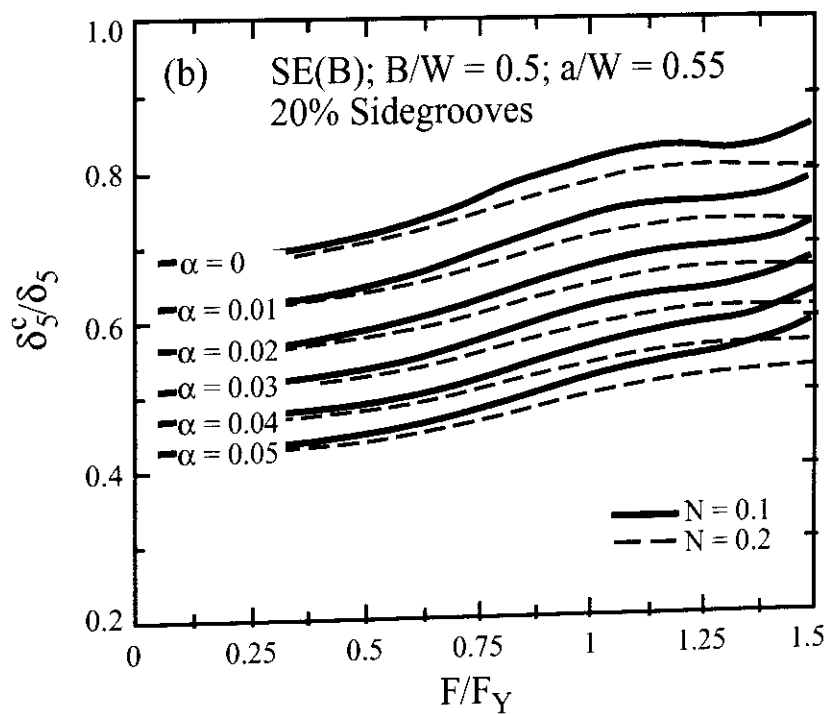
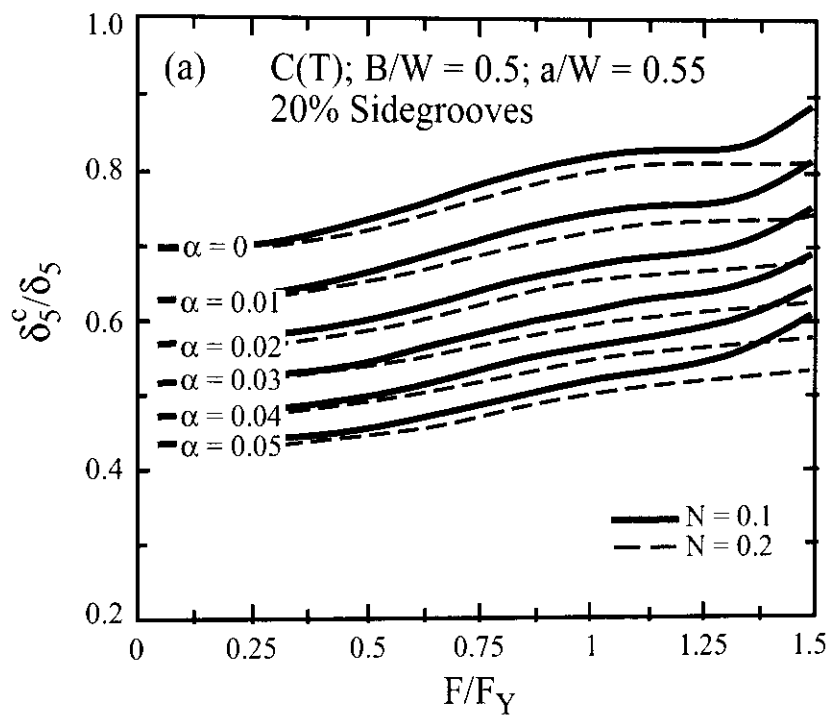


Figure A14.2: δ_5^c/δ_5 for sidegrooved specimens
a) C(T) specimens,
b) SE(B) specimens.

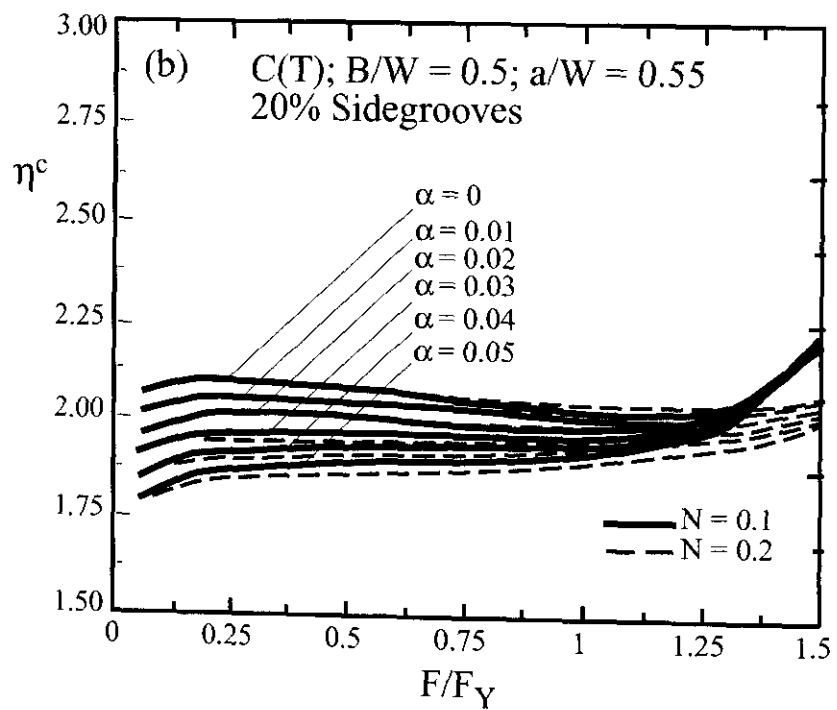
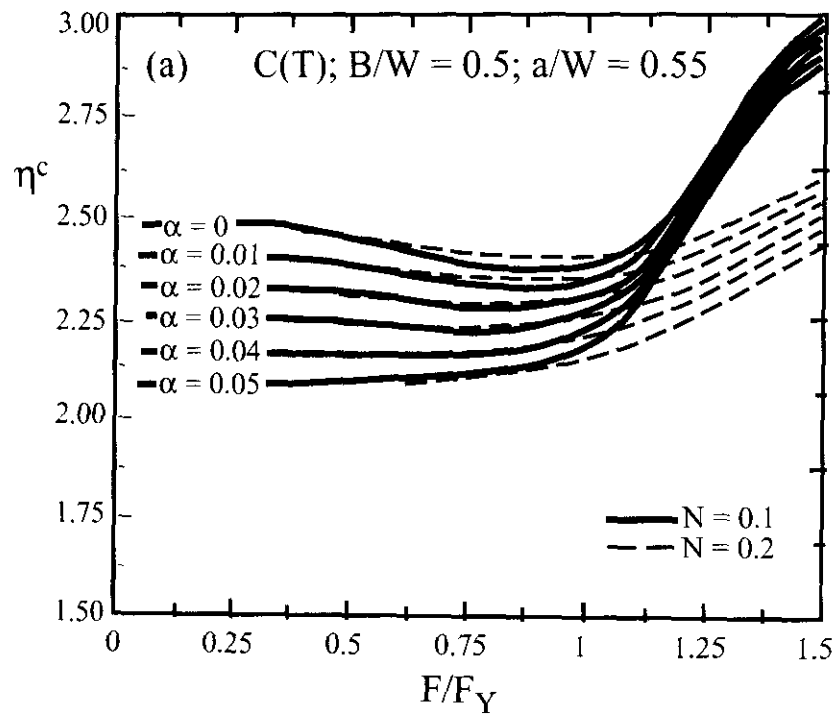


Figure A14.3: η^c factor for C(T) specimens

a) without sidegrooves,

b) with sidegrooves.

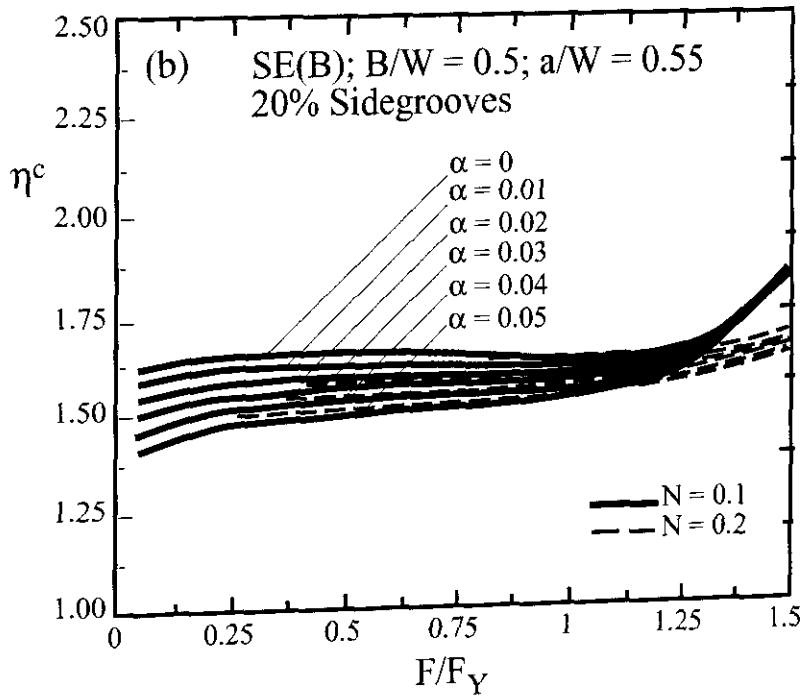
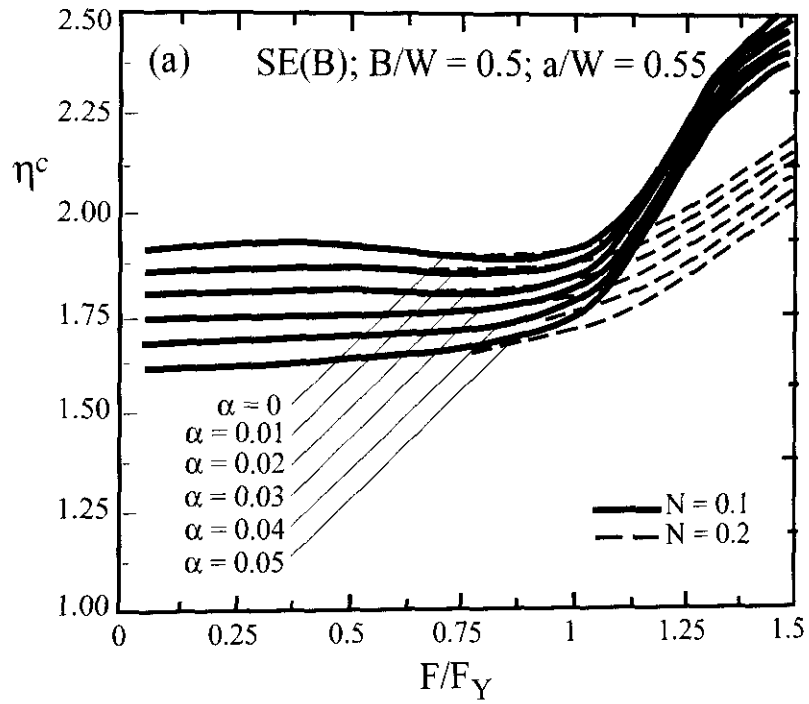


Figure A14.4: η^c factor for SE(B) specimens
a) without sidegrooves
b) with sidegrooves.

APPENDIX 15: Determination of the Crack Tip Opening Angle (CTOA)

The crack tip opening angle (CTOA) is a promising parameter for correlating stable crack extension. Its particular strength lies in describing large amounts of crack extension in thin-walled structures. However, due to the developing nature of CTOA determination, no standard procedure can be recommended. In the following, several techniques will be described which have been developed at BAM (Bundesanstalt für Materialforschung und -prüfung, Berlin), NASA Langley, and GKSS.

A15.1 Definitions

The CTOA is the angle included by the flanks of an extending crack, **Fig. A15.1**. After an initial transition period, the CTOA remains constant, i.e. independent of the amount of crack extension, **Fig. A15.2**. This constant angle is designated critical CTOA, ψ_c , which can be used for structural integrity assessments.

According to numerical analyses, the determination of the CTOA should be facilitated by the fact that the crack flanks remain linear during crack extension in these analyses, **Fig. A15.3**. The angle can this way be determined according to the relationship

$$\psi = \frac{\delta}{r_m}$$

where δ represents the opening displacement at the distance from the crack tip, r_m , **Fig. A15.1**. Ideally the distance r_m is held constant which can be easily done in finite element analyses. However, in a specific experimental method, δ is taken at a fixed location given by the fatigue precrack tip. Here $r_m = \Delta a$ and δ is given by δ_5 .

If ψ is to be determined experimentally in the neighbourhood of the extending crack tip, it turns out that in reality on a microscopic scale the crack flanks are quite irregular, making the determination of ψ difficult, **Fig. A 15.4**.

A15.2 Optical Microscopy (OM)

The OM method employs the following instruments [**A15.1**]:

- Long focal length microscope,
- Video camera with resolution of 512 x 512 pixels to obtain images of the stably tearing crack,
- Video recorder to store the images,
- PC with both monitor and software to precisely control the three-dimensional positioning of the microscope and also to analyze the images to obtain the CTOA.

To obtain clear images of the crack using OM, the surface of the specimen must be polished to a mirror finish and lighting of the crack region must be carefully controlled so that the crack tip region has optimum contrast and clarity. Three typical images obtained using OM are shown in **Fig. A15.5**. In the first image, **Fig. A15.5a**, a fatigue crack was grown approximately 0.75 mm under stable tearing. The second and third images, **Figs. A15.5b** and **A15.5c**, show the same crack after stable tearing of approximately 1.3 mm and 6 mm, respectively.

The CTOA is measured by recalling an individual image recorded on video tape and

- Locating the crack tip,
- Locating points on both crack surfaces in the range of 0.5–1.5 mm behind the crack tip,
- Fitting straight lines between the crack tip and each point and
- Computing the angle, ψ , between the straight lines.

The OM method can also provide the information on crack extension, Δa . Alternatively, crack extension can be determined using the methods described in **Appendix 5**.

Frequently the crack tip is difficult to define. In such cases, a four-point method [A15.2] is recommended as outlined in **Fig. A15.6**. Right behind the crack tip a pair of points on the crack flanks are identified. Within a distance of 1 to 1.5 mm another three to four pairs of points have to be identified.

The CTOA is then given by

$$\psi = \frac{1}{n} \sum \psi_i$$

where n is the total number of measured values satisfying the Δa_{\min} and Δa_{\max} requirements and

$$\psi_i = \frac{\delta_i - \delta_j}{r_i - r_j}$$

A15.3 Digital image correlation (DIC)

The DIC method employs the following instruments [A15.3]:

- 200 mm lens with 2X magnifier and several extension tubes,
- Translation stage for positioning of the video camera and following the growing crack,
- Video monitor to view the crack tip region,
- Video board to digitize images, and
- Microcomputer with software for controlling the image acquisition process and storing images.

The video camera is translated parallel to the specimen surface during the experiment so that the current crack tip remains within the field of view. After each translation of the video camera, the current image and previous image overlap by at least 50 pixels so that a continuous record of crack length is maintained in the event the crack grows beyond the current field of view.

Transverse magnification shall be at least 125 pixels per 1 mm. A high contrast random pattern is obtained by lightly spraying the specimen's surface with white acrylic paint and diffusely spreading black toner powder (from a laser printer) on the surface. The prepared specimen is to be baked at 200 °F for 25 minutes to adhere the powder to the surface. A typical set of images, obtained by the DIC before and during stable crack extension method is shown in **Figs. A15.7a** and **A15.7b**.

Because the DIC method obtains the displacement vector for a small subset, the general procedure is as follows:

- Choose a particular crack tip location and deformed image, D, for analysis.
- Choose a „reference“ image, R.
- Estimate the crack tip location in the deformed image, D.
- In the region of 0.5–1.5 mm behind the crack tip in image D, select pairs of subsets (each pair has one subset above the crack line and one subset below the crack line) that are a distance r_i behind the crack tip.
- Compute the crack opening displacement vector (u_i for upper and l_i for the lower subset) for each small subset using DIC.
- Subtract the displacement vectors for each pair of subsets.
- Estimate the normal vector for the crack line, n_i and
- Compute the angle for each pair of subsets using the equation

$$\psi = 2 \tan^{-1} [(du_i - dl_i)n_i/(2r_i)]$$

Fig. A15.7 shows two images and two pairs of subsets that were used to define ψ using DIC. Though the procedure described is straightforward, great care must be taken regarding:

Choice of „reference“ image

The DIC method uses finite-sized subsets to estimate the displacement of the center point. If the „reference“ image is an undeformed image, then the undeformed subsets will experience total strains exceeding 10 % during the fracture process most of which is plastic strain that is not recovered when the crack grows past a subset. The relative displacement used to estimate ψ will consequently be overestimated due to a combination of plasticity and offset of the subset center from the crack line. To minimize these difficulties, the „reference“ image shall be chosen to be a deformed crack configuration that is close to the current crack length. Thereby, the „reference“ image already will contain most of the intense plastic deformation that occurs during crack growth and the center point displacements will be relatively unbiased by plasticity.

Choice of subsets

Subsets have to be small, close to the crack line and of sufficient contrast for accurate DIC analysis. Experience has shown that, due to the random nature of the speckle pattern very few pairs of useful subsets are found in the region 0.5 to 1.5 mm behind the crack tip.

Errors in the measurement

The primary source of error in estimating ψ is in locating the current crack tip. This can be due to lack of contrast between painted surface and crack surfaces, small crack opening near the tip and a small amount of cracking of the thin paint layer near the tip. For these reasons, data for ψ is to be obtained by DIC using subsets further than 0.6 mm behind the crack tip. It should be borne in mind that overlapping images are needed.

The DIC can also provide information on crack extension, Δa . Alternatively crack extension can be determined using the methods described in **Appendix 5**.

A15.4 CTOA from δ_5 measurements

An approximate measure of ψ can be obtained from δ_5 measurements [**A15.3**, **A15.4**]:

$$\psi = \frac{d\delta_5}{da} .$$

Whereas this definition of ψ is very easy to exploit - using the δ_5 techniques recommended in **Appendix 4** – it seems to need further refinement as the available results are not unambiguous: **Figs. A15.8** and **A15.9a** show very good agreement with the CTOA as determined using FE analyses, whereas the agreement is less good in **Fig. A15.9b**.

A15.5 Infiltration

The infiltration technique represents a multiple specimen method. A number of nominally identical specimens are loaded up to different displacements. The infiltration material is given time to fill the crack wedge in the deformed condition and to form thereby a replica of the crack profile. The specimen is then unloaded and broken open to remove the replica and to determine the amount of crack extension as described in **Section 4.3**. The CTOA is determined from the profile of the replica. Sections through the replica can provide a through-thickness variation of the CTOA if desired.

A15.6 Finite element analyses

A possible approach is to assume a constant CTOA from initiation to instability and find by trial and error the ψ_c value which fits the maximum load. Various FE codes have already been used for determining the CTOA:

These FE codes have included two-dimensional constant-strain and linear-strain codes, a shell code, and three-dimensional linear-strain codes. The study of stable tearing behaviour for a variety of materials [A15.6] found that 0.5-mm constant-strain elements were required in the crack tip region, to fit the load-crack extension behaviour along the line of crack extension. Two other studies using a three-dimensional FE code [A15.7] and a shell code [A15.8] with linear-strain elements found that 1-mm size elements were sufficient to model stable tearing for a wide range of cracked specimens. If the crack length and uncracked ligament criteria ($a/B > 4$ and $b/B > 4$) are met, then the critical CTOA has been shown to be independent of specimen type (compact or middle crack tension). CTOA values so obtained have been used to predict the stable tearing behaviour of complex structures of thin-sheet aluminium alloy [A15.9].

Figs. A15.8 and A15.9 show early results which demonstrate the applicability of δ_5 for determining the CTOA. More recent experimental investigations performed at GKSS show, however, that, whereas excellent results were obtained for bend specimens, care is advised for tension geometries.

A15.7 Determination of the critical CTOA, ψ_c

The points of ψ versus Δa form the R-curve in terms of the CTOA, **Fig. A15.10**. The data between

$$\Delta a_{\min} = B$$

and

$$\Delta a_{\max} = W - a_0 - 4B$$

are used to determine ψ_c :

$$\psi_c = \frac{1}{N} \sum \psi_n$$

where N is the number of ψ values between the crack extension limits Δa_{\min} and Δa_{\max} .

NOTE: *These crack extension limits have been derived for thin-walled specimens.*

REFERENCES

- [A15.1] Dawicke, D.S. and Sutton, M.A., 1994, CTOA and crack-tunneling measurements in thin sheet 2024-T3 aluminium alloy, *Experimental Mechanics*, Vol 34, No. 4, 357–368.
- [A15.2] Heerens, J. and Schödel, M., 2003, On the determination of crack tip opening angle, CTOA, using light microscopy and δ_5 measurement technique, *Engineering Fracture Mechanics* 70, 417–426.

- [A15.3] Sutton, M.A., Turner, J.L., Bruck, H.A. and Chae, T.A., 1994, Full-field representation of discretely sampled surface deformation for displacement and strain analysis, *Experimental Mechanics*, Vol. 31, No. 2, 168–177.
- [A15.4] Brocks, W. and Yuan, H., 1991, Numerical studies on stable crack growth, in: Blauel, J.G. and Schwalbe, K.-H. (Eds.): *Defect Assessment in Components – Fundamentals and Applications*,ESIS/EGF 9, London, 19–33.
- [A15.5] Brocks, W. and Yuan, H., 1990, FE-Analysen des Risswachstumsverhaltens dünner Proben bei großem Risswachstum, BAM, Report BAM-1.01, 90/4.
- [A15.6] Newman, J.C., Jr., 1984, An elastic-plastic finite element analysis of crack initiation, stable crack growth and instability, *ASTM STP 833*, 93–117.
- [A15.7] Dawicke, D.S. and Newman, J.C., Jr., 1994, Residual strength predictions for multiple-site damage cracking using a CTOA criterion, *ASTM, STP 1332*, 815–829.
- [A15.8] Chen, C.S., Wawrzynek, P.A. and Ingraffea, A.R., 1999, Elastic-plastic crack growth simulation and residual strength prediction of thin plates with single and multiple crack, *ASTM STP 1332*, 97–113.
- [A15.9] Seshadri, B.R., Newman, J.C., Jr., Dawicke, D.S. and Young, R.D., 1999, Fracture analysis of the FAA/NASA wide stiffened panels, *Second Joint NASA/FAA/DoD Conference on Aging Aircraft*, NASA/CP-1999-208982, 513–524.
- [A15.10] de Koning, A. U., 1978, A contribution to the analysis of quasi-static crack growth, in: *Fracture 1977, Proceedings of the Fourth International Conference on Fracture*, Vol. 3A, Pergamon, 25–31.

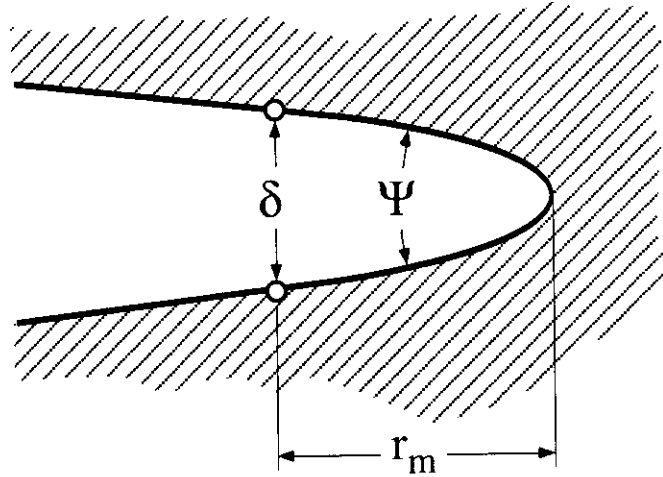


Figure A15.1: Definition of the CTOA.

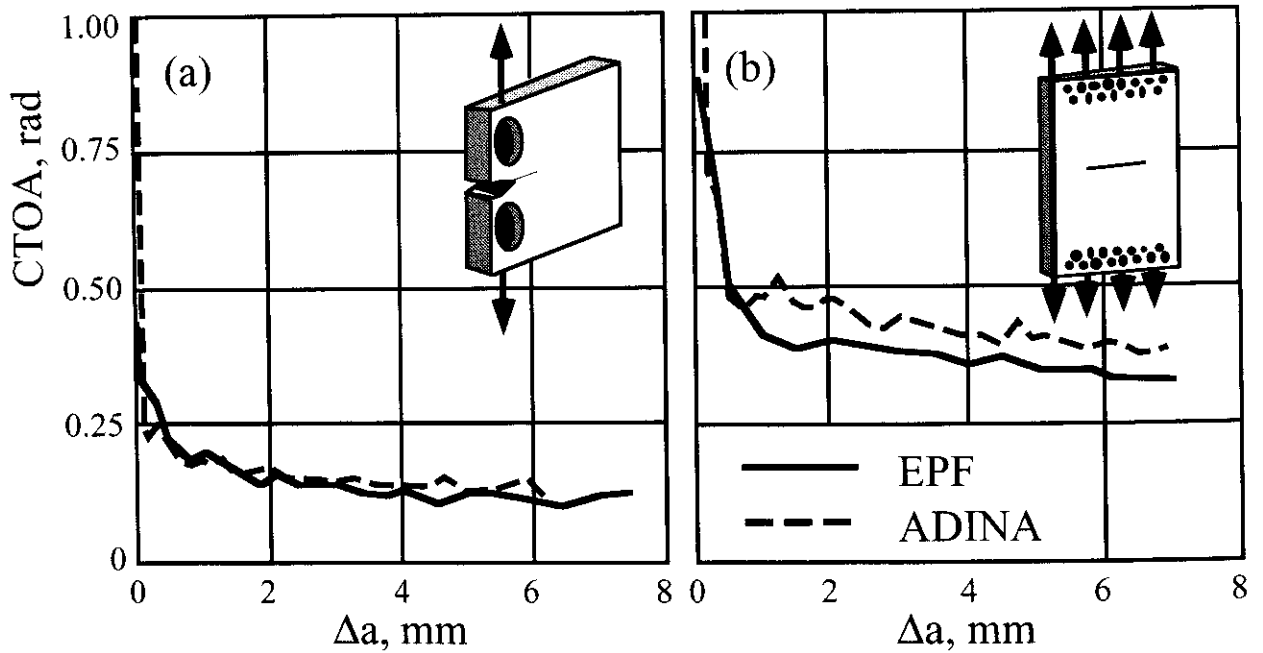


Figure A15.2: Variation of the CTOA with crack extension [A15.5];

a) C(T) specimen,

b) M(T) specimen,

It should be noted that the specimens do not meet the size requirements ($a_0/B > 4$, $b_0/B > 4$).

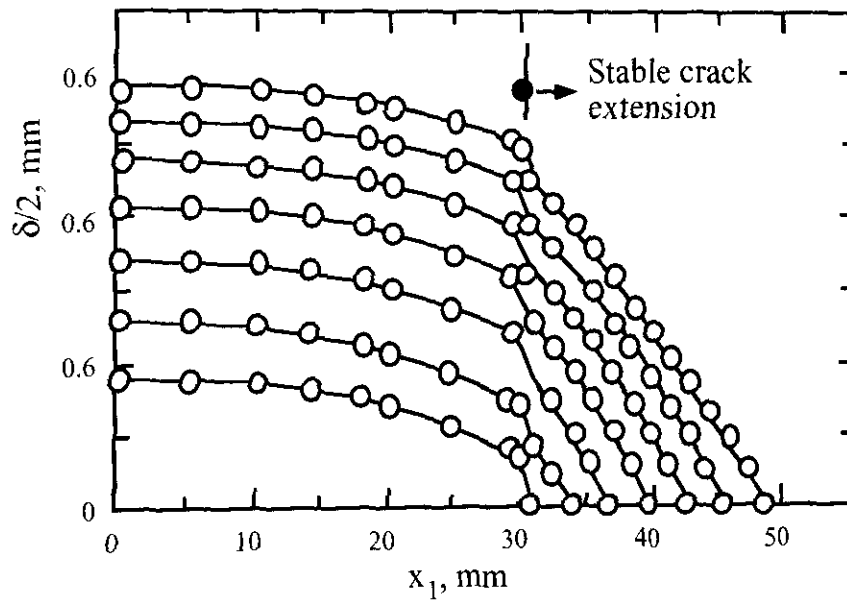


Figure A15.3: Finite element analysis of stable crack extension in Al 2024-T3 showing linear crack flanks [A15.10].

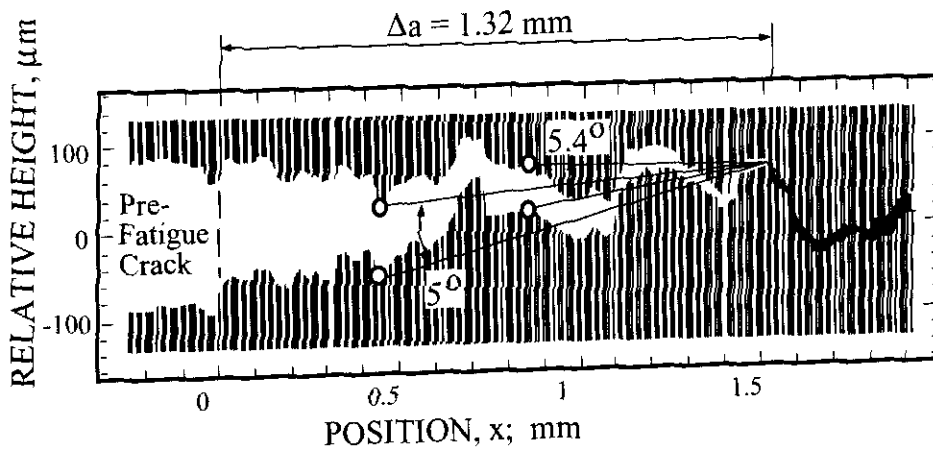
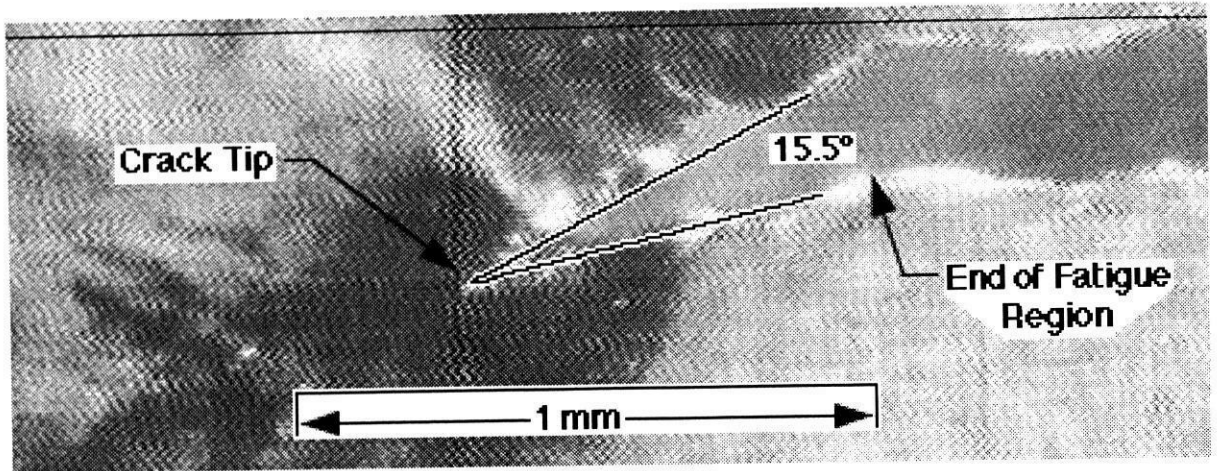
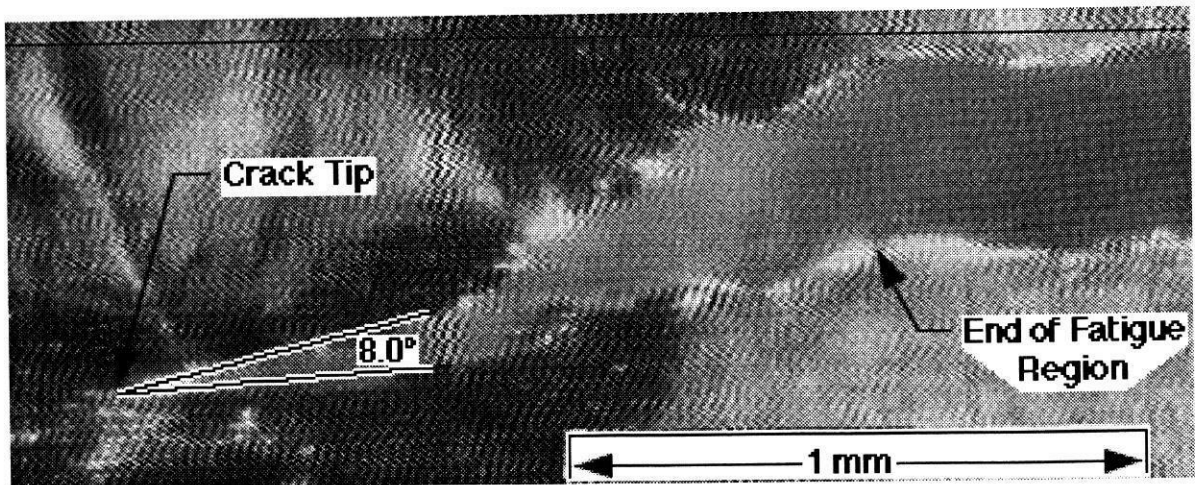


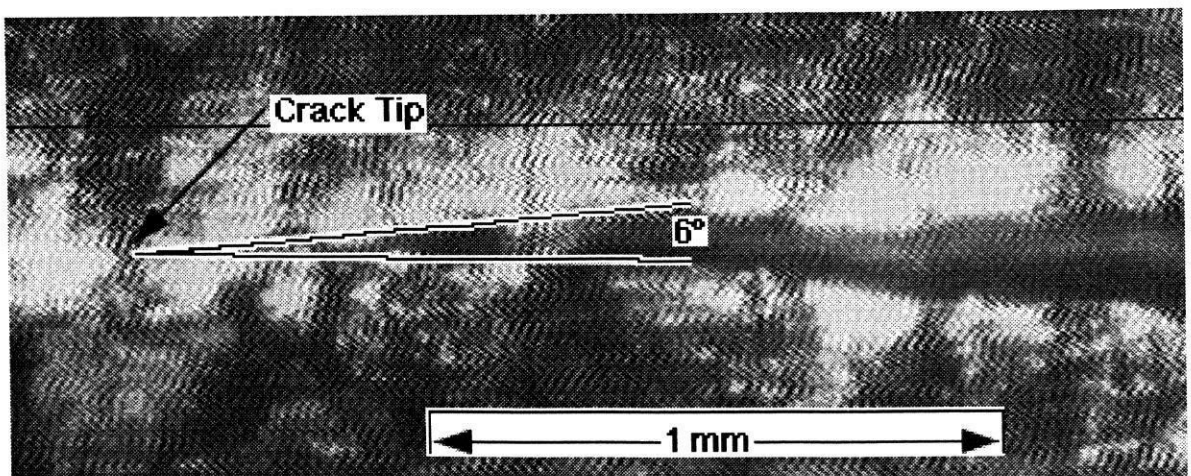
Figure A15.4: Irregularity of crack flanks complicates CTOA determination.



a.) OM image after about 0.75 mm of stable tearing



b.) OM image after about 1.3 mm of stable tearing



c.) OM image after about 6 mm of stable tearing

Figure A15.5: Typical OM images and CTOA measurements for stable tearing cracks in 2.3 mm thick 2024-T3 aluminium alloy [A15.1].

Figure A15.6:
Four-point method for determining the CTOA [A15.2].

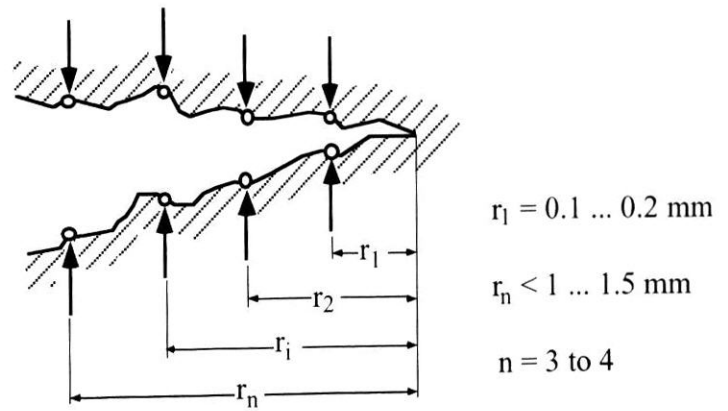
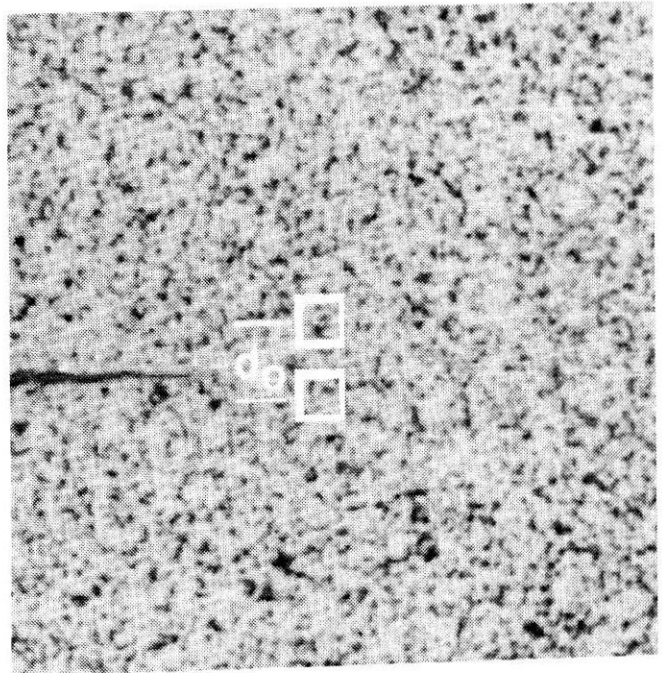
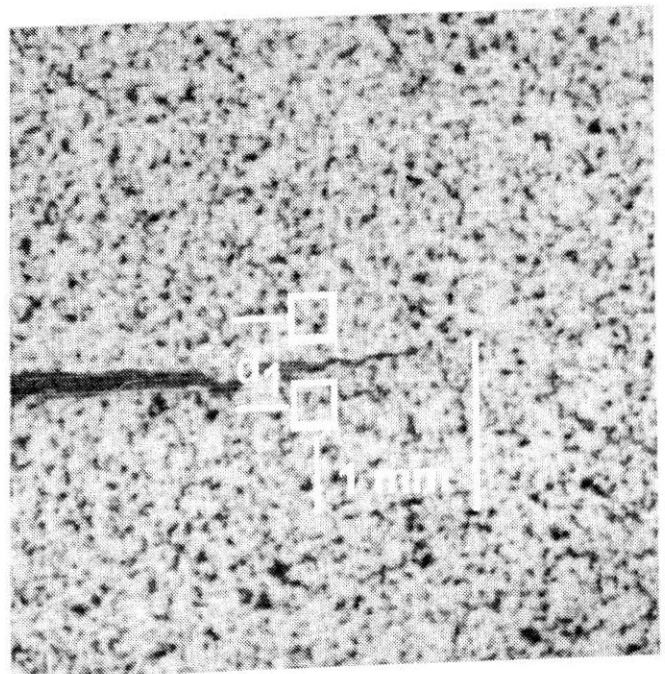


Figure A15.7:
DIC images of crack before and after crack extension [A15.1]:

a)
Current configuration of the fracture specimen,



b)
Configuration after crack extension.



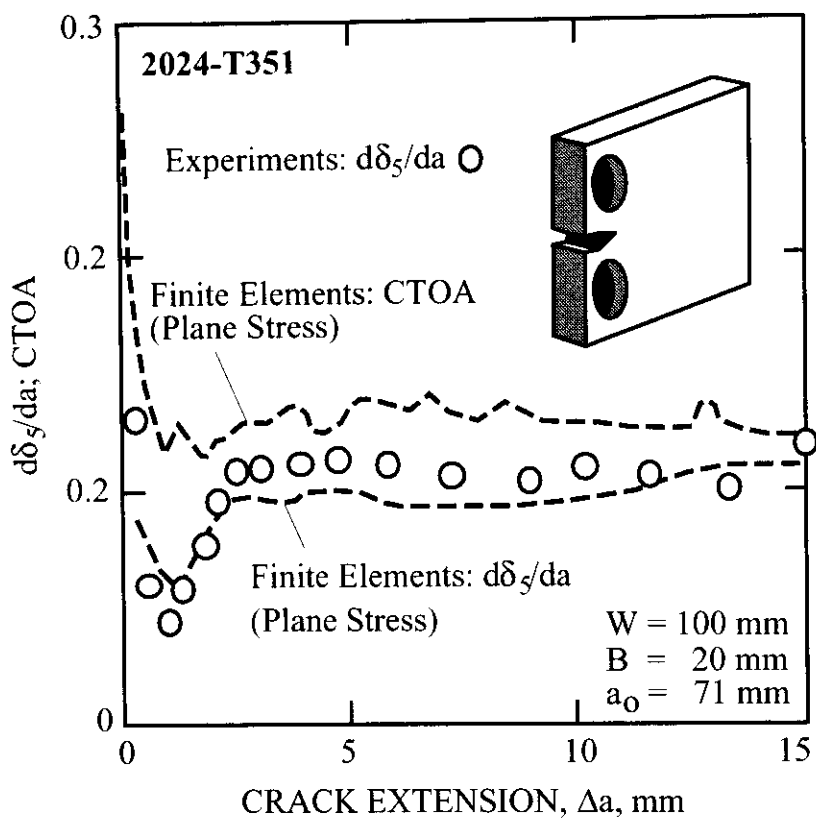
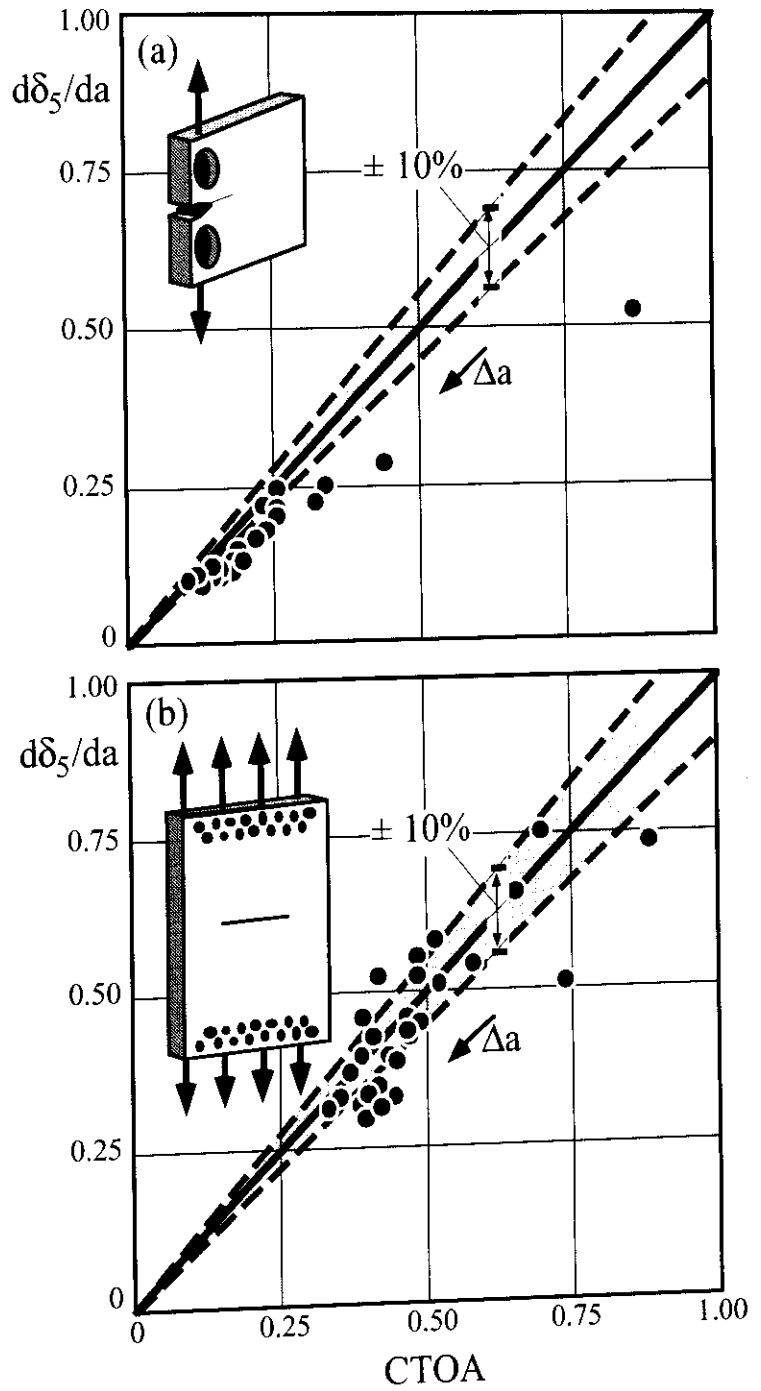


Figure A15.8:
CTOA and $d\delta_5/da$ for an aluminium alloy [A15.5].

Figure A15.9:
CTOA and $d\delta_5/da$ for two specimen geometries of the steel StE 460(3) [A15.5].



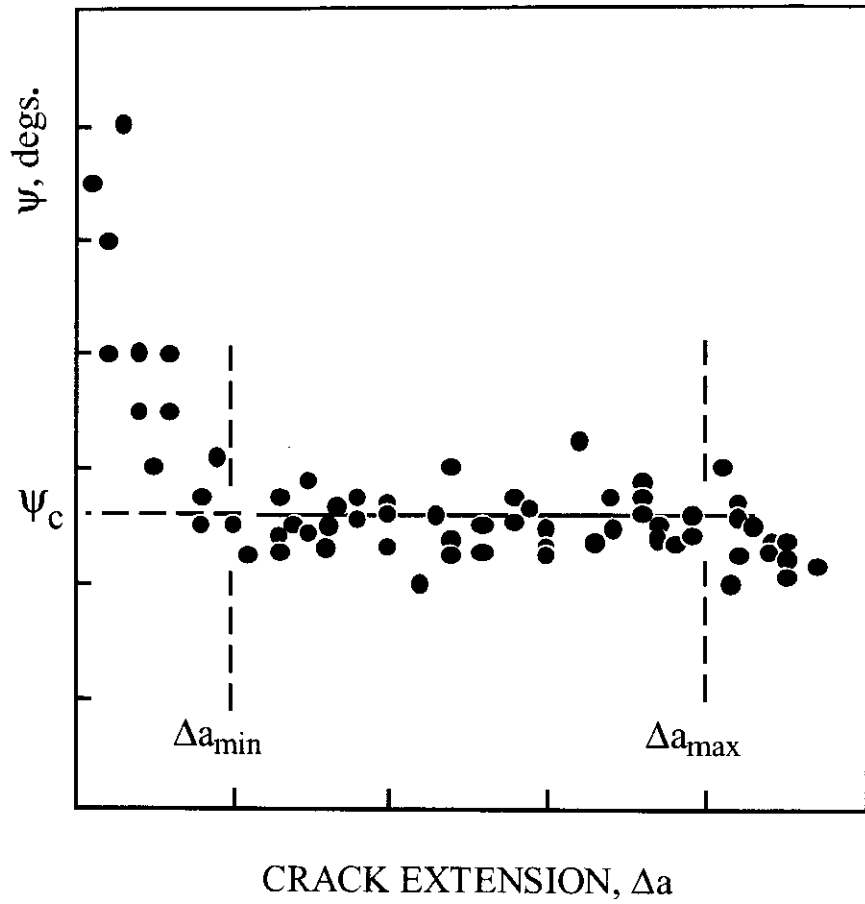


Figure A15.10: *Determination of the critical CTOA, ψ_c .*

APPENDIX 16: Determination of the Rate of Dissipated Energy, R.

The physical meaning of J as a crack tip field parameter vanishes as a consequence of ductile crack extension. Therefore, thoughts have been given to a physically more meaningful parameter for characterizing stable crack extension. The rate of dissipated energy, R , is regarded as a promising alternative to J [A16.1-A16.3]. It is defined by

$$R = \frac{1}{B} \left[\frac{dU}{d(\Delta a)} - \frac{dU_{el}}{d(\Delta a)} \right] = \frac{1}{B} \frac{dU_{dis}}{d(\Delta a)}$$

where U is the total work done on the specimen, U_{el} is the elastically stored energy, and U_{dis} is the dissipated energy.

R-curves for the rate of dissipated energy can be derived from J-R-curves [A16.3, A16.4]:

$$R = \frac{W-a}{\eta} \frac{dJ_{pl}}{d(\Delta a)} + J_{pl} \frac{\gamma}{\eta} \quad \text{for C(T) and SE(B) specimens}$$

with

$$\begin{aligned} \eta &= 2.0 + 0.522 (1-a/W) && \text{for C(T) specimens} \\ \eta &= 2.0 && \text{for SE(B) specimens} \\ \gamma &= 1.0 + 0.76 (1-a/W) && \text{for C(T) specimens} \\ \gamma &= 1.0 && \text{for SE(B) specimens} \end{aligned}$$

and

$$R = (W-a) \frac{dJ_{pl}}{da} \quad \text{for M(T) specimens.}$$

In the above equations,

$$J_{pl} = J - J_{el} = J - \frac{K^2}{E}.$$

The shape of a R - Δa curve, **Fig. A16.1**, is the same as that of a ψ - Δa curve, **Fig. A15.10**. The R - Δa curve can be analytically expressed using [A16.5]

$$R = R_{\infty} \left[1 + \alpha \exp\left(-\lambda \frac{\Delta a}{W}\right) \right]$$

where R_{∞} is the stationary value of R attained after a certain amount of crack extension, α and λ are fit parameters.

An example of such an analysis is shown in **Figs. A16.2** and **A16.3**.

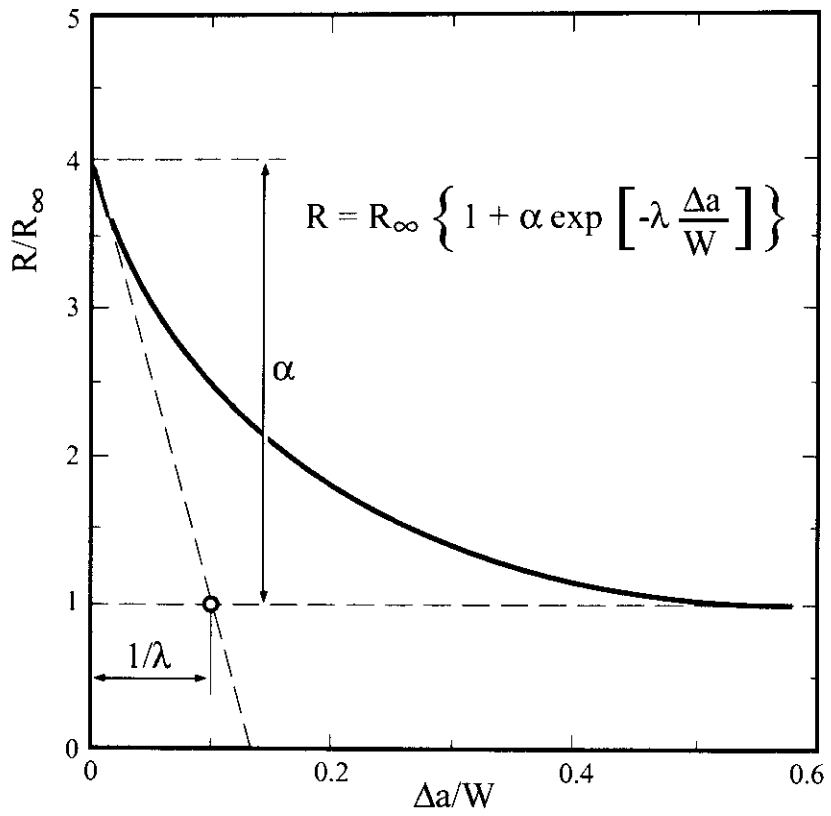


Figure A16.1: Fit function for a crack extension resistance curve on the basis of the rate of dissipated energy [A16.5].

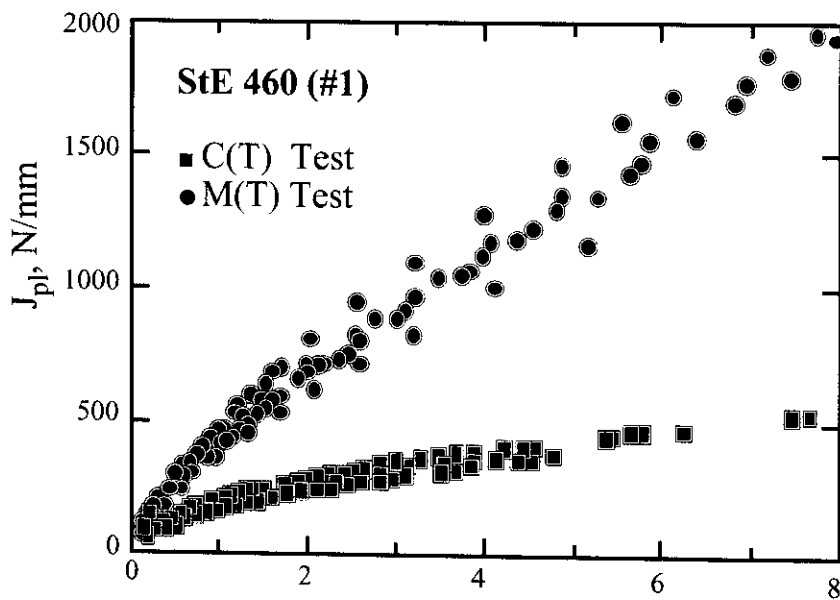


Figure A16.2: J - R -curves obtained on C(T) and M(T) specimens of the steel S+E460 [A16.6].

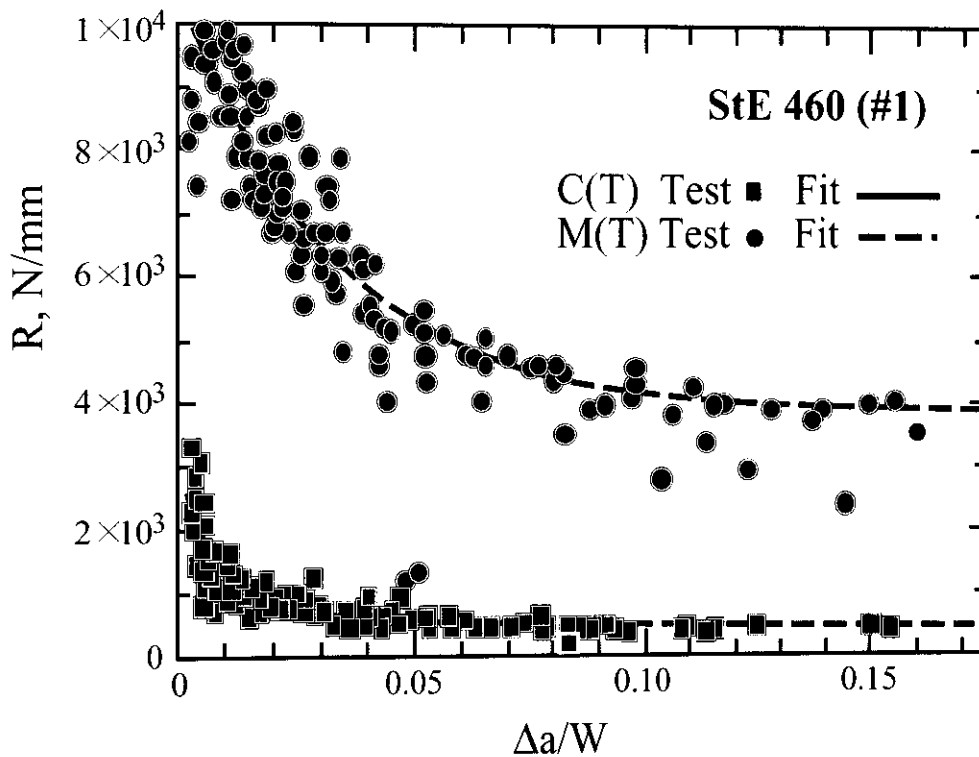


Figure A16.3: *R*-curves on the basis of the rate of dissipated energy, derived from the data in Fig. A16.2 [A16.6].

REFERENCES

- [A16.1] Turner, C.E., 1990, A re-assessment of ductile tearing resistance (Part I and II), Fracture Behaviour and Design of Materials and Structures (Ed. Firrao, D.) Vol. II, Proc. ECF8, 933-949 and 951-968, Engineering Materials Advisory Services LTD, Cradley Heath, U.K.
- [A16.2] Turner, C.E. and Kolednik, O., 1994, Application of the energy dissipation rate and arguments to stable crack growth, Fatigue and Fracture of Engng. Materials and Structures, 17, 1109-1127.
- [A16.3] Siegmund, T. and Brocks, W., 2000, A numerical study on the correlation between the work of separation and the dissipation rate in ductile fracture, Engineering Fracture Mechanics 67, 139-154.
- [A16.4] Memhard, D., and Klemm, W., 1992, Zusammenhang zwischen Risslaufenergie und J-Risswiderstandskurven, Berichtsband 24. Sitzung des DVM-Arbeitskreises Bruchvorgänge, 291-302, Deutscher Verband für Materialforschung und -prüfung, Berlin.
- [A16.5] Brocks, W., 1998, Charakterisierung des Risswiderstandes mit Hilfe der Energie-dissipationsrate: Einflüsse von Material, Probenform und -größe, Technical Note GKSS/WMG/98/6 (internal report), Institute of Materials Research, GKSS Research Centre, Geesthacht, Germany.
- [A16.6] Aurich, D., et al., 1990, Analyse und Weiterentwicklung bruchmechanischer Versagenskonzepte, Forschungsbericht 174, Bundesanstalt für Materialforschung und -prüfung, Berlin.

EFAM DOCUMENT IMPROVEMENT PROPOSAL		
1. Document I.D. EFAM GTP 02	2. Document Date: December 2002	3. Document Title: The GKSS test procedure for determining the fracture behaviour of materials
4. Recommended Improvement (Section no.)		
5. Reason for Recommendation		
6. Author of Recommendation		
Name:	Organisation:	
Address:	Phone: Fax: E-mail:	7. Date of Submission

send to: Prof. Karl-Heinz Schwalbe
GKSS-Forschungszentrum Geesthacht GmbH
Max-Planck-Str. 1
D-21502 Geesthacht, Germany
Fax: +49 (0) 4152-872534
schwalbe@gkss.de